Influence of summer snowfall on discharge emanating from the Gangotri glacier

by

Kirk Gunnar Larsen

A thesis submitted for the degree of
master of science

School of Environment and Life Sciences
College of Science and Technology
University of Salford, UK

2017

Contents

List of Figures

List of Tables

This thesis is dedicated to the late Professor David N. Collins, without whom this thesis would not be possible. For this I am eternally thankful ...

Rest in peace

Acknowledgements

I would first like to thank the late Professor David N. Collins, who first ignited my love for Alpine glaciers leading me to undertake postgraduate study in the area. I will never forget David's expertise, kind heartedness and approachability, not to mention the incredible field trips. For these opportunities and experiences I am immensely grateful, making my time at the University of Salford as great as it was.

My gratitude is also extended to both Dr Neil Entwistle and Dr Robert Williamson for their help and support given throughout the duration of my postgraduate study, in particularly during the difficult past year. Their approachable and helpful manner has been outstanding and without their guidance the completion of this thesis would not have been possible. For this I am truly indebted.

I also wish to thank both of my parents Gary and Alison Larsen as well as Linda Owens for the unrivalled support and encouragement they have supplied during my study. This has been utterly invaluable to me and for this I am also sincerely thankful.

Furthermore, I would also like to thank my friends who often provided necessary distraction from time to time. Thanks also go to my fellow student George Pea, who has been great company throughout both my undergraduate and postgraduate study, often providing much needed camaraderie.

I would also like to thank NERC for the funding of this project, without which its completion would not be possible.

Declaration

This is to certify that the copy of my thesis, which is presented for the degree of Master of Science by research, embodies the results of my own course of research, has been completed by myself and has been viewed by my supervisor before presentation.

Signature:_____   Date:_____

Abstract

Study of Himalayan glaciers are important for a number of reasons including hydroelectric power, drinking water supply, irrigation & water resources. The aim of this investigation was to determine how summer snowfall events between 2001 & 2004 influenced runoff flowing from Gangotri glacier, located in the Garhwal region of the Himalayas. This was achieved by collating air temperature, precipitation and discharge data for the study area. Data were used to determine the hydrological regime within catchment and to establish the general influence that air temperature and precipitation have on discharge, using regression and correlation analysis. Using a temperature lapse rate the daily average elevation for the 0 °C isotherm was calculated. This differentiated days in which snowfall events would cover a large majority of the glacier through filtering elevation. Correlation analysis was used to assess the relationship between air temperature and discharge; before, during and after these precipitation events. It was found that air temperature was the driving factor for discharge with R^2 results ranging from 0.38 to 0.67 for the study period, whereas between discharge and precipitation R^2 ranged from 0 to 0.16. Under lowering 0 °C isotherm filters the relationship between air temperature and discharge became weaker for all years apart from 2004, whereas the relationship between discharge and precipitation became more negative for 2001 & 2004. These findings suggest a decreasing influence of air temperature and presence of snowfall, where an increase in precipitation causes a decrease in discharge. During three specific snowfall events correlation between discharge and air temperature before the snowfall event was positive, during the period of snow cover was negative and after the snowpack had depleted returned to a positive correlation. Results show that such snowfall events appeared to have a dampening effect on discharge for around 5 to 7 days.

Chapter 1

Introduction

Glaciers and ice caps occupy around 10% of the Earth's land mass concentrated primarily in polar regions, but are important in that they hold nearly 77% of total fresh water. Himalayan glaciers alone store around $12\,000\,\text{km}^3$ of fresh water and source some of the worlds largest rivers such as the Indus, Ganga and Brahmaputra (Dyurgerov and Meier, 2005; Ninh, 2007). The Himalayas are both the highest and youngest mountain range in the world, boasting the largest glacial coverage outside of the polar regions and are sometimes referred to as 'the third pole' (Dyurgerov, 2001; Khan *et al.*, 2017; Pandey *et al.*, 1999; Singh *et al.*, 2014).

The Indian region of the Himalayas contains around 9 575 glaciers spanning an area of nearly $40\,000\,\text{km}^2$ (Raina and Srivastava, 2014; Sangewar *et al.*, 2009). Himalayan glaciers and their study is of increasing importance to India for a number of reasons including hydroelectric power, drinking water supply, irrigation and other water resources. The demand for these resources is also increasing due to pressures from industrial development and urbanisation as a result of rapid population growth (Singh *et al.*, 2011).

Understanding glacial response to meteorological conditions including summer snowfall events is also of increasing importance, due to a warming climate. A large majority of Himalayan glaciers have experienced decline over the last

century due to climate change, evident in a number of studies including those conducted by Bahuguna *et al.*, (2007), Kulkarni and Bahuguna, (2002), Kulkarni *et al.*, (2007), and Yao *et al.*, (2007). It has also been suggested by the Intergovernmental Panel on Climate Change that total glacier mass within Alpine regions could decline by up to a quarter by 2050 and around half by 2100 (Watson *et al.*, 1996). The decline of glaciers within the Himalayan region would be detrimental to near 500 million inhabitants who rely on meltwater derived from glaciers within major rivers (Rees and Collins, 2006).

The potential effects of a warming climate on glaciers are displayed in Figure 1.1 from a study conducted by Hock *et al.*, (2005), who investigated the response of glacial discharge to climatic warming.
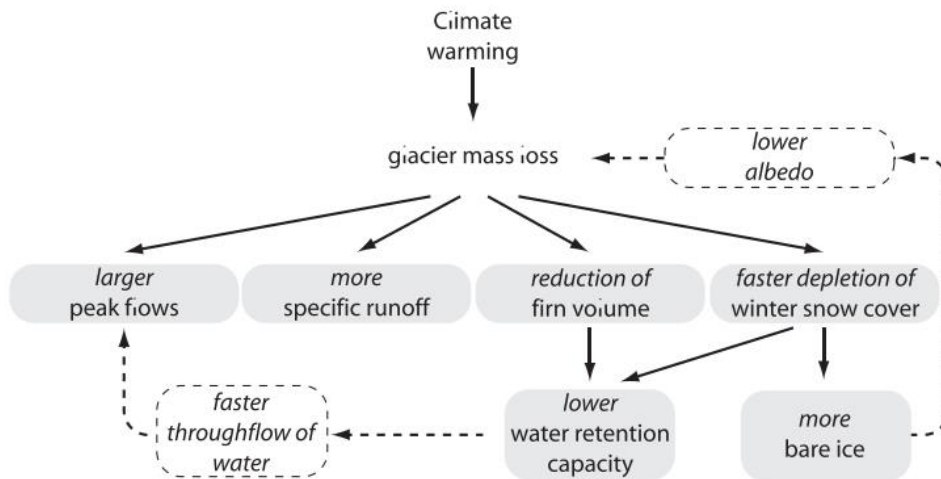
Figure 1.1: Effects of a warming climate on discharge from a glacier (Hock *et al.*, 2005).

The diagram illustrated in Figure 1.1 displays the effect mass loss through climatic warming has on glaciers including larger peak flows, more specific runoff, reduction of firn volume and faster depletion of winter snow cover. The depletion of winter snow cover is one of the most influential effects, as this leaves more bare ice exposed to radiation leading to more glacier mass loss and the further effects this causes (Hock *et al.*, 2005). During a warming climate melting of glacier ice will lead to greater discharges, but this supplementary

flow cannot be sustained and will eventually begin to decrease and disappear as the glacier declines in mass (Rees and Collins, 2006).

Within the Himalayas, monsoonal rainfall during summer plays a large role on the status of glaciers. The monsoon is predominantly caused by high upper-tropospheric air temperatures above the Tibetan Plateau, through warming of the land mostly situated at elevations above 3500 m. This produces a temperature gradient between the Indian Ocean and Tibetan Plateau, causing warm and moist air to rise upwards over the Himalayas which cools and produces clouds forming the monsoon (Fu and Fletcher, 1985; Immerzeel *et al.*, 2009; Zhisheng *et al.*, 2011).

The Indian summer monsoon weakens from east to west meaning the Himalayas can be split into 4 zones (Figure 1.2). Zone 1, furthest west, represents a region mainly controlled by westerlies as opposed to monsoonal influences. Glaciers located within the region of Zone 1 are influenced mainly by winter precipitation. Zone 2, located over the Karakoram and western region of the Himalayas, experiences both influence from monsoonal rainfall and a small influence from the westerlies. Zone 3 is located in the Central Himalayan region and is predemonantly influenced by monsoonal rainfall including parts of Tibet, Nepal and India, with many glaciers within this zone debris covered. Moreover, Zone 4 is located over the eastern most area where many of the glaciers are summer accumulation type due to domination of the summer monsoon (Khan *et al.*, 2017).

Distribution of monsoonal rainfall within the Bhagirathi basin containing Gangotri glacier is evident in Figure 1.3. It is apparent that more rainfall occurs at lower elevations of the basin, but some still occurs at higher elevations over the glacier. If air temperature is low, causing a low elevation of the 0 °C isotherm during monsoonal rainfall, precipitation will fall as snow and cover the glacier.
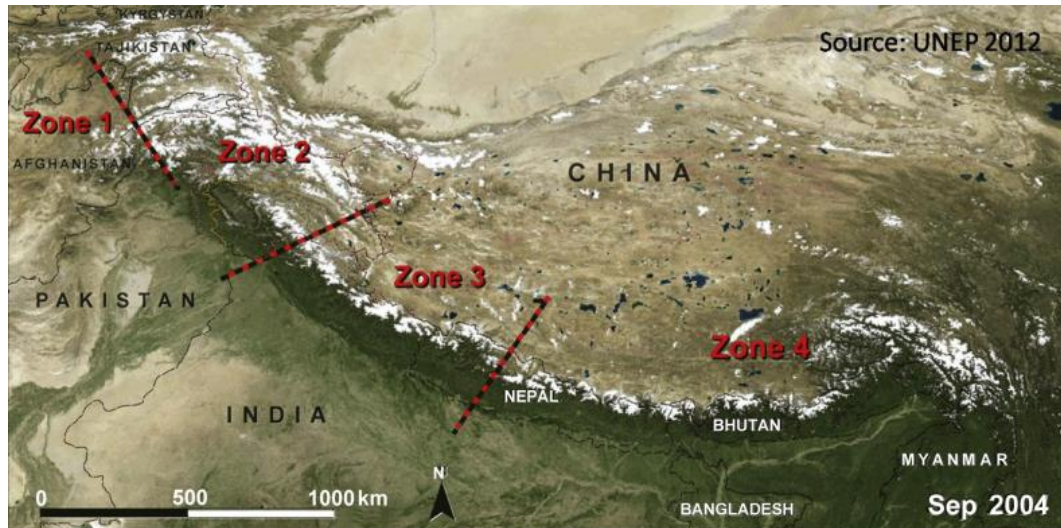
Figure 1.2: Four major climatic zones present within the Himalayas (Khan *et al.*, 2017).
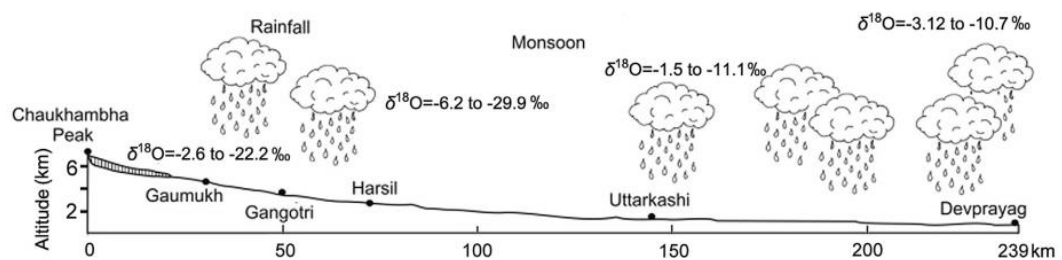
Figure 1.3: Schematic diagram of monsoon rainfall over Gangotri glacier and Bhagirathi basin at differing elevations (Khan *et al.*, 2017).

Literature directly investigating the effect of summer snowfall events on discharge from glacierised basins appears to be rare, especially within the Himalayan region. This may partly be due to difficulties recording data regarding meteorological conditions within the Himalayas and discharge from glacierised basins. Poor accessibility to high altitudes, harsh weather and precipitous terrains may cause logistical problems for transportation of equipment (Singh *et al.*, 2005b). The area of study is of importance as summer precipitation events have the potential to offset melt for short periods of time within summer months, which may slightly extend the life span of a glacier, especially those which experience monsoonal rainfall.

Work displayed in following chapters attempts to understand the effect that specific summer snowfall events have on discharge from a highly glacierised basin, located in the Indian Himalayas. It is hypothesised that a summer precipitation event which falls as snow will have a dampening effect on discharge, despite an increasing air temperature. It is also thought that as the elevation of the 0 °C isotherm decreases, the relationship between precipitation and runoff will become negative and the relationship between air temperature and runoff will become weaker.

1.1 Theses outline

This thesis comprises of seven chapters including introduction, study area, background, methods, results, discussion and conclusion. The introduction includes a small background to the general topic area, explains why this area of research is important and hypothesises what this investigation expects to find. Introduction also includes aim & objectives, which sets out what the study aims to achieve and describes objectives in order to meet this aim.

Study area aims to provide information about the immediate region in which the investigation is based and the background aims to provide an insight into the current understanding of each subsection through examining current literature in the field. Subsections include the 0 °C isotherm and summer snow-

fall, retreat of Gangotri glacier and other Himalayan glaciers and Himalayan streamflow.

The methods chapter entails how the data were gathered regarding discharge, air temperature and precipitation with the data analysis utilised. Chapter 5 quantifies results of the investigation in detail, comprising of sections regarding general air temperature, precipitation and discharge for the summers of 2001-2004, the interaction between discharge and precipitation, interaction between discharge and air temperature in relation to the elevation of the 0 °C isotherm and displays specific summer snowfall events with response of discharge. Chapter 6 contains the discussion, explaining and accounting for results within Chapter 5, with the utilisation of literature. The discussion will attempt to explain year to year trends in discharge, air temperature and precipitation, general influence of air temperature and precipitation on discharge, interaction of air temperature and precipitation with discharge in relation to the elevation of the 0 °C isotherm as well as relationship between discharge, air temperature and precipitation during specific summer snowfall events.

The conclusion will provide an overall summary of main themes and findings presented within this thesis, and describe how the aim and objectives were met. Concluding remarks regarding limitations of the study and considerations for future research in the topic area are also included.

1.2   Aim & objectives

The overall aim of the research is to investigate how summer snowfall events influence discharge emanating from Gangotri glacier. This is to provide an insight as to the effect a specific snowfall event over the ablation area of the glacier has on runoff, utilising calculation of the 0 °C isotherm elevation. The period under analysis occurred between May and October ranging from 2001 & 2004, using data regarding precipitation, discharge and air temperature. Specific objectives developed to achieve this aim were to:

1. Determine the discharge and meteorological regime for Gangotri glacier.

Gathering previously collected meteorological data will allow for determination of the discharge and meteorological regime within the immediate area of the glacier.

2. Establish daily average elevation of the 0 °C isotherm for each summer day.

Calculating the elevation of the 0 °C isotherm for each summer day will enable the determination of precipitation type (rain or snow) over Gangotri glacier.

3. Identify precipitation events where snowfall covers a large amount of the ablation zone.

Summer precipitation events which fall as snow over a majority of the glacial area, identified through the third objective will allow for the fulfilment of the overall aim of the study. This is by collaborating such precipitation events with discharge and air temperature in order to observe their direct effect on river flow.

Chapter 2

Study Area

The Himalayan arc spans a length of around 2 500 km with a width of 200 km to 250 km, crossing through India, China (Tibet), Bhutan, Nepal and Pakistan as displayed in Figure 2.1 (Le Fort, 1975). The Himalayas were formed around 40-50 million years ago, when the Indian subcontinent collided with Asia following the breakup of Pangea. Due to their low density and buoyancy neither plate subducted, causing the crust between two continents to thicken through compressional forces. This produced rapid uplift forming the Himalayas, which still continues today (Molnar, 1986).

The Himalayas are often referred to as 'the water towers of Asia', due to large amounts of snow and ice which are present supplying water via rivers to millions of people. Meltwater which emanates from snow and ice feeds a number of large river systems including the Brahmaputra, Ganges, Yangtze, Mekong and the Yellow Rivers. The river basins cover a vast expanse of around 9 million km^2, of which 2.8 million km^2 are within the Hindu Kush region of the Himalayas alone. There are an estimated 54 000 glaciers located within the region spanning an overall area of around 61 000 km^2 (Bajracharya and Shrestha, 2011).

Figure 2.1: Span of the Himalayas across Pakistan, India, Nepal, Bhutan and China.

The primary area of study is the Bhagirathi basin located within the North West Garhwal region, Uttarakhand. This area contains Gangotri glacier which is the largest of glaciers located within Garhwal as displayed in Figure 2.2, adapted from a map created by Sharma and Owen, (1996). Gangotri glacier will be the primary glacier investigated, spanning an elevation of 4000 m to 7000 m and is one of the main sources of the Bhagirathi River.

The total area of different elevation zones for the Bhagirathi basin and their individual percentage of total basin area are illustrated in Figure 2.3 created by Singh *et al.*, (2008). In 1999 Bhagirathi basin contained around 238 glaciers covering nearly 12% of the basins total area, with the Bhagirathi River flowing from this valley being one of the main tributaries to the Ganga (Dobhal and Mehta, 2010). Gangotri glacier itself is a product of a number of joining glaciers including Swachand, Maiandi, Ghanohim and Kirti glaciers, with Chaturangi glacier (Figure 2.2) also joining until 1971, before retreating 100 m (Vohra, 1988).
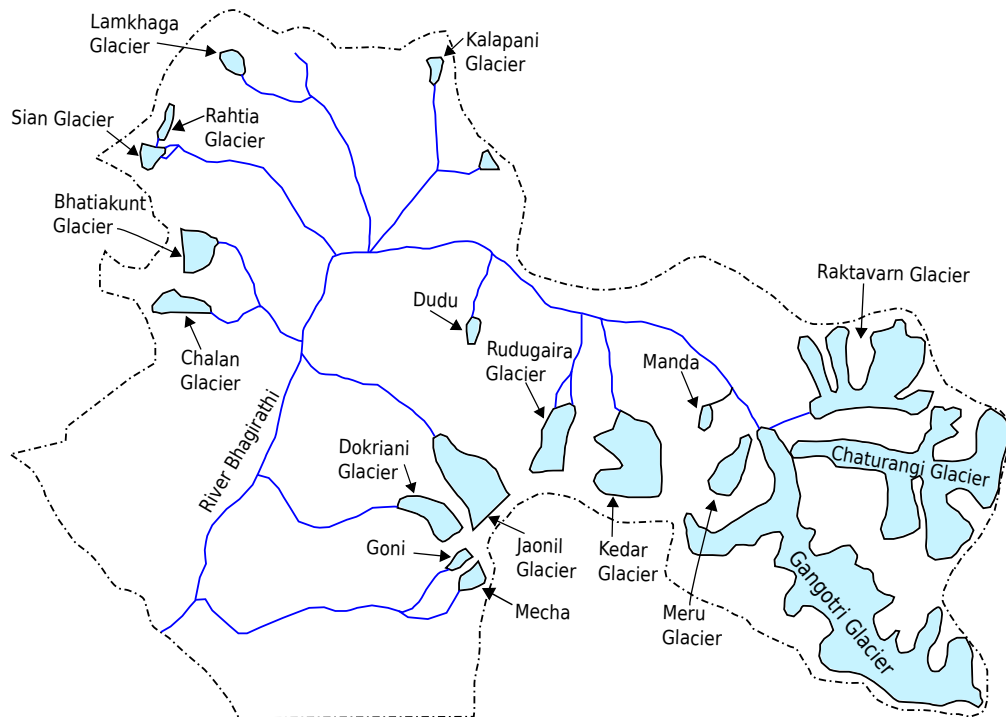
Figure 2.2: The North West Garhwal Himalaya displaying glaciers and rivers within Bhagirathi basin (Adapted from Sharma and Owen, (1996)).
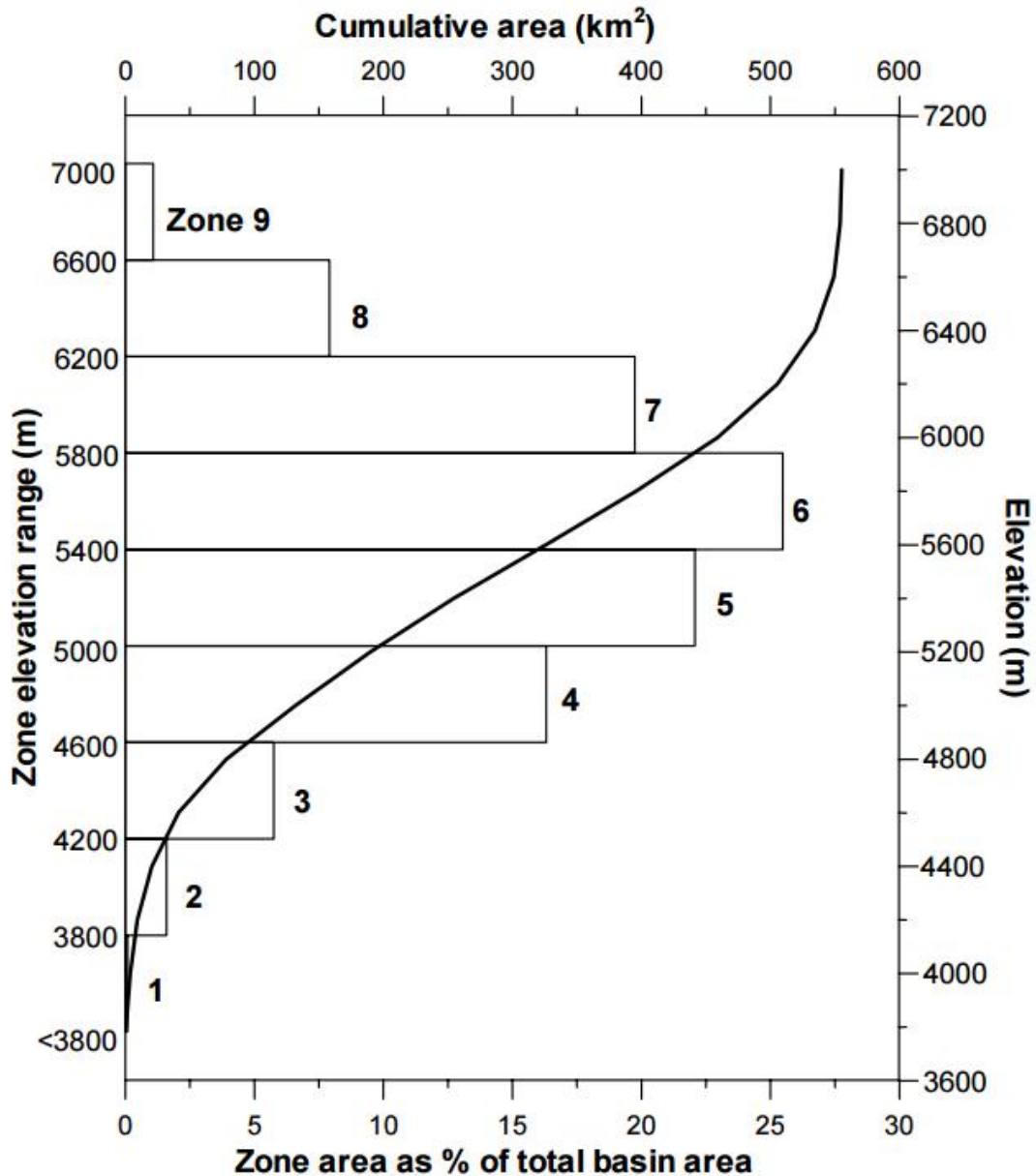
Figure 2.3: Elevation zones as a percentage of the Bhagirathi basin and an area-elevation curve (Singh *et al.*, 2008).

In terms of geomorphology, the Bhagirathi basin is located within an active and relatively young tectonic mountain range. Bhagirathi basin has steep sides extending down to the Bhagirathi River, which flows east-northeast to west-southwest through a V-shaped valley (Mathew *et al.*, 2007). The region in

which Bhagirathi basin lies is still seismically active and continues to experience rapid uplift exposing augen gneiss, quartzites, phylites and granites. A combination of fluvial incision, heavy monsoonal rainfall and earthquakes also mean that mass movements such as landslides are relatively common (Barnard *et al.*, 2004).

A recent example of a mass movement event that occurred in Bhagirathi basin was investigated by Haritashya *et al.*, (2006) who studied hydro-meteorological conditions of a storm that occurred in June 2000, causing unusually high levels of precipitation on the upper region of the river. The storm induced a number of rockslides/landslides between the snout of Gangotri glacier and Gangotri town causing damage such as that displayed in Figure 2.4.

Figure 2.4: Damage sustained by a major rockslide affecting Gangotri town. (Haritashya *et al.*, 2006).

In addition to causing damage to the town, a rockslide blocked the Bhagirathi River 3 km downstream of the Gangotri glacier initiating the creation of a temporary artificial lake. The artificial lake later burst temporarily causing a

sudden high river flow downstream peaking at $124\,\mathrm{m}^3\,\mathrm{s}^{-1}$. This resulted in a rise of the river bed of around 3 m and a change in the rivers course (Haritashya *et al.*, 2006).

The valley containing Gangotri Glacier is a U-shaped valley, which is around $1.5\,\mathrm{km}$ wide where the glacial snout lies. Downstream of the glacial snout the valley is marked by a number of debris cones, out-wash plains and recessional moraines formed by previous glacial extent. The Bhagirathi River has incised a V-shaped valley into the bottom of the U-shaped valley, as displayed in Figure 2.5 due to its high velocity caused by a steep gradient. The geographical location within the Gangotri valley of each cross section are further illustrated in Figure 2.6.

The fast flowing nature of the Bhagirathi River provides high sediment transport capacity during peak flow, carrying sediments associated with glacial erosion. Where the river experiences low gradients in wide areas of the valley there is much deposition of glacial outwash, creating multiple channels of a braided pattern (Bali *et al.*, 2003).
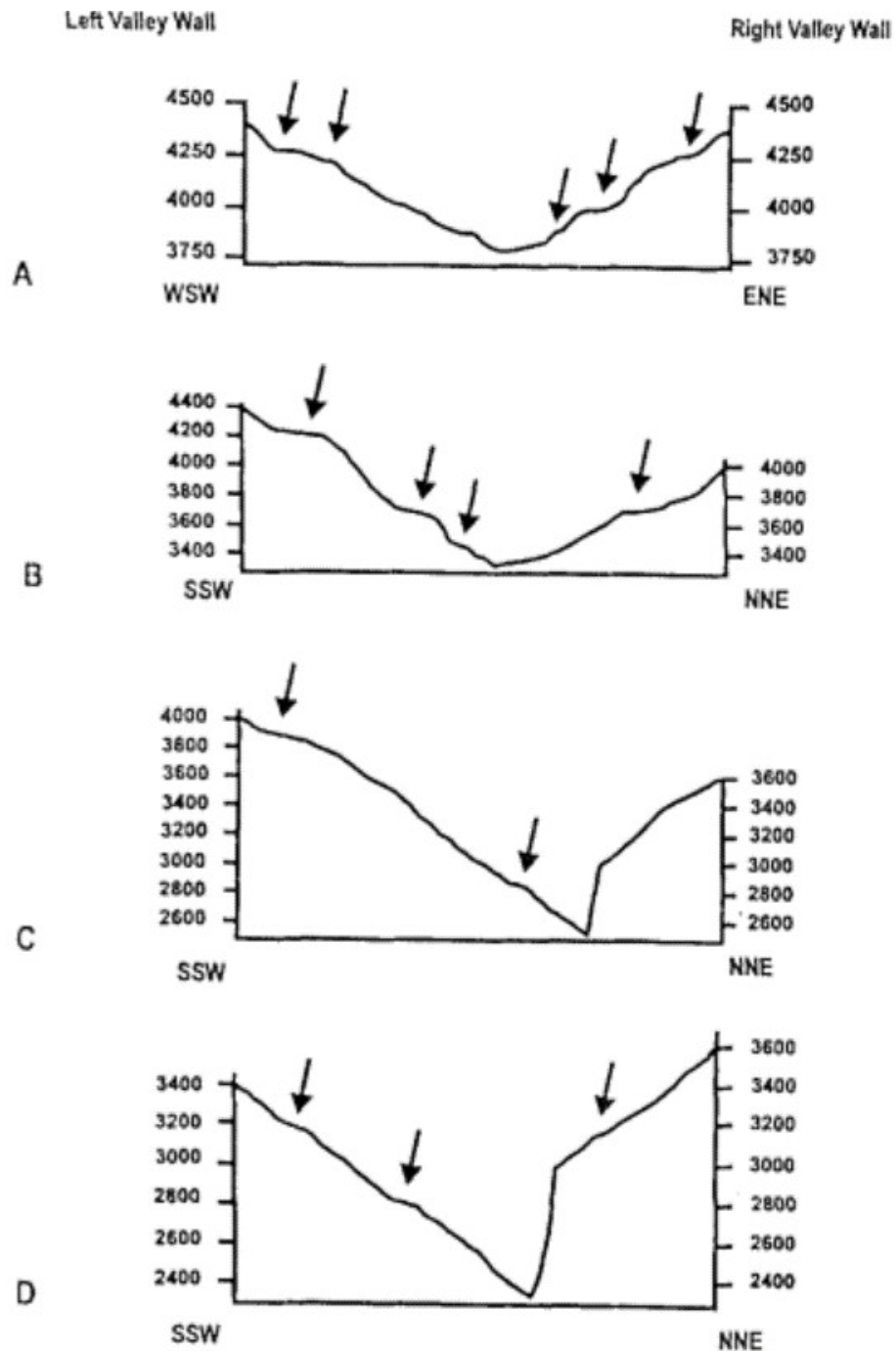
Figure 2.5: Cross sectional profile of Gangotri valley at varying distances from the glacial snout (A. 2 km, B. 15 km, C. 23 km, D. 25 km), with glacially eroded terraces marked by arrows (Bali *et al.*, 2003).
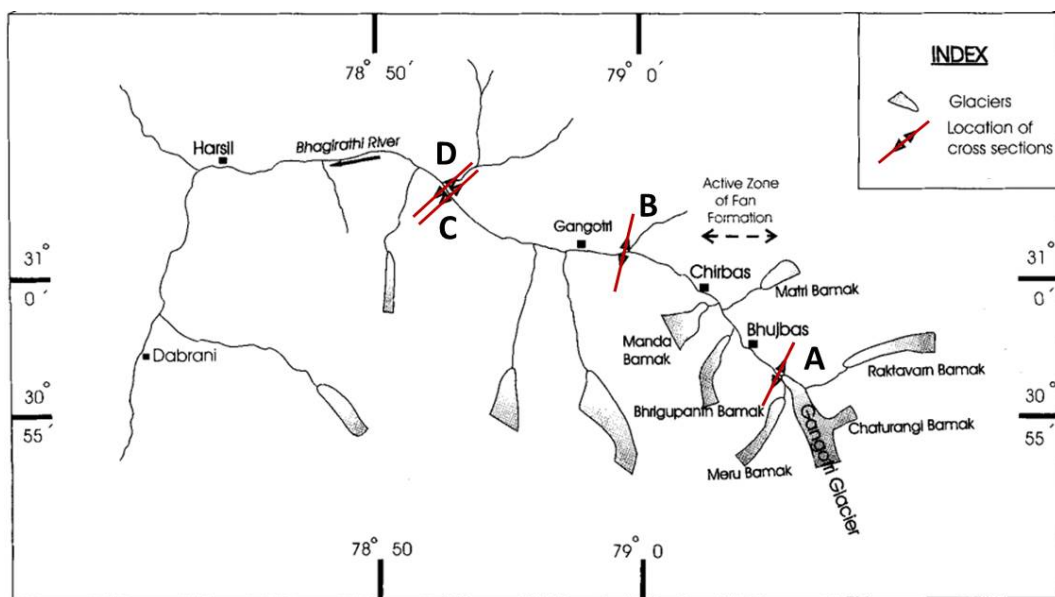
Figure 2.6: Plan view of Gangotri valley including locations of each cross section illustrated in Figure 2.5 (Bali *et al.*, 2003).

Chapter 3

Background

Gangotri glacier and wider Himalaya have been the subject of investigation by many researchers for a number of years regarding glacial retreat and discharge from glacierised basins, such as that containing Gangotri glacier. Such research is of particular importance for planning and management of water resources and also the design and operation of engineering projects including hydropower (Singh *et al.*, 2005a). Alford and Armstrong, (2010) state that as a result of retreat; Ganga, Brahmaptra and other rivers located in North India could become more seasonal rivers in future, with decline of glaciers in the Himalayas. This suggests that research of streamflow from glacier fed rivers will become of increasing importance as glaciers decline, building upon those already conducted.

3.1 The 0°C isotherm and summer snowfall

Elevation of the 0 °C isotherm is of great importance to glaciers around the world, but is an area which has experienced little research focusing particularly on high mountain glaciers, especially within the Himalayas. This is due to a lack of high elevation weather stations which can only partly be substituted by remote sensing (Bolch *et al.*, 2012). Diaz *et al.*, (2003) defines the 0 °C

isotherm or 'freezing level' as "The elevation above sea level at which the air temperature is close to 0 °C". Elevation of the 0 °C isotherm determines whether precipitation falls as rain or snow, effectively splitting basins into two zones whereby precipitation which falls below the 0 °C isotherm falls as rain and above falls as snow, evident in Figure 3.1 (Collins, 1998b).

Glaciers that encounter heavy monsoonal rainfall during summer are often summer accumulation type and changes in air temperature at high altitude in these regions may alter their accumulation pattern (Higuchi and Ohata, 1996). Figure 3.1 displays how changes in elevation of the 0 °C isotherm determines areas within a glacierised basin which receive rain or snow, and also displays how movement of the transient snow line effects the percentage of snow covered and snow free areas.
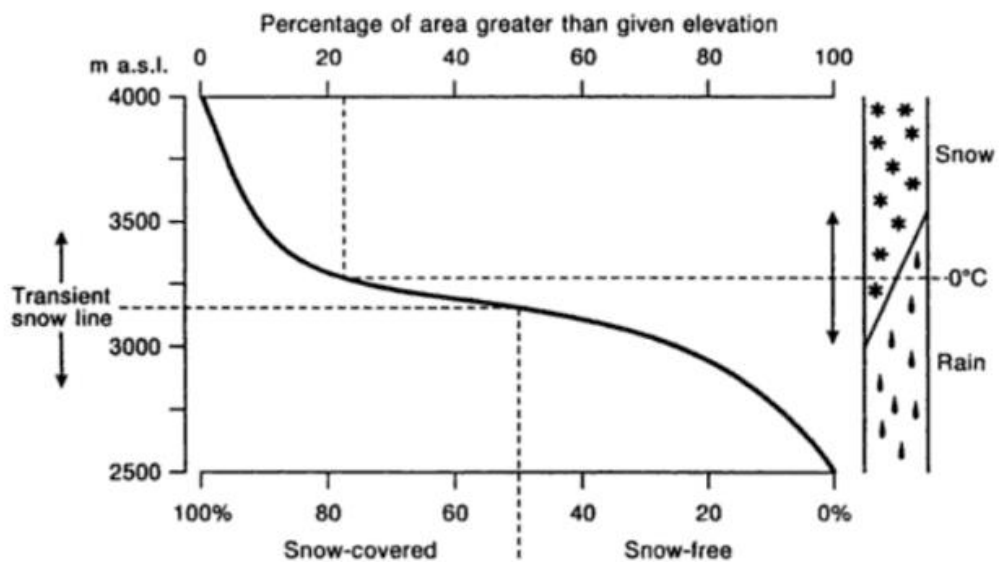
Figure 3.1: How vertical movements of the 0 °C isotherm partitions differing areas of a basin into parts which precipitation falls as rain or snow, and how movement of the transient snow line influences the snow covered and snow free areas of a basin (Collins, 1998b).

A study conducted by Zhang *et al.*, (2010) investigated response of runoff to movement of the summer 0 °C isotherm over the Xinjang region. It was found that there was a strong positive relationship between 0 °C isotherm height

and runoff, as displayed in Figure 3.2. This indicates that as elevation of the 0 °C isotherm increases, as do measurements of runoff and vice versa. This is because as the height of the 0 °C isotherm increases, it is usually followed by a glaciers equilibrium line creating a larger ablation area and therefore more runoff during summer. The regression coefficient between variables is also high at 0.74, indicating that 74% of the runoff value can be explained by height of the 0 °C isotherm.
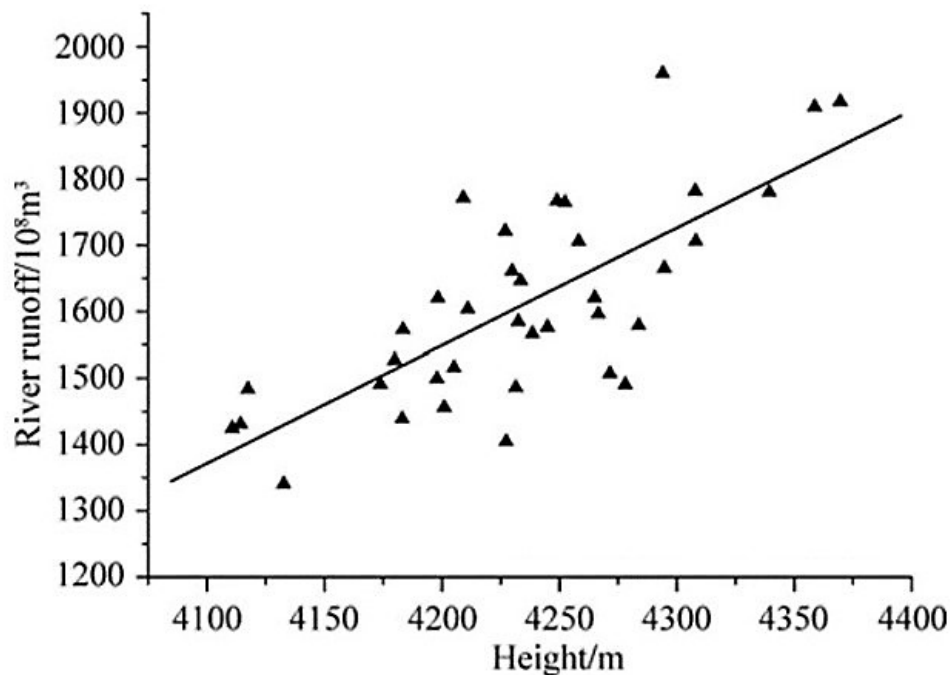
Figure 3.2: Linear regression displaying the relationship between 0 °C isotherm height and runoff from Xinjang (Zhang *et al.*, 2010).

Wang *et al.*, (2014) investigated freezing level heights in High Asia utilising NCEP/NCAR reanalysis and its effects on glacier changes. Figure 3.3 displays the findings of Wang *et al.*, (2014) in terms of relationship between freezing level height and mass balance for a large number of glaciers.

All glaciers investigated in Figure 3.3 encounter a negative relationship of differing severities between mass balance and freezing level heights. Glaciers which show the most severe negative relationships are Urumqi No.1 and Shum-

skiy (Figure 3.3d & 3.3e). Whereby as atmospheric freezing level height increases, mass balance of each glacier steeply decreases. This indicates that as air temperature potentially increases in the future, height of the freezing level will also increase and therefore decrease the mass balance of a number of glaciers, causing shrinkage. This is evident in areas such as Eastern Tianshan, Altai and Qilian Mountains which are all areas that have experienced largely increasing trends of freezing level heights (Wang *et al.*, 2014).

Moreover, a study conducted by Zhang and Guo, (2011), using atmospheric air temperature gathered from the Chinese radiosonde network, found upward trends for the freezing level height between 1958 and 2005 which appeared to be consistent with retreat of the High Asian cryosphere. Figure 3.4 published by Zhang and Guo, (2011) shows that equilibrium line altitude for Ürümqi glacier follows patterns displayed by freezing level height, indicating a strong relationship between the two.
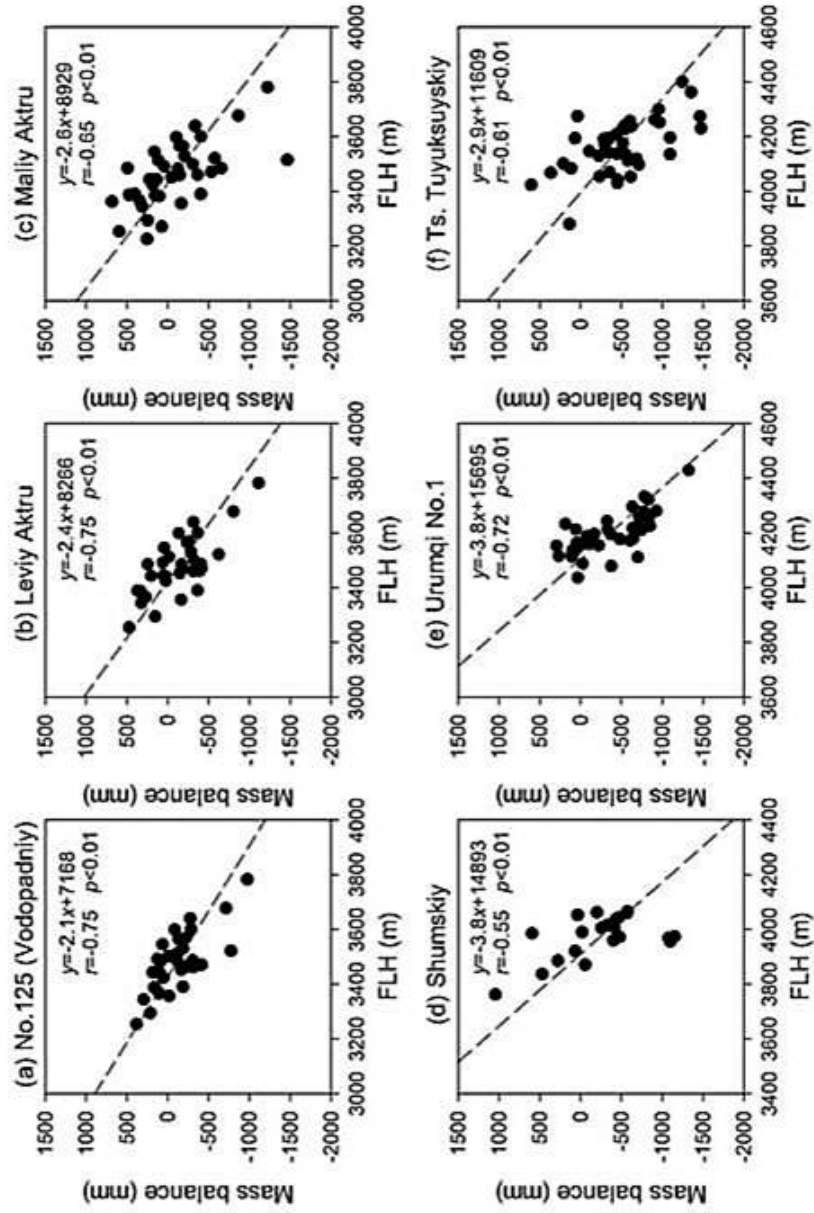
Figure 3.3: Linear relationship between freezing level heights and mass balance for a number of glaciers located in High Asia (Wang *et al.*, 2014).(**Continued...**)
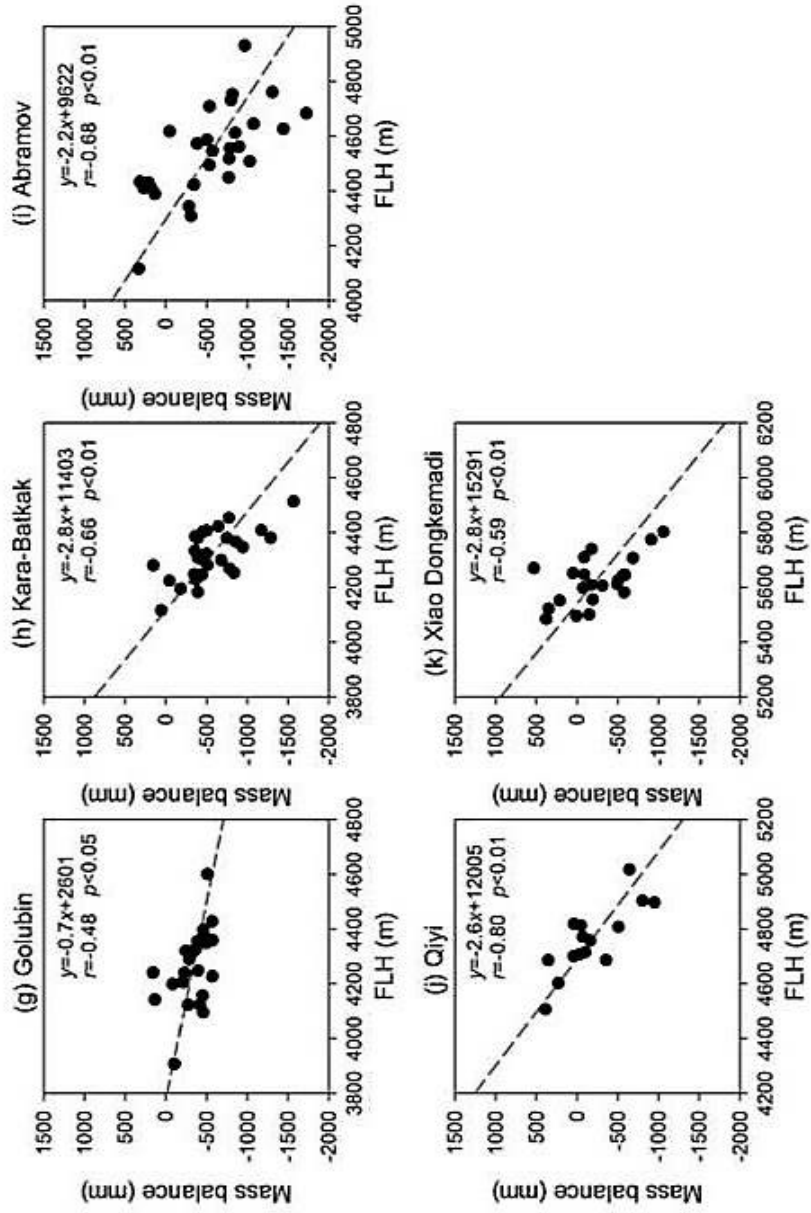
Figure 3.3: Linear relationship between freezing level heights and mass balance for a number of glaciers located in High Asia (Wang *et al.*, 2014).(**Concluded.**)
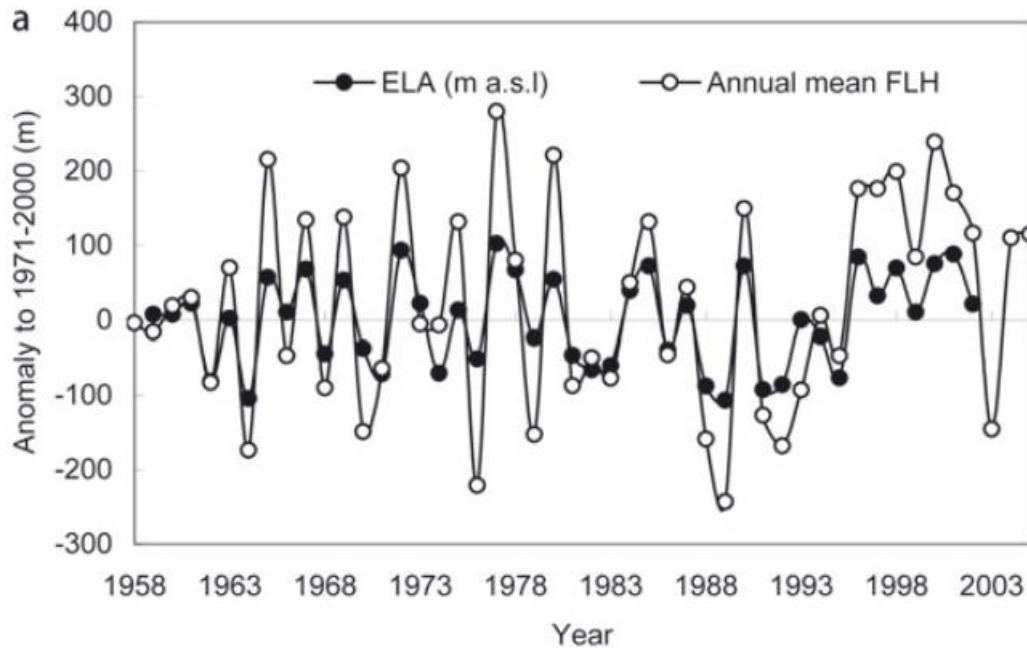
Figure 3.4: Changes in equilibrium line altitude (ELA) and freezing level height (FLH) between 1958 and 2003 for Ürümqi glacier (Zhang and Guo, 2011).

The primary source of heat for glacial melt is derived from incoming shortwave solar radiation. Surface albedo of a glacier essentially determines how much shortwave solar radiation is absorbed and how much is reflected, measured on a scale from 0 - 1. Ice surface albedo ranges from around 0.4 - 0.6, whereas the surface albedo of fresh snow is around 0.9. This difference in surface albedo has a large influence on the volume of runoff produced and also effects glacial mass balance. On June 21 when solar radiation reaches its maximum, much snow cover gathered from the previous winter will still be present resulting in much of the incoming solar radiation being reflected. As the transient snowline retreats exposing large areas of bare ice, the surface albedo of the glacier will reduce causing an increase in melt rate and therefore runoff. Additionally, if altitude of the freezing level is low during a large summer precipitation event it can cause snow to fall on exposed glacial ice as opposed to rain. The addition of fresh snow may temporarily raise the albedo of the glacial surface and offset discharge despite large amounts of solar radiation (Collins, 1998a).

This is demonstrated in a study conducted by Oerlemans and Klok, (2004), who investigated the effect of summer snowfall on glacier mass balance for Morteratschgletscher, Switzerland with their findings displayed in Figure 3.5.
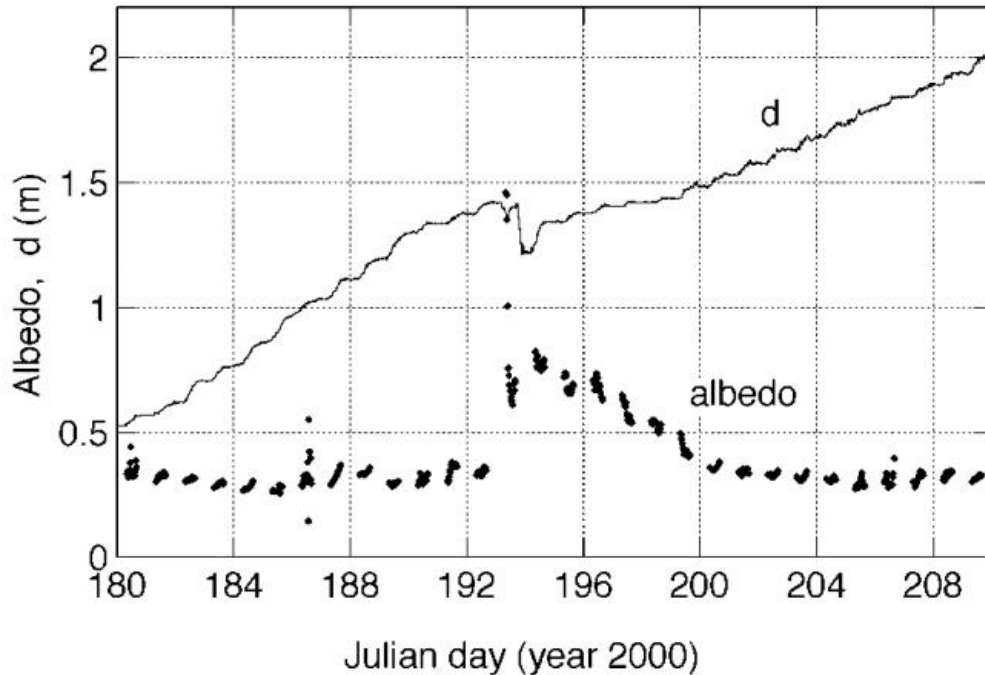
Figure 3.5: Distance to the surface (d) and surface albedo for the Morteratschgletscher between Julian days 180 (June 28) and 210 (July 28) for the year 2000 (Oerlemans and Klok, 2004).

Results displayed in Figure 3.5 demonstrate distance to surface of the glacier measured using a sonic ranger and surface albedo (half hourly between 0800-1600), with measurements taken between Julian days 180 (June 28) and 210 (July 28) during 2000. The snowfall event occurs on Julian day 192 (July 10) shown by distance to surface of the glacier decreasing indicating build up of a snowpack. Corresponding with build up of the snowpack, albedo of ice in the study area increases from 0.3 to around 0.75. Low albedo of fresh snow can be explained by melting beginning almost immediately slightly lowering its albedo, but still protects underlying glacial ice (Oerlemans and Klok, 2004). Oerlemans and Klok, (2004) concluded that heavy summer snowfall events have a large impact on glaciers such as those located in Switzerland, by

reducing the amount of absorbed radiation and simultaneously adding mass.

A study regarding the role of snow-albedo feedback and warming of high elevation Himalayas was conducted by Ghatak *et al.*, (2014). Using Community Climate System Model version 4 and Geophysical fluid Dynamics Laboratory model, Ghatak *et al.*, (2014) found that surface albedo decreases more at higher elevations than lower elevations due to retreat of the 0 ° isotherm and snow line. Decrease in surface albedo and consequential increase in absorbed solar radiation causes an increased loss of snowpack, triggering warming over Central Asian mountains, Himalayas and Karakoram. A study conducted by Fujita, (2008) investigated influence of precipitation seasonality on mass balance, also concluded that decreased summer snowfall on glaciers would cause accelerated melting through a lowering of surface albedo.

3.2 Retreat of the Gangotri glacier and other Himalayan glaciers

According to Jain, (2008) Gangotri glacier has only experienced 18 km of retreat over a period of around 4000 years, when the snout of Gangotri glacier was positioned at Gangotri temple. Gangotri glacier advanced during the little ice age between the 16th and 18th centuries, but has experienced rates of recession between 22 m and 27 m per year over the past few decades. Jain, (2008) also studied the effect that retreat of Gangotri glacier would have on the Ganga. It was found that although Gangotri glacier had retreated around 22-27 m per year, there was no profound effect on flow of the Ganga and may have little effect as it continues to retreat in the future, as beyond the nearby Haridwar its sole influence on the Ganga dwindles to less than 4%.

Retreat of Gangotri glacier was also investigated by Kumar *et al.*, (2007) using rapid static and kinematic GPS survey. Using the GPS in rapid static mode revealed Gangotri glacier had experienced differing rates of retreat between 1935 and 2004, with total retreat during this period being 1519.13 m as dis-

played in Table 3.1. Table 3.1 also shows that rate of retreat declined to 17.15 ma^{-1} between 1971 to 2004 as opposed to 26.50 ma^{-1} recorded between 1935 and 1971.

Table 3.1: Total recession and rate of retreat for Gangotri glacier between 1935 and 2004 (Kumar *et al.*, 2007).

Duration (yrs)	Total recession (m)	Period (yrs)	Rate (ma^{-1})
1935–71	954.14	36	26.50
1971–2004	564.99	33	17.15

Gangotri glacier was further investigated by Negi *et al.*, (2012) who monitored the glacier using remote sensing and ground observations. It was found that prevailing wet snow conditions have caused slope scouring leading to soil and debris deposition onto the surface of Gangotri glacier. This debris cover is said to be one of the main factors causing fast melting of the glacier and appears to be impacting the glaciers health in an influential manner, finding overall glacial area loss to be 6%. Figure 3.6 displays boundaries of the Gangotri glacier for 1962 and 2006. It is evident that the glacier has experienced retreat, concentrated around its snout and trunk particularly on the eastern area.
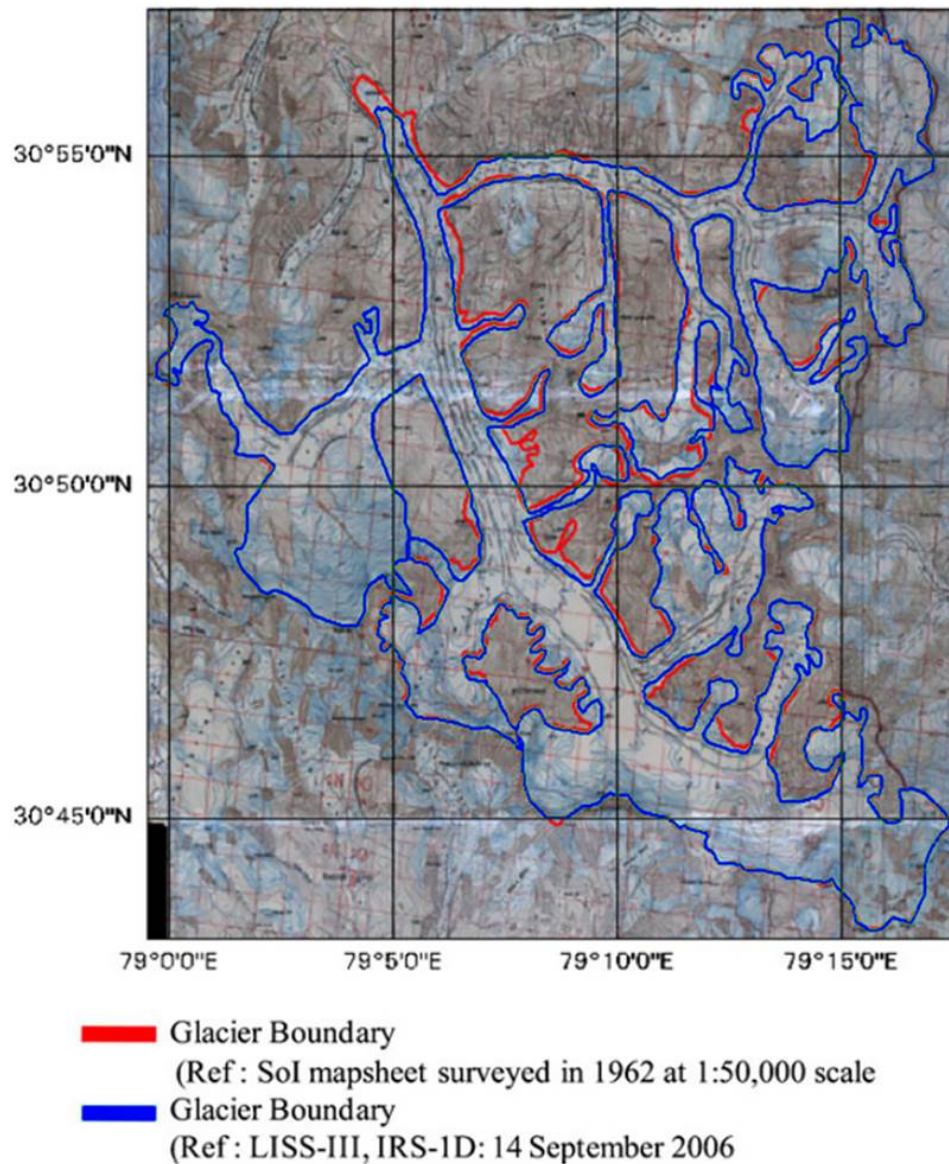
Figure 3.6: Glacier boundaries of the Gangotri glacier for 1962 and 2006 (Negi *et al.*, 2012).

An investigation conducted by Bhambri and Bolch, (2009) mapping glaciers in the Indian Himalayas produced a graph displaying cumulative length changes of Indian Himalayan glaciers including Gangotri glacier as displayed in Figure 3.7.

26
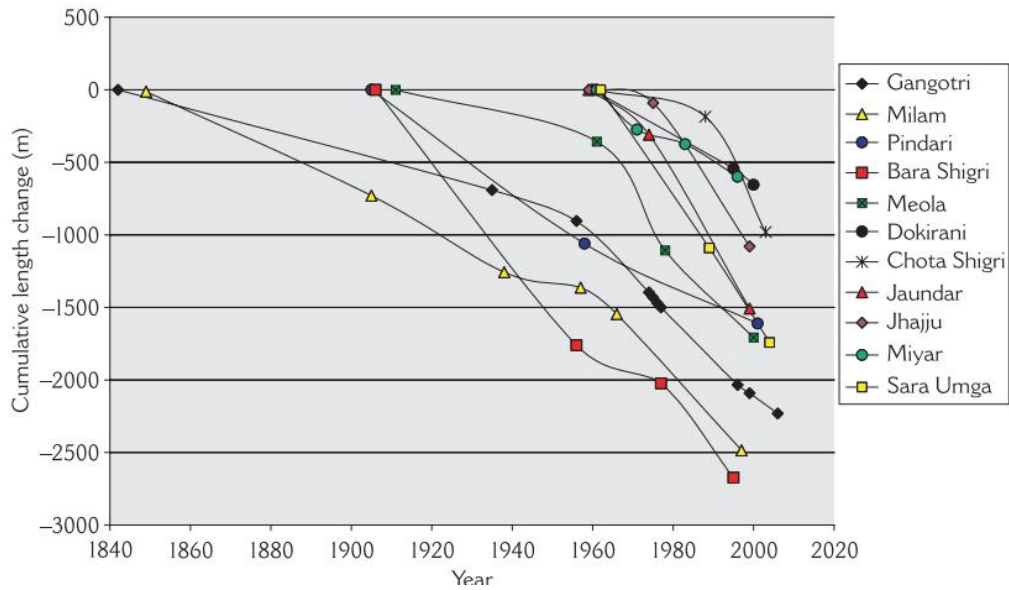
Figure 3.7: Cumulative length changes of selected glaciers located within the Indian Himalaya (Bhambri and Bolch, 2009).

Findings of Bhambri and Bolch, (2009) within Figure 3.7 indicate that Gangotri glacier declined at a steady rate between years 1840 and 1960. After 1960 Gangotri glacier along with a number of other glaciers begin to experience a rapid shortening of cumulative length, indicating rapid retreat for all glaciers selected. With regards to Gangotri glacier in particular, cumulative length change appears to drop from around $-1000\,\mathrm{m}$ in 1960 to around $-2250\,\mathrm{m}$ in 2009, much steeper than cumulative length change experienced between 1840 and 1960 of around $-900\,\mathrm{m}$ over a longer period of time.

Bhambri *et al.*, (2011) also investigated glacial retreat using remote sensing in the Himalayas but focused on those located within the Garhwal Himalaya, including Gangotri glacier. Figures 3.8 & 3.9 display area changes for Tara Bamak glacier and Gangotri glacier between 1968 and 2006.
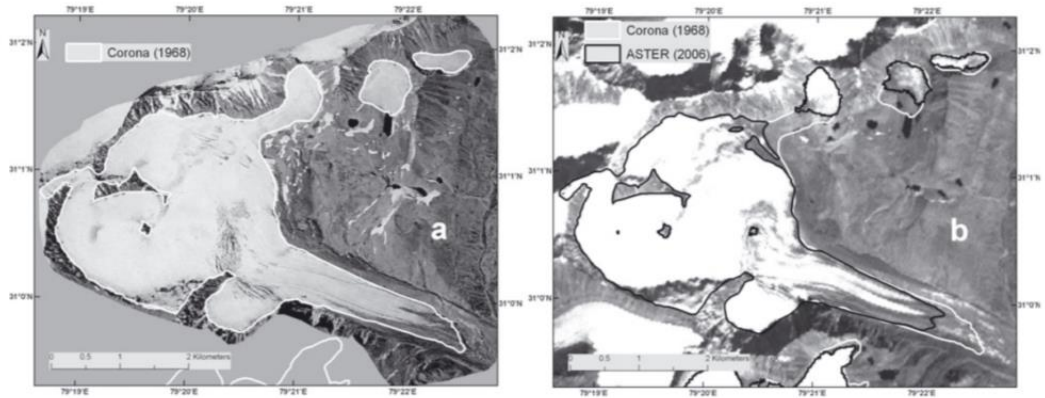
Figure 3.8: Images gathered via remote sensing of Tara Bamak glacier during 1968 (a) and 2006 (b) (Bhambri *et al.*, 2011).
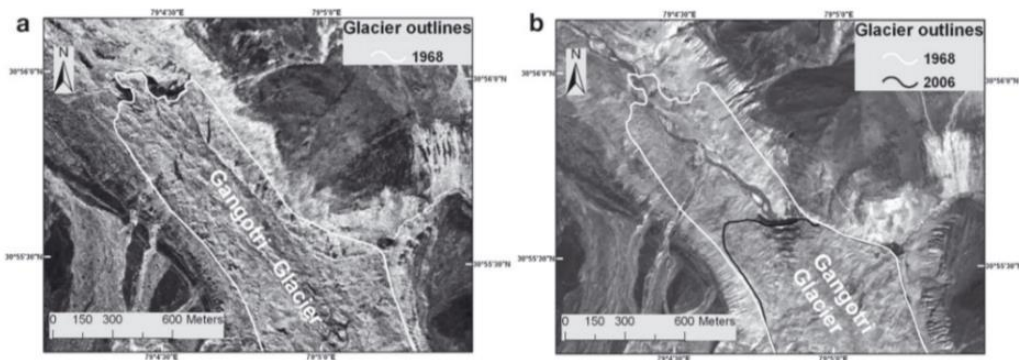
Figure 3.9: Images gathered via remote sensing of the frontal area of Gangotri glacier during 1968 (a) and 2006 (b) (Bhambri *et al.*, 2011).

Results obtained by Bhambri *et al.*, (2011) (Figures 3.8 & 3.9) show large changes in both glaciers between 1968 & 2006. The image of Tara Bamak glacier in Figure 3.8a is a Corona image taken in 1968, the outline of which is laid over an ASTER image taken in 2006 (Figure 3.8b). It is evident that much of retreat suffered by Tara Bamak glacier has not only been effecting the snout, but has also experienced retreat in its north-eastern region by splitting of an ice mass from the main body.

In terms of Gangotri glacier, the 1968 Corona image (Figure 3.9a) and 2006 Cartosat-1 image (Figure 3.9b) focus on the snout. It is clear from Figure 3.9 that the snout of Gangotri glacier has experienced much retreat between 1968 and 2006 with the amount of area lost around $0.38 \, \text{km}^2$. Bhambri *et al.*, (2011) state that the number of glaciers located in Garhwal Himalaya increased from 82 to 88 between 1968 and 2006 due to fragmentation of large glaciers, with recession rates between 1990 and 2006 increasing.

There has also been much research conducted on glacial retreat for many other glaciers located in the Himalayas. Bolch *et al.*, (2012) conducted research regarding the cumulative length changes of a number of Himalayan glaciers, the findings of which displayed in Figure 3.10.
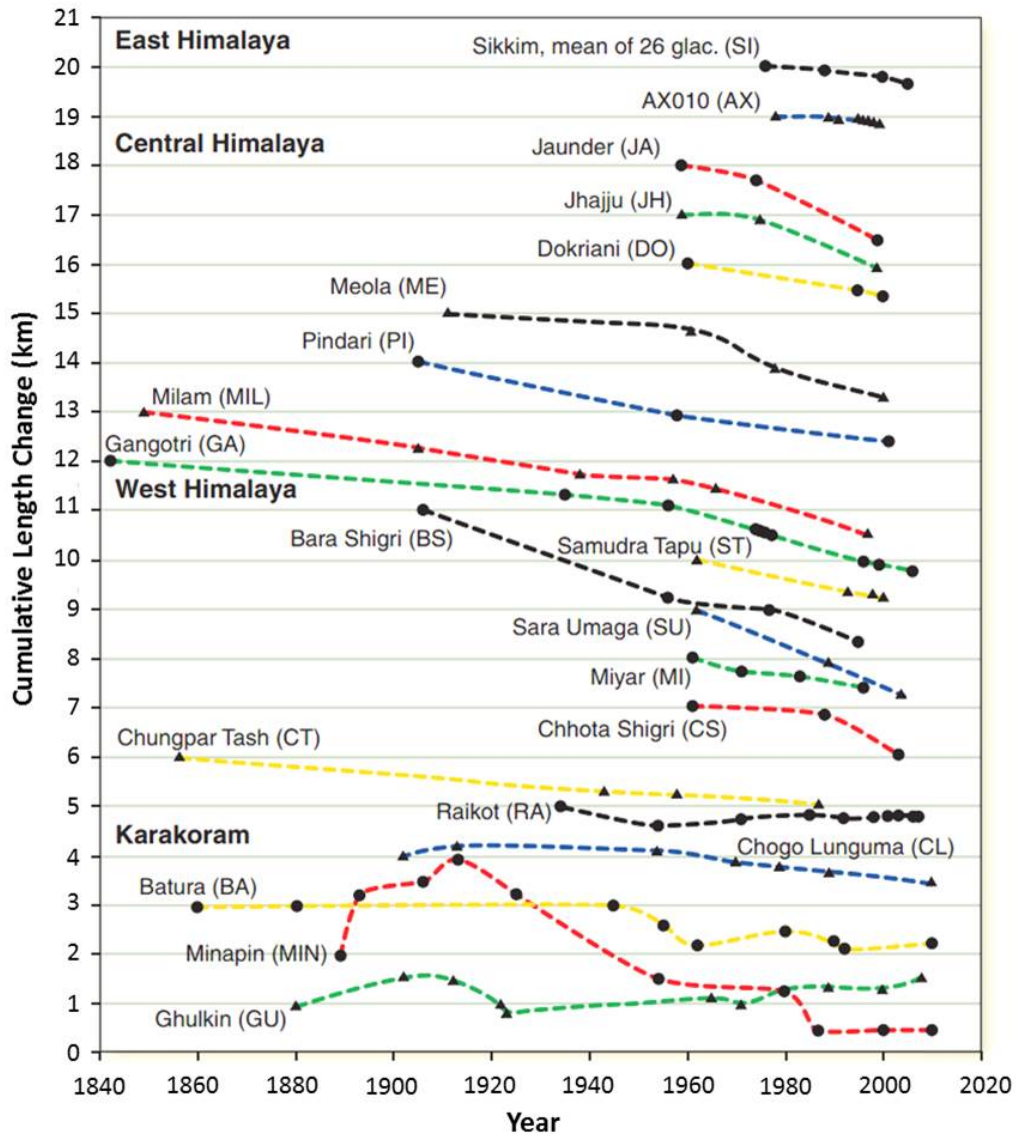
Figure 3.10: Cumulative length changes of glaciers located in the east, central and west Himalaya with the Karakoram region (Bolch *et al.*, 2012).

It is clear from Figure 3.10 that a large majority of glaciers located in the Himalayas are experiencing retreat, especially after the 1970s. All appear to be retreating apart from Batura, Minapin and Ghulkin located in the Karakoram region, which all appear to be in advance or stable. It was also found that 25% of glaciers located within the eastern Hindu Kush region were either advancing

or stable between years 1976 and 2007.

Glacial retreat in the Himalayas was also investigated by Dobhal and Mehta, (2010), who focused on Dokriani glacier using fixed date observations at the end of ablation period each year. It was found that Dokriani glacier has experienced large changes in elevation and surface morphology. Between 1962 and 1991 total retreat of Dokriani glacier was measured at around 480 m meaning the average rate of retreat for this period was 16.5 m/yr. Rate of retreat increased to 17.8 m/yr between 1991 and 2000, but declined to 15.7 m/yr between 2000 and 2007 indicating that the rate of terminus retreat has recently declined (Dobhal and Mehta, 2010).

3.3 Himalayan streamflow

The Indian monsoon also has a large influence on streamflow from glaciers located in eastern and central Himalayas. The findings of Singh *et al.*, (2000) suggested a prominent role of monsoonal rainfall in determining runoff from Dokriani glacier during July and August. Graphs illustrated in Figure 3.11 demonstrate cumulative discharge and rainfall for Dokriani glacier created by Thayyen *et al.*, (2005). The smooth curve of discharge measured throughout the ablation season of each year shows a similar trend to that of rainfall over the same period of time. Although discharge and rainfall show a similar trend, Thayyen *et al.*, (2005) concluded that rise in discharge during the monsoon period is more related to rising summer air temperatures as opposed to increased rainfall contribution.
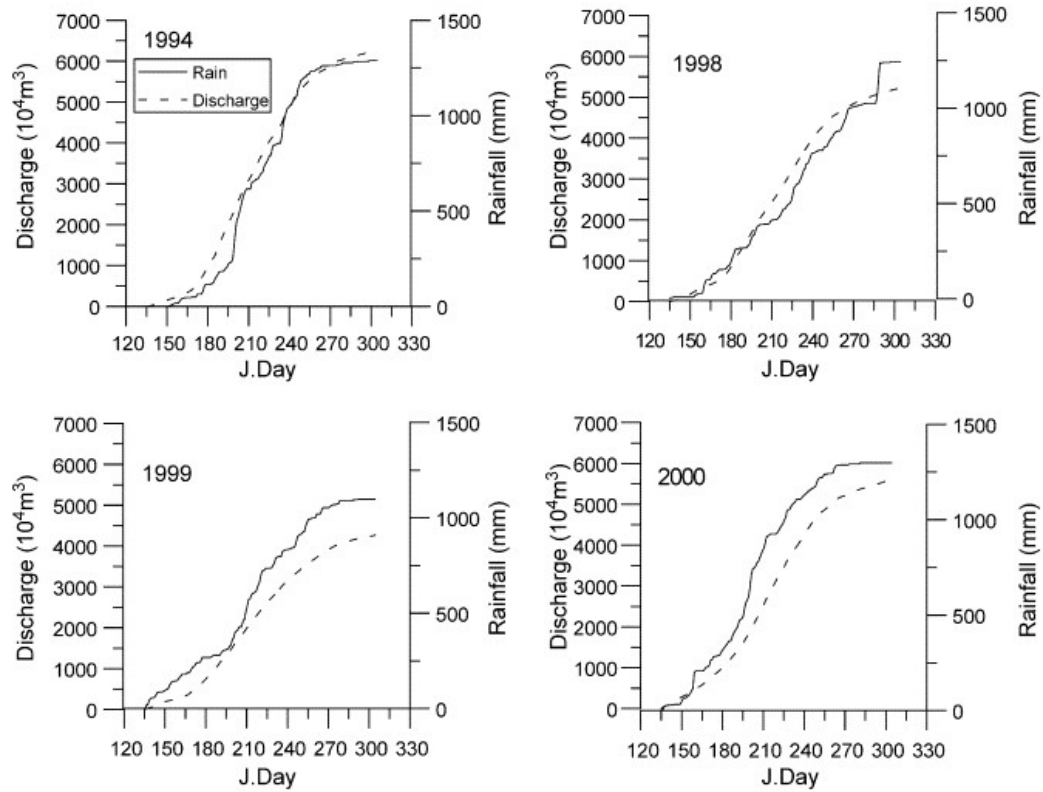
Figure 3.11: Cumulative rainfall and discharge flowing from the Dokriani glacier throughout the ablation season for the years 1994, 1998, 1999 and 2000 (Thayyen *et al.*, 2005).

Seasonal variation of daily total discharge and measured daily total suspended sediment for Batura glacier is illustrated within Figure 3.12, from April to October. It is evident from Figure 3.12 that discharge begins to rise in early May, with the rise of the transient snowline during late June almost doubling discharge before rapidly decreasing after early August. This is caused by movement of the transient snowline which in turn causes the ablation zone of the glacier to grow, creating a marked increase in discharge observed during the summer period as the albedo of snow (0.9) is much higher than that of ice (0.6).
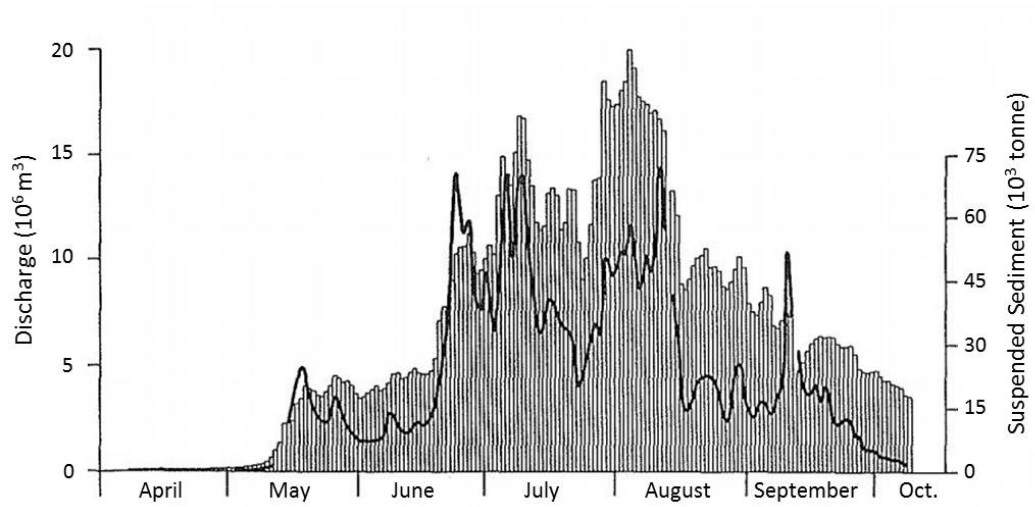
Figure 3.12: Daily total discharge (columns) and measured daily total suspended sediment (line) from the Batura glacier between April & October 1990 (Collins and Hasnain, 1995).

Moreover, Singh *et al.*, (2005a) also investigated variations in discharge and suspended sediment but on a diurnal scale from Gangotri glacier. Measurements for discharge were gathered at a gauging site established at Bhojbasa, around 3 km downstream of the terminus of Gangotri glacier. Figure 3.13 displays diurnal variations of discharge for 2001.
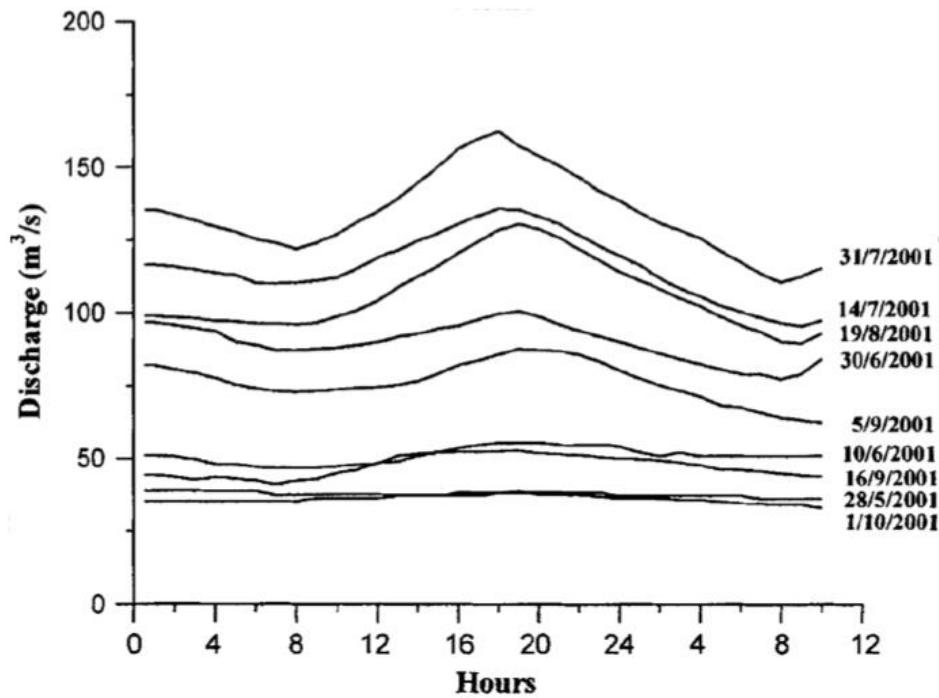
Figure 3.13: Diurnal discharge measured at Bhojbasa for Gangotri glacier, regarding clear days of the ablation period 2001 (Singh *et al.*, 2005a).

Findings of Singh *et al.*, (2005a) displayed in Figure 3.13 show a similar trend to those displayed in Figure 3.12 by Collins and Hasnain, (1995). It is evident in Figure 3.13 that discharge begins to rise in June and achieves its highest level during July, before beginning to decline. Results in Figure 3.13 also indicate that during the first part of the melt season (May-June), discharge is determined by extent of snow cover within the basin and snow depth (Singh *et al.*, 2005a).

Discharge was also investigated by Thayyen and Gergan, (2010) for Dokriani glacier between 1998 and 2004 measured at Tela and Gujjar Hut. As with previous figures, Figure 3.14 shows that discharge flowing from Dokriani glacier also peaks between July and August. It is also displayed in Figure 3.14 that discharge over the summer of 2004 is much less than that recorded for 1998 at both stations, gradually decreasing over the years. It is also evident that

34

discharge from the glacier has begun to decrease over the years, despite percentage contribution from the glacier catchment increasing.
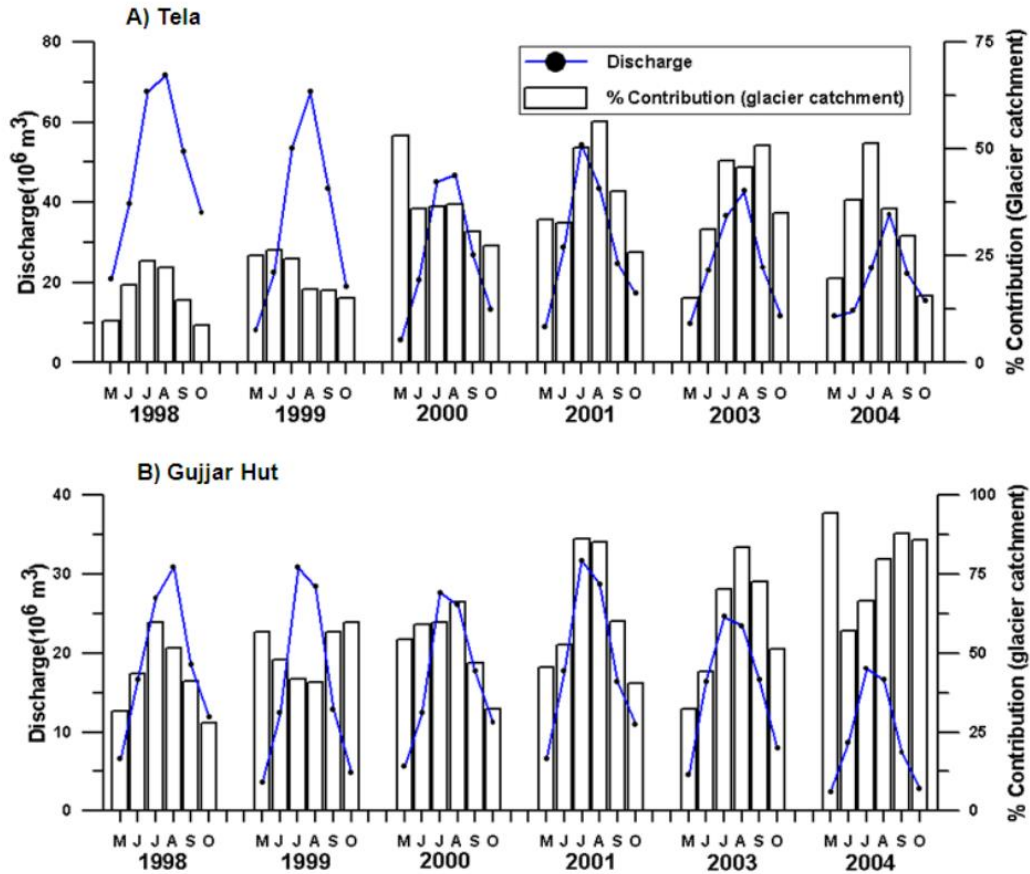
Figure 3.14: Monthly summer variations of discharge at (A) Tela and (B) Gujjar Hut and percentage contribution from the glacier catchment (Thayyen and Gergan, 2010).

An investigation conducted by Arora *et al.*, (2008) uses the SNOWMOD model to research how potential increases in air temperature by $+1\,^\circ$C, $+2\,^\circ$C and $+3\,^\circ$C affect streamflow from Chenab river basin, located in the western Himalayas with an elevation ranging from 305 to 7500 m and a total glacierised area of $2.280\,\mathrm{km}^2$. The results in Figure 3.15 display total streamflow for Chenab River measured at Salal between 1996 and 1999 with a simulated $+2\,^\circ$C scenario for the same period.
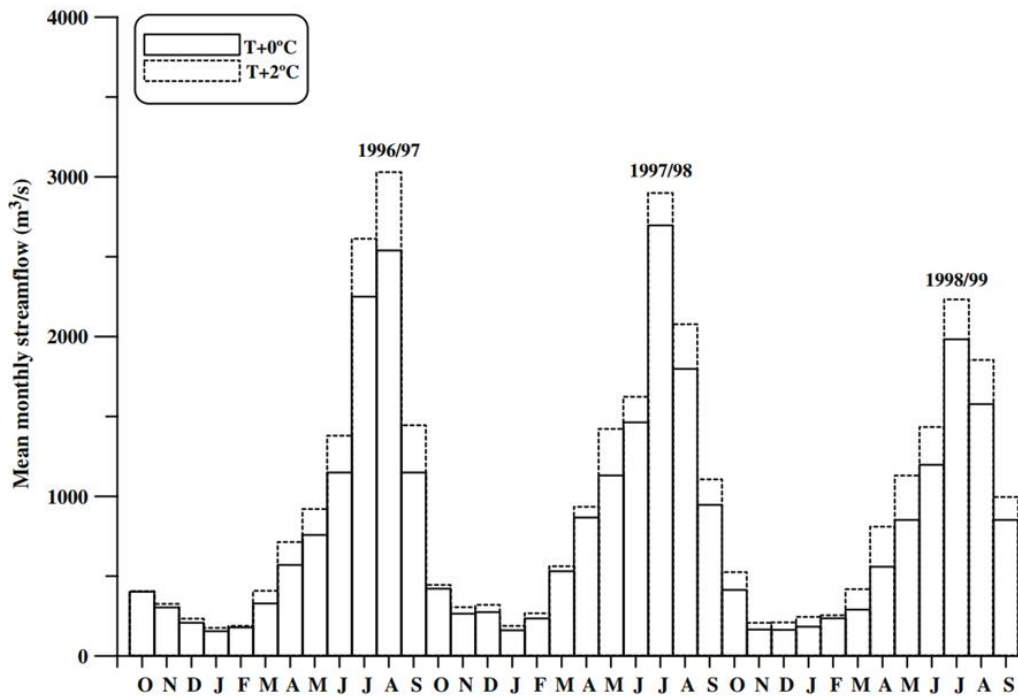
Figure 3.15: Mean monthly streamflow for Chenab River at Salal at current air
temperature and $+2\,^{\circ}$C (Arora *et al.*, 2008).

The findings of Arora *et al.*, (2008) displayed in Figure 3.15 show that with
an air temperature increase of $+2\,^{\circ}$C timing of when peak flow occurs for the
river remains the same around July and August. But their magnitude often
increases with an average increase of 19%, although this is not reflected within
winter streamflow.

Discharge originating from Dunagiri glacier in response to climate was the topic
of research for Srivastava *et al.*, (2014). Dunagiri glacier lies at an altitude of
4200 m and is located within the Garhwal Himalaya of India. The study
focuses on years 1985, 1987, 1988 and 1989 over the ablation season from July
to September utilising daily values of discharge for each year, results of which
are displayed in Figure 3.16.
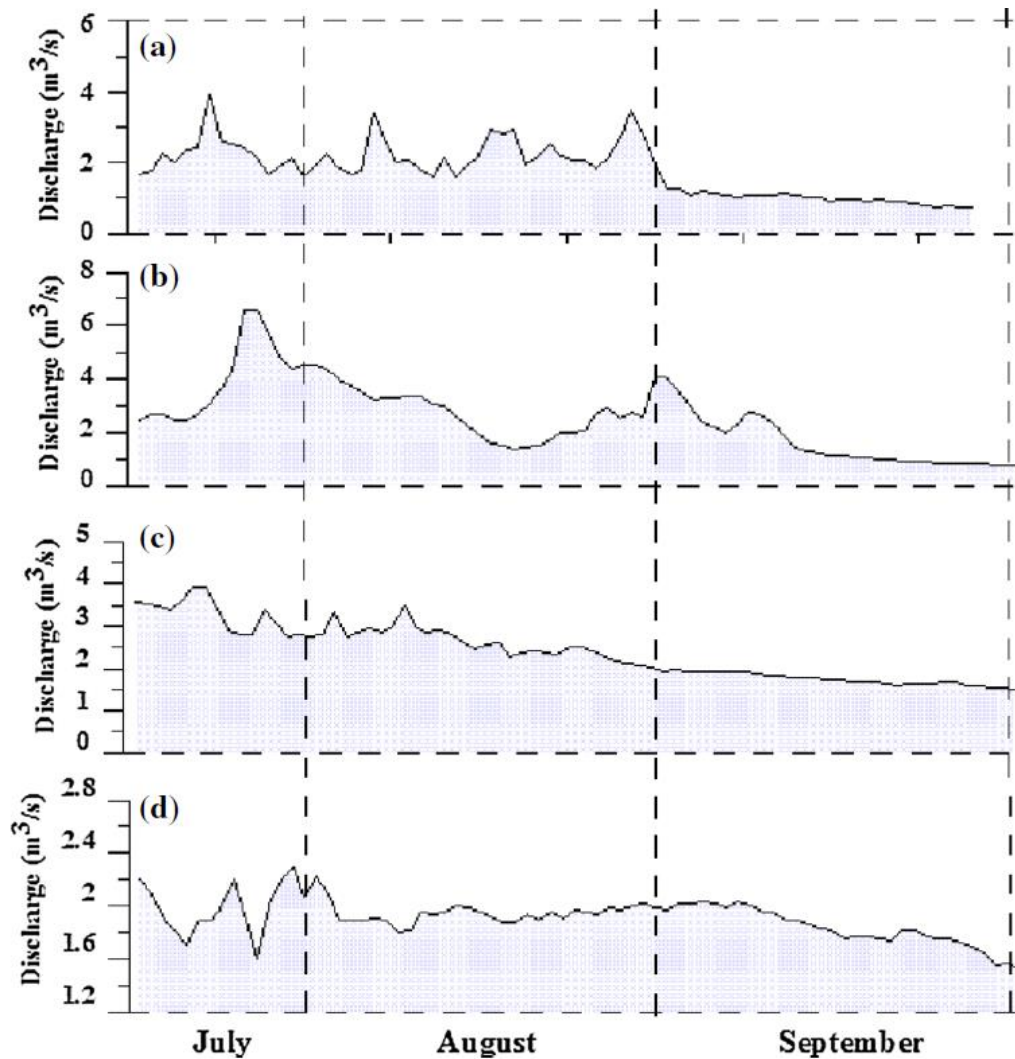
Figure 3.16: Daily discharge from July to August from Dunagiri glacier for 1985 (a), 1987 (b), 1988(c) and 1989 (d) (Srivastava *et al.*, 2014).

Daily discharge displayed in Figure 3.16 shows that the largest peaks in discharge for each year occur within July, with August displaying both increasing and decreasing trends from year to year and September indicating a generally decreasing trend for each year. Srivastava *et al.*, (2014) also found that ablation of Dungiri glacier was exponentially correlated with mean air temperature attaining a strong R^2 value of 0.79, also finding very little correlation between ablation and precipitation.

Chapter 4

Methods

Discharge data were obtained for Gangotri glacier between May & October from 2001 to 2004. Precipitation and air temperature observations for the same period, collected at Bhojbasa were also obtained. In the Indian Himalaya, streamflow and meteorological monitoring sites located at high altitudes nearby to glaciers are rare and most of which do not measure regularly, indicating an inadequate hydrological and meteorological network in this area. This makes acquisition of a long and complete data series on hydrometeorology for the Gangotri glacier and other glaciers difficult with few data sources (Bolch *et al.*, 2012; Chalise *et al.*, 2003; Gurung *et al.*, 2017; Singh *et al.*, 2006b).

4.1 Discharge data

Data gathered by Singh *et al.*, (2006b) for discharge deriving from Gangotri glacier was measured around 3 km downstream of the snout. This area was chosen as it met requirements of being a single channel with low turbulence and was an accessible location. On the bank of the river a stilling well and concrete wall were constructed with an automatic water level recorder placed on the stilling well, in order to monitor changing water levels. A graduated staff gauge

was also installed in order to calibrate the automatic recorder using manual measurements. Discharge was estimated using a velocity-area technique, with surface velocity of discharge measured utilising wooden floats and was found to be between $0.5\,\mathrm{m\,s^{-1}}$ and $4.5\,\mathrm{m\,s^{-1}}$, with mean velocity calculated by reducing surface velocity by 10%. The area of cross section was measured using sounding rods at the beginning and end of the melt season.

A stage-discharge relationship was then created for each year, in order to convert measurements of water levels from the automatic water level recorder into discharges utilising data collected from a range of flow stages. Figure 4.1 displays the stage-discharge relationship created for 2000.
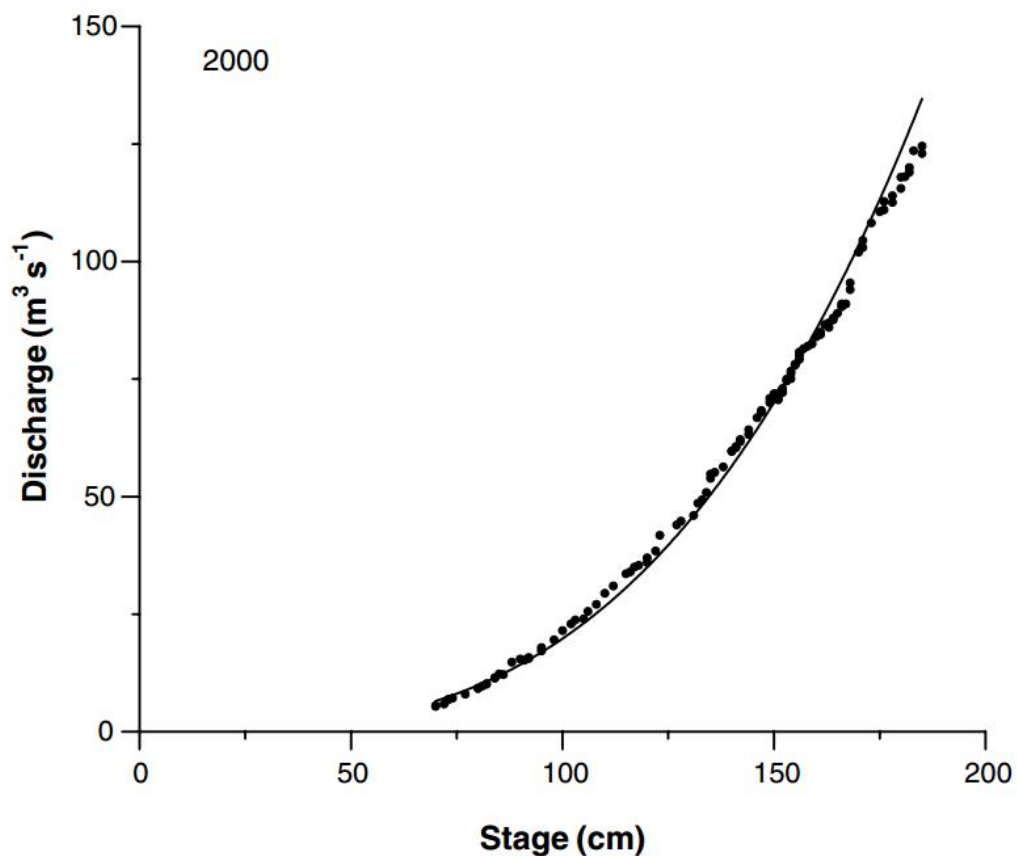
Figure 4.1: Stage-discharge relationship established for the ablation season of 2000, 3 km downstream of the Gangotri glacier (Singh *et al.*, 2006b).

The method of estimating discharge for a river through the velocity-area technique has also been utilised by a number of other studies including those conducted by Chhetri *et al.*, (2016), Hood and Hayashi, (2015), Kumar *et al.*, (2016), and Srivastava *et al.*, (2014).

4.2   Air temperature and precipitation data

Air temperature and precipitation data for Gangotri glacier were collected by Singh *et al.*, (2005b), by establishing a meteorological observatory nearby to the glacier terminus on the valley floor, situated at around 3800 m above sea level. The meteorological observatory used to collect relevant data was equipped with a range of equipment including maximum and minimum thermometers, anemometer, a self recording rain gauge, an ordinary rain gauge, dry and wet bulb thermometers, evaporimeter, hydrograph, wind vane, a sunshine recorder and anemometer.

Timings for data collection taken by Singh *et al.*, (2005b) were in concordance with practice used by the India Meteorological Department providing daily values for minimum and maximum air temperature and daily total values for precipitation.

4.3   Data analysis

Data for discharge, air temperature and precipitation were collated in order to perform data analysis investigating the 0 °C isotherm, summer snowfall events and the effect these summer snowfall events had on discharge.

Daily average air temperature was first calculated from the maximum and minimum data and was then used to work out daily average elevation of the 0 °C isotherm using a temperature lapse rate. The temperature lapse rate used is derived from a study conducted by Singh *et al.*, (2008), who investigated and estimated different components of streamflow from Gangotri glacier, using

a temperature lapse rate of 0.6 °C/100 m. A number of other studies also found the temperature lapse rate of mountain regions to be between 0.5 and 0.7 °C/100 m including those conducted by de Scally, (1997), Hagemann *et al.*, (2013), Luetschg *et al.*, (2008), Singh and Jain, (2002; 2003), and Six and Vincent, (2014).

Elevation of the 0 °C isotherm was calculated by using an equation based on that utilised by both Singh and Jain, (2003) and Singh *et al.*, (2008) in order to calculate air temperature at specific elevations using only one meteorological observatory, as given below:

$$T_{i,j} = T_{i,base} - \delta(h_j - h_{base}) \tag{4.1}$$

where Singh and Jain, (2003) and Singh *et al.*, (2008) describe components as $T_{i,j}$ being a measure of mean daily temperature on the ith day, in the jth zone measured in (°C); $T_{i,base}$ is daily mean temperature (°C) on the ith day at the meteorological observatory, h_j is hypsometric mean elevation (m) of the zone investigated, h_{base} is elevation of the meteorological observatory (m) and δ is the temperature lapse rate for the area (°C/100 m).

Equation 4.1 was then modified in order to calculate daily average elevation of the 0 °C isotherm within the basin containing Gangotri glacier as given below:

$$E_{iso} = \left(\frac{T_{i,base}}{\delta}\right) + h_{base} \tag{4.2}$$

where E_{iso} is elevation of the 0 °C isotherm; $T_{i,base}$ is mean daily temperature (°C) on the ith day measured at the meteorological observatory, δ is the temperature lapse rate for the area (0.6 °C/100 m) and h_{base} is the elevation of the meteorological observatory.

Once established, Equation 4.2 was then applied to average air temperature for each Julian day available using a temperature lapse rate of 0.6 °C/100 m, for 2001 to 2004 collected by Singh *et al.*, (2005b).

Further to calculating the average elevation of the 0 °C isotherm for each Julian

day, data were then filtered to only show air temperature, precipitation and discharge on Julian days where the 0 °C isotherm was positioned below certain elevations within the basin; including 5500 m, 5000 m and 4500 m. The starting elevation of 5500 m was chosen as this is around the mid point of Gangotri glacier and subsequent filter elevations (5000 m & 4500 m) were chosen to give an insight into how discharge was influenced by summer snowfall covering almost the entire area of the glacier. Equation 4.1 was also used in order to calculate average air temperature for each Julian day at the same elevations used to filter data regarding the elevation of the 0 °C isotherm.

Once the data had been filtered for each elevation, correlation and regression analysis were then performed on the data in order to determine the interaction between summer snowfall events, discharge and elevation of the 0 °C isotherm. Filters were also used to identify individual summer snowfall events, which were isolated and investigated in order to gather a more detailed account of their specific effect on discharge. This was achieved using correlation analysis on three specific periods around selected precipitation events. The first period was before the snowfall event occurred, second was the snowfall event including duration of which the snow cover endured and the third period was immediately following snowpack depletion.

Chapter 5

Results

The following section displays the results and analysis of this investigation including air temperature, precipitation and discharge for the study period, interaction between discharge and precipitation along with air temperature in relation to altitude of the 0 °C isotherm and specific summer snowfall events with the response of discharge.

5.1 Air temperature, precipitation and discharge for the summers of 2001-2004

Discharge, air temperature and precipitation collected by Singh *et al.*, (2006b) and Singh *et al.*, (2005b) for the summers of 2001 to 2004 are displayed in Figures 5.1 to 5.4.

Over the summer of 2001 (Figure 5.1), daily average air temperature displays a generally arcing trend, although greatly fluctuates. The first value occurs on Julian day 121 (May 1) with a temperature of 7.75 °C, which shows a generally rising trend before reaching 14.25 °C on Julian day 188 (July 7) which is also recorded on Julian day 202 (July 21). After the value of 14.25 °C on Julian day 202 (July 21), air temperature then begins to display a downwards trend,

reaching its lowest value of 2.85 °C on Julian day 292 (October 19) after a sharp drop from 8.35 °C on Julian day 283 (October 10). This occurs just before the last value of 5.15 °C on Julian day 293 (October 20). Air temperatures of 14.25 °C recorded on Julian days 188 (July 7) and 202 (July 21), are 0.35 °C (2.52%) higher than any other peak air temperature recorded within the time period. The lowest value of 2.85 °C is 2.25 °C (44.12%) lower than any other period of low air temperature recorded, before a drop in air temperature which occurred on Julian day 283 (October 10). The average air temperature for 2001 was 9.84 °C.

Daily precipitation for 2001 is also illustrated. Although there appear to be a number of summer precipitation events, none of that which occur are of a considerably high magnitude, with average summer precipitation for the year only reaching 2.35 mm. The largest precipitation event recorded occurs on Julian day 136 (May 16) with a value of 10.4 mm, 0.6 mm (6.12%) higher than any other precipitation event recorded for that year. Total precipitation for the summer of 2001 was 131.35 mm.

The trend within daily discharge in Figure 5.1 characterises a sharp increase, peaking on Julian day 203 (July 22) with $176.70 \, \mathrm{m^3 \, s^{-1}}$, rising from the lowest value of $8.50 \, \mathrm{m^3 \, s^{-1}}$ on Julian day 121 (May 1). After two large drops in discharge between the largest peak occurring on Julian day 203 (July 22) and the second peak of $174.00 \, \mathrm{m^3 \, s^{-1}}$ on Julian day 226 (August 14), discharge begins to steadily decline before reaching $20.80 \, \mathrm{m^3 \, s^{-1}}$ on Julian day 293 (October 20). Two peaks occurring on Julian days 203 (July 22) and 226 (August 14) were $32.50 \, \mathrm{m^3 \, s^{-1}}$ (22.54%) and $29.80 \, \mathrm{m^3 \, s^{-1}}$ (20.67%) higher respectively than any other high flow event for discharge recorded. The lowest recorded discharge for 2001 ($8.50 \, \mathrm{m^3 \, s^{-1}}$) occurs on Julian day 121 (May 1) attaining $12.30 \, \mathrm{m^3 \, s^{-1}}$ (59.13%) lower than any other low flow event.
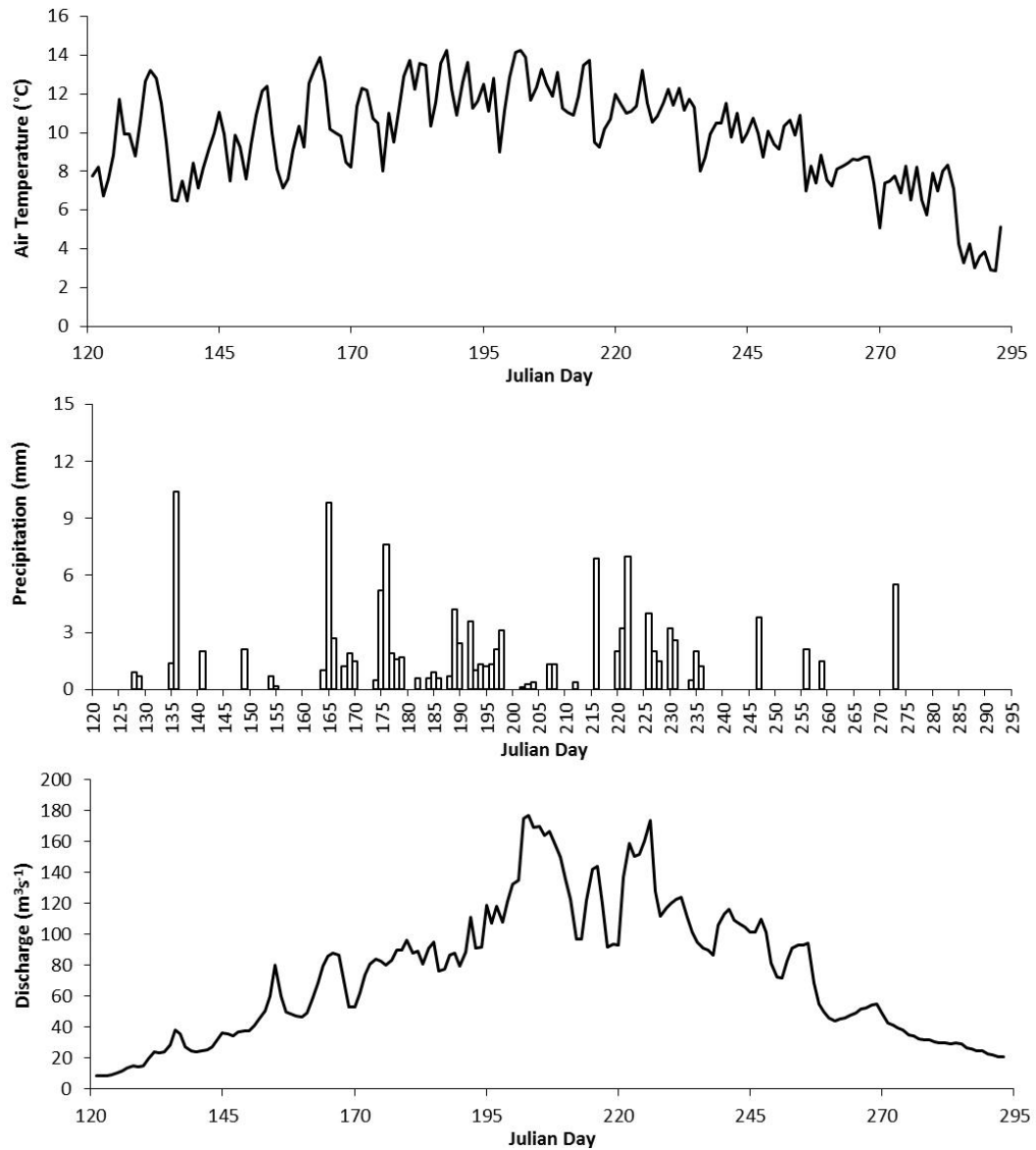
Figure 5.1: Daily average air temperature (°C) at an elevation of 3800 m and daily total precipitation (mm) measured nearby to the snout of Gangotri glacier, with daily average discharge measured 3 km downstream for 2001 between Julian days 121 (May 1) and 293 (October 20).

Similarly to daily average air temperature for 2001, data for 2002 (Figure 5.2) also shows a generally arcing trend, but appears to encounter more extreme temperature variations. The series begins on Julian day 128 (May 8) at 8.45 °C and initially shows a generally rising trend, although displaying large variations in air temperature. Examples of such variation include that recorded for Julian day 141 (May 21), indicating an unusually low value of 4.55 °C and the highest of the series for Julian day 175 (June 24) with 16.00 °C (1.65 °C warmer than any other peak for 2002). After Julian day 198 (July 17) daily average air temperature then begins to show a decreasing trend reaching its lowest point on Julian day 250 (September 7) with an average temperature of 1.75 °C closely followed by Julian day 256 (Septeber 13) with 2.10 °C, only 1.00 °C (36.36%) and 0.65 °C (23.64%) lower than any other low temperature event recorded in the series. The series then ends on Julian day 293 (October 20) with 3.50 °C and an average air temperature for the year of 9.25 °C.

Precipitation recorded for 2002 (Figure 5.2), displays almost entirely different characteristics to that of 2001. Between Julian days 120 (April 30) & 215 (August 3) there only appears to be a small summer precipitation events, highest of which occurring on Julian day 135 (May 15) producing 4.7 mm of precipitation. Between Julian days 216 (August 4) & 257 (September 14) there appears to be a large number of precipitation events, most are high in magnitude. Precipitation appears to build up, starting on Julian day 216 (August 4) with 15.3 mm followed by a series of smaller events before reaching 47.0 mm on Julian day 251 (September 8). This is then followed by the largest precipitation event, occurring on Julian day 256 (September 13) with a value of 72.2 mm, 25.2 mm (53.62%) higher than 47.0 mm recorded previously. After the largest precipitation event, there is then a smaller event on Julian day 257 (September 14) reaching only 3.5 mm and thereafter no more precipitation is recorded. Total precipitation recorded for 2002 is 368.8 mm.
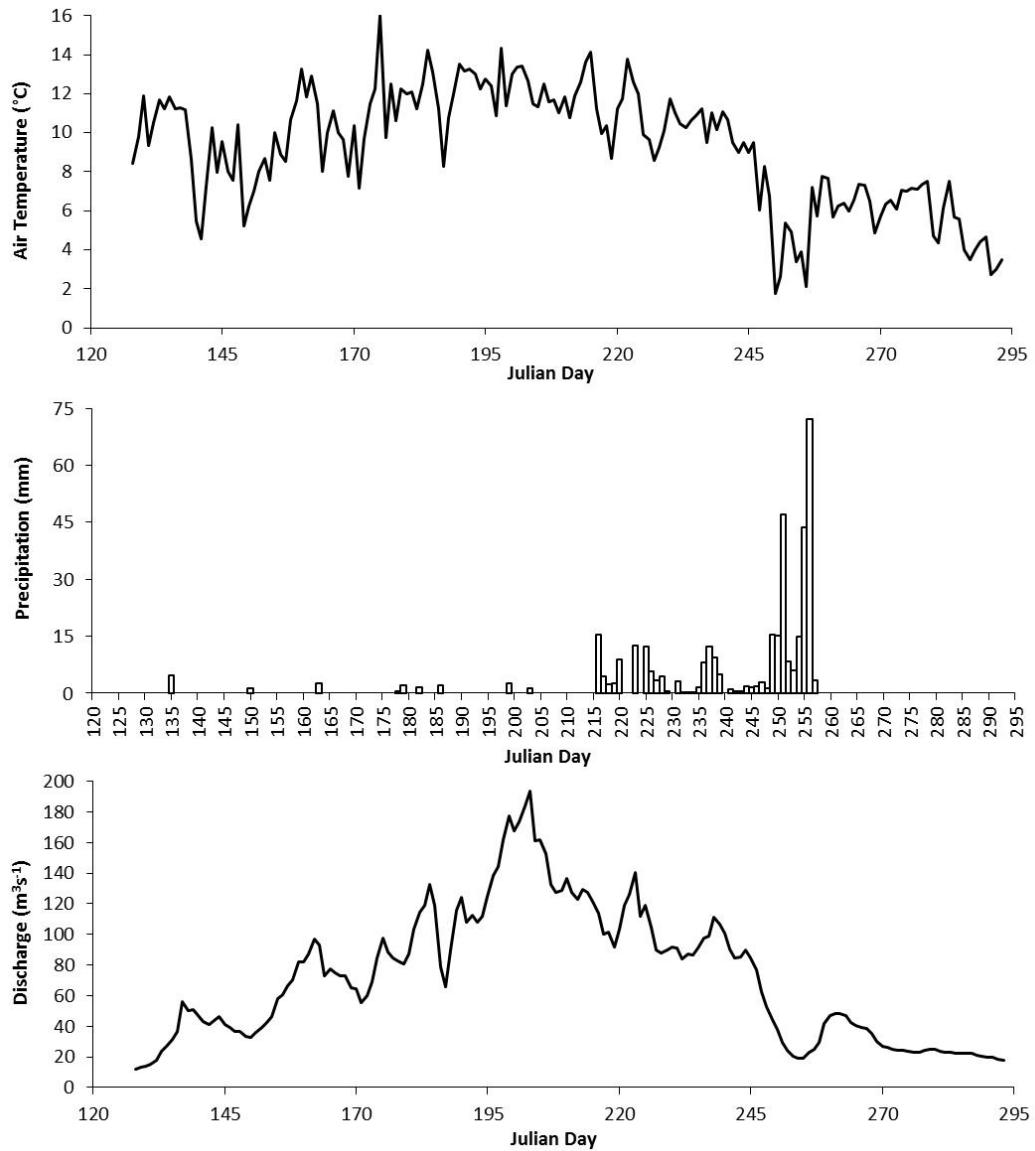
Figure 5.2: Daily median air temperature (°C) at an elevation of 3800 m and daily total precipitation (mm) measured nearby to Gangotri glacier, with daily average discharge measured 3 km downstream for 2002 between Julian days 128 (May 8) and 293 (October 20).

Figure 5.2 displays discharge for 2002, with a similar trend to 2001. Data for discharge begins on Julian day 128 (May 8) at the lowest value within the series of $12.00\,\mathrm{m^3\,s^{-1}}$, $5.70\,\mathrm{m^3\,s^{-1}}$ (32.20%) lower than any other low flow event. Discharge begins to display a rapidly increasing trend with a large amount of fluctuation, reaching a peak on Julian day 203 (July 22) with a value of $193.50\,\mathrm{m^3\,s^{-1}}$. Discharge attained on Julian day 203 (July 22) appears highest for 2002, $16.00\,\mathrm{m^3\,s^{-1}}$ (9.01%) higher than the closest peak recorded 4 days earlier on Julian day 199 (July 18). After $193.50\,\mathrm{m^3\,s^{-1}}$ is recorded discharge starts rapidly decreasing to a value similar to that at which it began, ending with $17.70\,\mathrm{m^3\,s^{-1}}$ on Julian 293. A large and sharp drop in discharge also occurs between Julian days 244 (September 1) and 254 (September 11), where it decreases from $89.80\,\mathrm{m^3\,s^{-1}}$ on Julian day 244 (September 1) to $19.20\,\mathrm{m^3\,s^{-1}}$ on Julian day 254 (September 11), with an overall decrease during this period of $70.60\,\mathrm{m^3\,s^{-1}}$ (78.62%).

Daily air temperature for 2003 (Figure 5.3) shows a distinct arcing trend similar to that for 2001. The series begins on Julian day 129 (May 9) with an average air temperature of $4.25\,^\circ$C, after which the average air temperature begins to rapidly rise before reaching the largest peak on Julian day 185 (July 4) with $13.50\,^\circ$C. After the peak on Julian day 185 (July 4), air temperature then drops to $7.15\,^\circ$C on Julian day 192 (July 11), before rising once again to $13.35\,^\circ$C on Julian day 205 (July 24) only $0.15\,^\circ$C (1.11%) lower than the previous peak. After the second peak occurring on Julian day 205 (July 24), daily air temperature then begins to display an overall decreasing trend, reaching its lowest point of $1.50\,^\circ$C on Julian day 292 (October 19), $0.90\,^\circ$C (37.5%) lower than any other low point. Following this low point average air temperature begins slightly increasing and ends on a value of $2.75\,^\circ$C on Julian day 293 (October 20). The average air temperature measured over 2003 between Julian days 129 (May 9) & 293 (October 20) was $9.14\,^\circ$C.
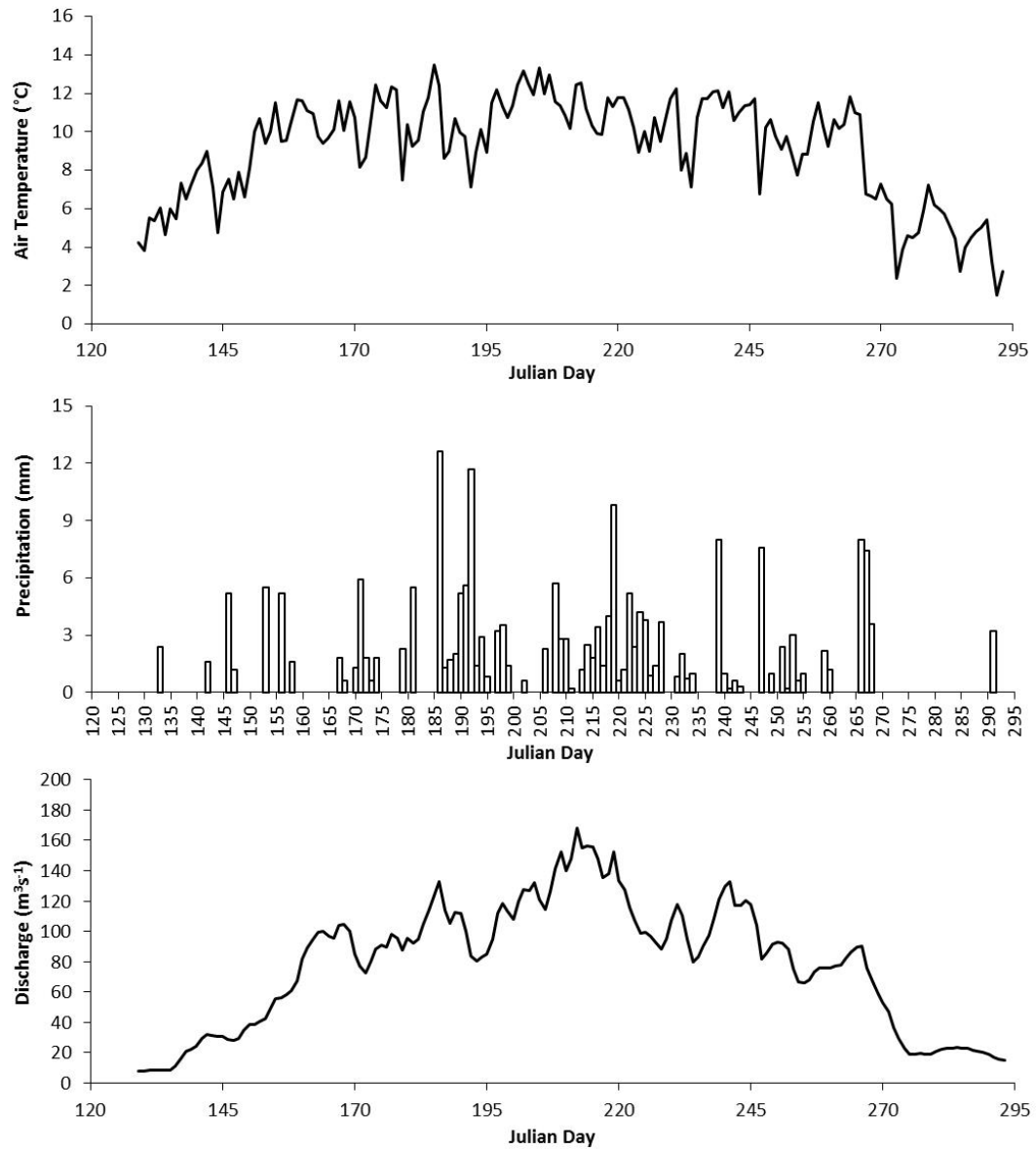
Figure 5.3: Daily median air temperature (°C) at an elevation of 3800 m and daily total precipitation (mm) measured nearby to Gangotri glacier, with daily average discharge measured 3 km downstream for 2003 between Julian days 129 (May 9) and 293 (October 20).

Daily total values of precipitation are also displayed for 2003. Precipitation recorded for 2003 shows similar frequency of events to that recorded for 2001, although the magnitude of events that occur in 2003 appear to be somewhat larger. The largest summer precipitation event appears to arise on Julian day 186 (July 5) with a small value of 12.60 mm, as compared with that achieved for 2002 displayed in Figure 5.2. The peak precipitation event for this series is also only 0.90 mm (7.69%) larger than the secondary peak occurring 6 days later on Julian day 192 (July 11), with a value of 11.7 mm. Total precipitation measured for 2003 is 215.50 mm, considerably higher than that measured for 2001, yet still substantially lower than that of 2002.

Discharge from Gangotri glacier for 2003 is displayed in Figure 5.3. As with 2001 and 2002, 2003 further exhibits an acutely similar trend. The time series begins on Julian day 129 (May 9) with a value of $8.00 \, \text{m}^3 \, \text{s}^{-1}$, which then begins a steady rise to the highest value recorded for 2003 of $167.90 \, \text{m}^3 \, \text{s}^{-1}$ on Julian day 212 (July 31), though not as sharply as that presented in Figure 5.2. The peak recorded on Julian day 212 (July 31) is $15.50 \, \text{m}^3 \, \text{s}^{-1}$ (10.17%) larger than any other visible spike in discharge. Furthermore, Figure 5.3 exhibits that after the peak is recorded on Julian day 212 (July 31), discharge begins to rapidly drop to a value of $14.80 \, \text{m}^3 \, \text{s}^{-1}$ on Julian day 293 (October 20) where the series ends. The starting daily discharge value and also the lowest on Julian day 129 (May 9) of $8.00 \, \text{m}^3 \, \text{s}^{-1}$ appears to be $11.00 \, \text{m}^3 \, \text{s}^{-1}$ (57.89%) lower than any other low flow event for 2003.

Daily average air temperature and discharge with daily total precipitation for 2004 is displayed in Figure 5.4. Daily air temperature for 2004 appears quite different to that displayed for 2001 & 2003, but does bear resemblance to daily average air temperature for 2002, only showing a slight arc throughout the series with many and often large fluctuations.

Figure 5.4: Daily median air temperature (°C) at an elevation of 3800 m and daily total precipitation (mm) measured nearby to Gangotri glacier, with daily average discharge measured 3 km downstream for 2004 between Julian days 128 (May 7) and 286 (October 12).

The first measurement of daily average air temperature recorded for 2004 occurs on Julian day 128 (May 7) at 8.80 °C, before rising to the highest temperature of the series at 14.50 °C on Julian day 184 (July 2). This peak is 0.50 °C (3.57%) higher than the second highest peak recorded on Julian day 208 (July 26). Before reaching the highest daily average air temperature, 2004 appears to encounter a prolonged period of low air temperatures between Julian days 143 (May 22) and 167 (June 15), reaching a low point on Julian day 145 (May 24) with 4.2 °C. Although air temperature rises again on Julian day 167 (June 15) to 13.5 °C, this is short lived as it drops to 7.00 °C on Julian day 178 (June 26). After the highest peak of temperature is achieved on Julian day 184 (July 2) daily average air temperature begins to display a declining trend until the end of the series, finishing at the coldest recorded temperature at 0.00 °C on Julian day 286 (October 12) (3.50 °C lower than any other drop in air temperature recorded). The average air temperature recorded for 2004 was 9.73 °C.

Daily total precipitation for 2004 (Figure 5.4) appears to be similar to that for 2003, in terms of magnitude and frequency of events despite attaining a singular large storm event. The largest precipitation event to occur during 2004 is on Julian day 267 (September 23) with a large amount of 44.30 mm, 28.70 mm(183.97%) higher than any other precipitation event during that year. There is a large cluster of precipitation events occurring between Julian days 209 (July 27) & 238 (August 25) with only 3 days during this period receiving no precipitation, reaching a total of 96.90 mm over a 29 day period and accounting for 44.55% of total precipitation. Total precipitation to fall over the summer of 2004 is recorded as 217.50 mm.

Discharge measured for 2004 is also present in Figure 5.4. Despite displaying a trend similar to that of previous years, it appears that the near central peak of discharge is not as pronounced as those displayed for 2001 to 2003. The data series begins on Julian day 128 (May 28) with a value of 10.88 $m^3 s^{-1}$ and proceeds to show a generally rapid increase, reaching its highest point on Julian day 218 (August 5) at 149.78 $m^3 s^{-1}$. This is closely followed by a value of discharge recorded on Julian day 221 (August 8) with 149.60 $m^3 s^{-1}$.

Values of discharge recorded at the peak were only marginally larger than any other by $8.70\,\mathrm{m^3\,s^{-1}}$ (6.17%) and $8.52\,\mathrm{m^3\,s^{-1}}$ (6.04%) respectively. After these peaks are achieved discharge then begins to display a decline before ending on Julian day 286 (October 12) with $23.80\,\mathrm{m^3\,s^{-1}}$. The lowest value for discharge was recorded on Julian day 130 (May 9), soon after measurements began with $9.76\,\mathrm{m^3\,s^{-1}}$, $24.31\,\mathrm{m^3\,s^{-1}}$(71.35%) lower than any other low flow event.

Table 5.1 displays total precipitation calculated for each summer investigated over the study period. Table 5.2 shows average discharge and air temperature with the average precipitation event calculated for each summer.

Table 5.1: Total precipitation for the summers of 2001 to 2004.

	Total Precipitation (mm)
2001	131.35
2002	368.80
2003	215.50
2004	217.50

Table 5.2: Average discharge, precipitation event and air temperature for summers 2001 to 2004.

	Average Discharge ($\mathrm{m^3\,s^{-1}}$)	Average Precipitation Event (mm)	Average Air Temperature (°C)
2001	73.98	2.35	9.84
2002	72.20	8.02	9.25
2003	78.18	2.95	9.14
2004	78.42	3.88	9.73

Highest average discharge is evident for 2004 attaining $78.42\,\mathrm{m^3\,s^{-1}}$ as displayed in Table 5.2. Despite attaining highest average discharge, 2004 does not display highest average air temperature or highest average precipitation event placing second highest for average air temperature and second highest

for both total precipitation and average precipitation event. The year which encounters lowest average discharge is 2002 with $72.20\,\text{m}^3\,\text{s}^{-1}$. Average air temperature for 2002, displayed in Table 5.2 is also low with the second lowest value of $9.25\,°\text{C}$ but has a good correlation with discharge of 0.76. 2002 also records the highest amount of precipitation out of any other year by a considerable amount with $368.80\,\text{mm}$, which has negative correlation with discharge of -0.40. This large amount of precipitation is also evident in Table 5.2, displaying an average summer precipitation event of $8.02\,\text{mm}$. The negative correlation of -0.40 between discharge and precipitation for the summer of 2002 is considerably more negative than any other year, with the closest being -0.12 for 2004.

The year which displays highest daily average air temperature is 2001 with $9.84\,°\text{C}$ closely followed by 2004 with $9.73\,°\text{C}$. Although 2001 records the highest average air temperature, it only displays a correlation between daily average discharge and daily air temperature of 0.63. The correlation between daily average discharge and daily average air temperature of 0.63 for 2001 is also reflected in 2004 with 0.62. 2001 furthermore displays the lowest level of total precipitation measured with $131.35\,\text{mm}$, also evident in Table 5.2, where the average precipitation event was only $2.35\,\text{mm}$.

5.2 Interaction between discharge and precipitation in relation to the elevation of the 0 °C isotherm

The following series of graphs display the relationship between precipitation and discharge for each summer. These include unfiltered data and data filtered for when the 0 °C isotherm is positioned below 5500 m, 5000 m and 4500 m, with each graph including its regression equation and subsequent R^2.

The relationship between precipitation and discharge for each summer, utilising an unfiltered dataset is evident in Figure 5.5. Discharge and precipitation do not appear to have a strong relationship in any of the years presented. The strongest relationship is displayed for 2002 (Figure 5.5B) with an R^2 of 0.16, with a correlation of -0.40 for the same year. The only other year which displays a relationship is 2004 (Figure 5.5D), with a poor R^2 of 0.02 and a correlation of -0.12.

The weakest relationship present within the unfiltered dataset is for 2003 (Figure 5.5C) displaying an R^2 of 2E-06 (0.00). This indicates a weak relationship between discharge and precipitation within the unfiltered data for this year, which is also reflected in correlation with a value of 0.00. The relationship for 2003 is similarly poor to that displayed for 2001 (Figure 5.5A), with an R^2 of 0.00 and a weak correlation of -0.02.
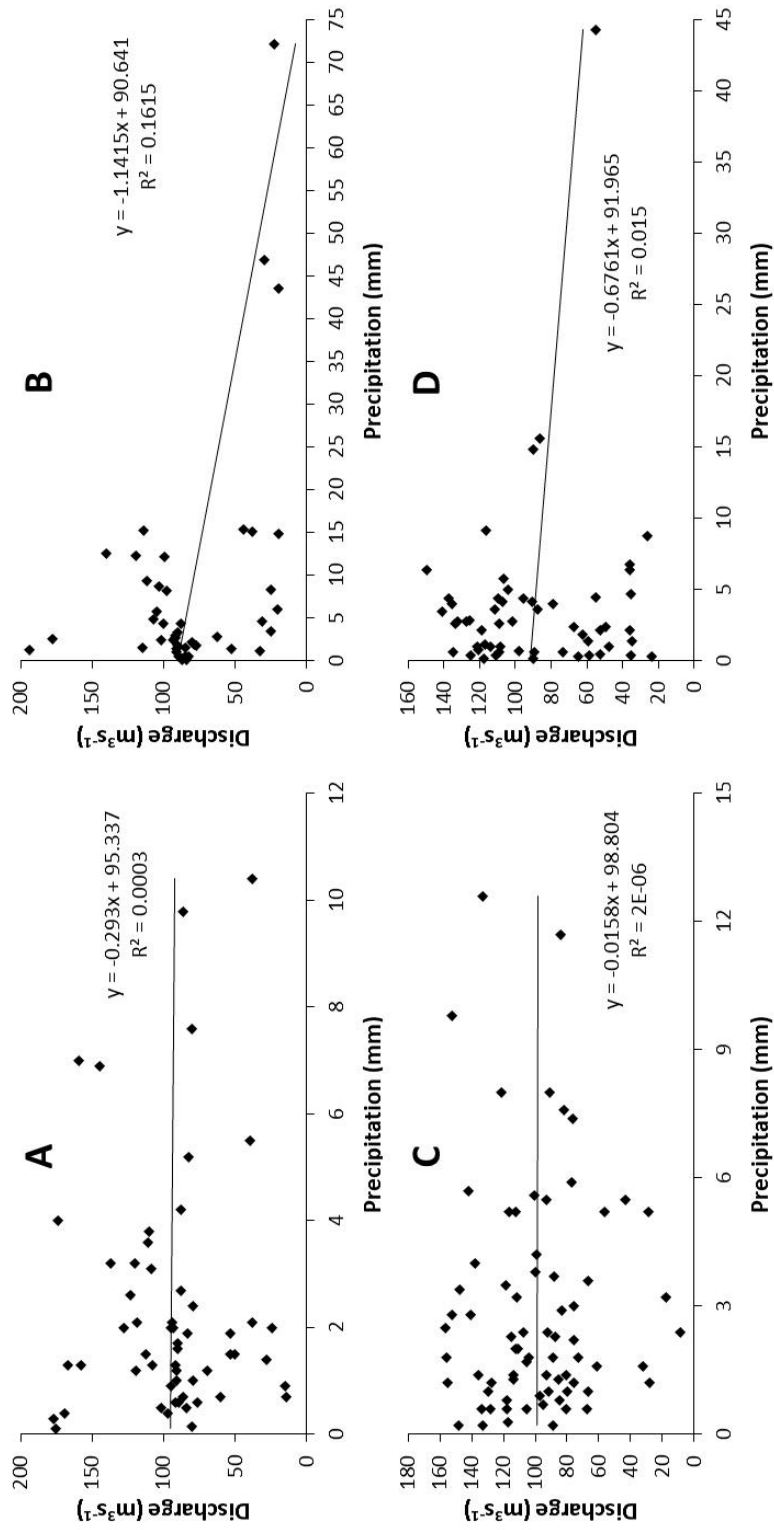
Figure 5.5: Discharge and precipitation for 2001 (A), 2002 (B), 2003 (C) and 2004(D), with their R^2 values and equations.

Values for discharge and precipitation which occur when the 0 °C isotherm is positioned below 5500 m for each year investigated are displayed within Figure 5.6. As with Figure 5.5, it is immediately evident that the year which has the strongest relationship between discharge and precipitation is 2002 (Figure 5.6B). The R^2 for this year is 0.24 with a corresponding negative correlation of -0.49. Compared to the unfiltered data (Figure 5.5), the relationship between discharge and precipitation for 2002 appears to have improved when filtered, as shown by an increase in R^2 of 0.08 and an increase in correlation by 0.09.

Similarly to 2002 (Figure 5.6B), 2001 (Figure 5.6A) and 2003 (Figure 5.6C) also show an increase in relationship between discharge and precipitation but only by a small fraction. The R^2 for 2001 changes from a relationship of 0.00 to a positive relationship of 0.05, evident from the linear trend line. This change is also evident within correlation for the less than 5500 m 0 °C isotherm filtered data for 2001, which changes from -0.02 to 0.22. R^2 for 2003 also portrays an increase in relationship between discharge and precipitation, increasing from 2E-06 (0.00) to 0.01. The increase in relationship is negative as displayed by the trend line and correlation which increases from 0.00 to a negative of -0.11.

Contrary to other summers investigated, 2004 (Figure 5.6D) does not appear to have the same response to the less than 5500 m 0 °C isotherm filter. The relationship between discharge and precipitation becomes worse with the R^2 decreasing to 0.00 from 0.02. The decrease in relationship between the two variables for 2004 is also evident in correlation which decreases from -0.12 to -0.02.
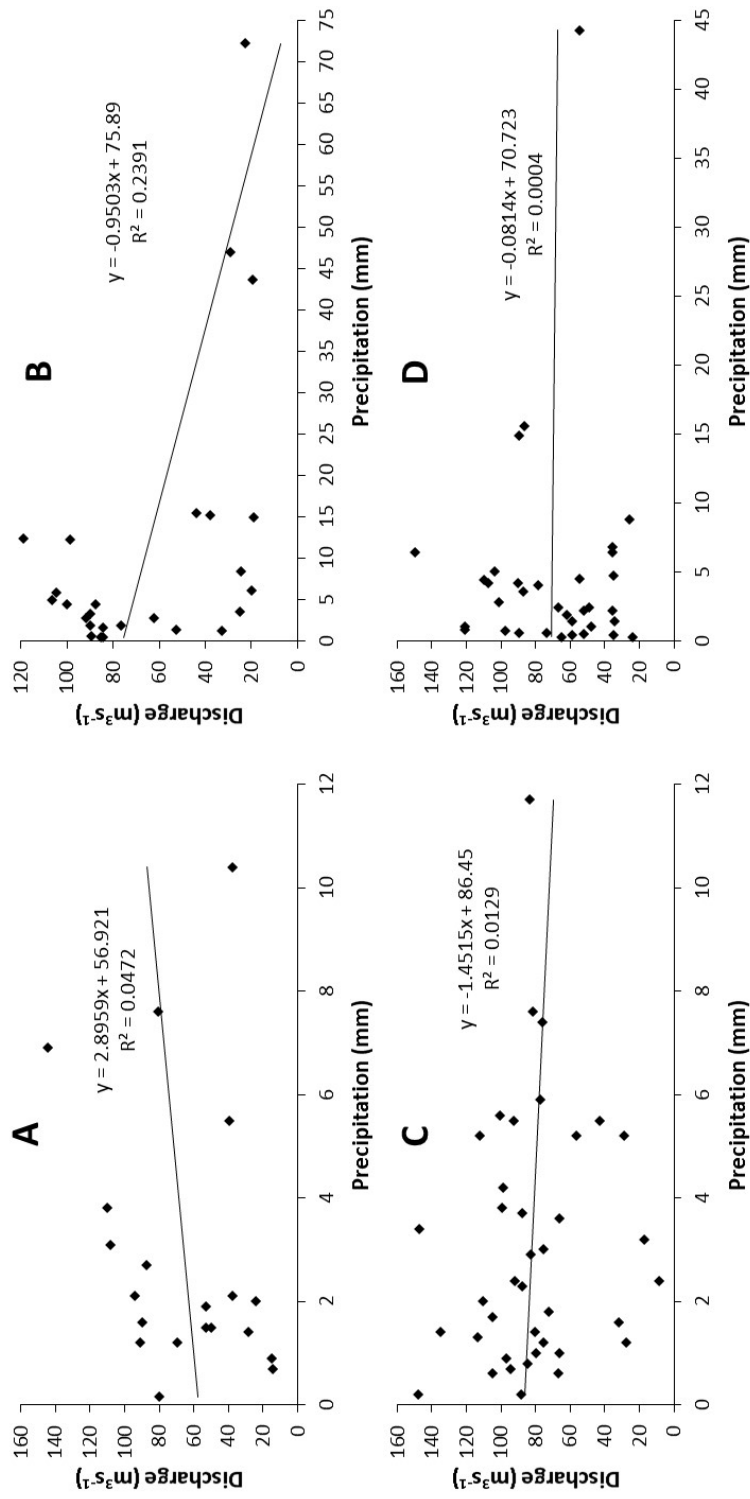
Figure 5.6: Discharge and precipitation for 2001 (A), 2002 (B), 2003 (C) and 2004(D) filtered for when the 0 °C isotherm was positioned below 5500 m, with their R^2 values and equations.

The relationship between discharge and precipitation for when the 0 °C isotherm was positioned below an elevation of 5000 m is illustrated in Figure 5.7. The first most notable change in relationship between discharge and precipitation is evident for 2003 (Figure 5.7C), displaying a positive relationship via the trend line as opposed to the slightly negative trend line displayed in Figure 5.6C. An R^2 of 0.34 for 2003 indicates an increase of 0.33 from its R^2 of 0.01 under the less than 5500 m 0 °C isotherm filter. The relationship flips from a negative correlation of -0.11 under the less than 5500 m 0 °C isotherm filter to a positive correlation of 0.59 under the less than 5000 m 0 °C isotherm filter.

2004 (Figure 5.7D), encounters a similar response to the less than 5000 m 0 °C isotherm filter as 2003 (Figure 5.7C). The relationship between precipitation and discharge for 2004 increases to an R^2 of 0.05 from 0.00. Correlation also changes from a negative of -0.02 under the 5500 m 0 °C isotherm filter to a positive of 0.23 under the 5000 m 0 °C isotherm filter.

Opposing the switch from a negative relationship to a positive, 2001 (Figure 5.7A) indicates a switch from a positive relationship to a negative via the trend line. This switch is also displayed within the correlation, changing from a value of 0.22 to -0.32. The R^2 also increases by 0.05 to 0.10 under the less than 5000 m 0 °C isotherm filter, from 0.05 under the less than 5500 m 0 °C isotherm filter.

Under the less than 5000 m 0 °C isotherm filter 2002 (Figure 5.7B) appears to display a weaker negative relationship between precipitation and discharge as shown by a reduction in the R^2 from 0.24 (Figure 5.6B) to 0.11 (Figure 5.7B). This reduction is also evident within correlation between precipitation and discharge under filters reducing from -0.49 to -0.34.
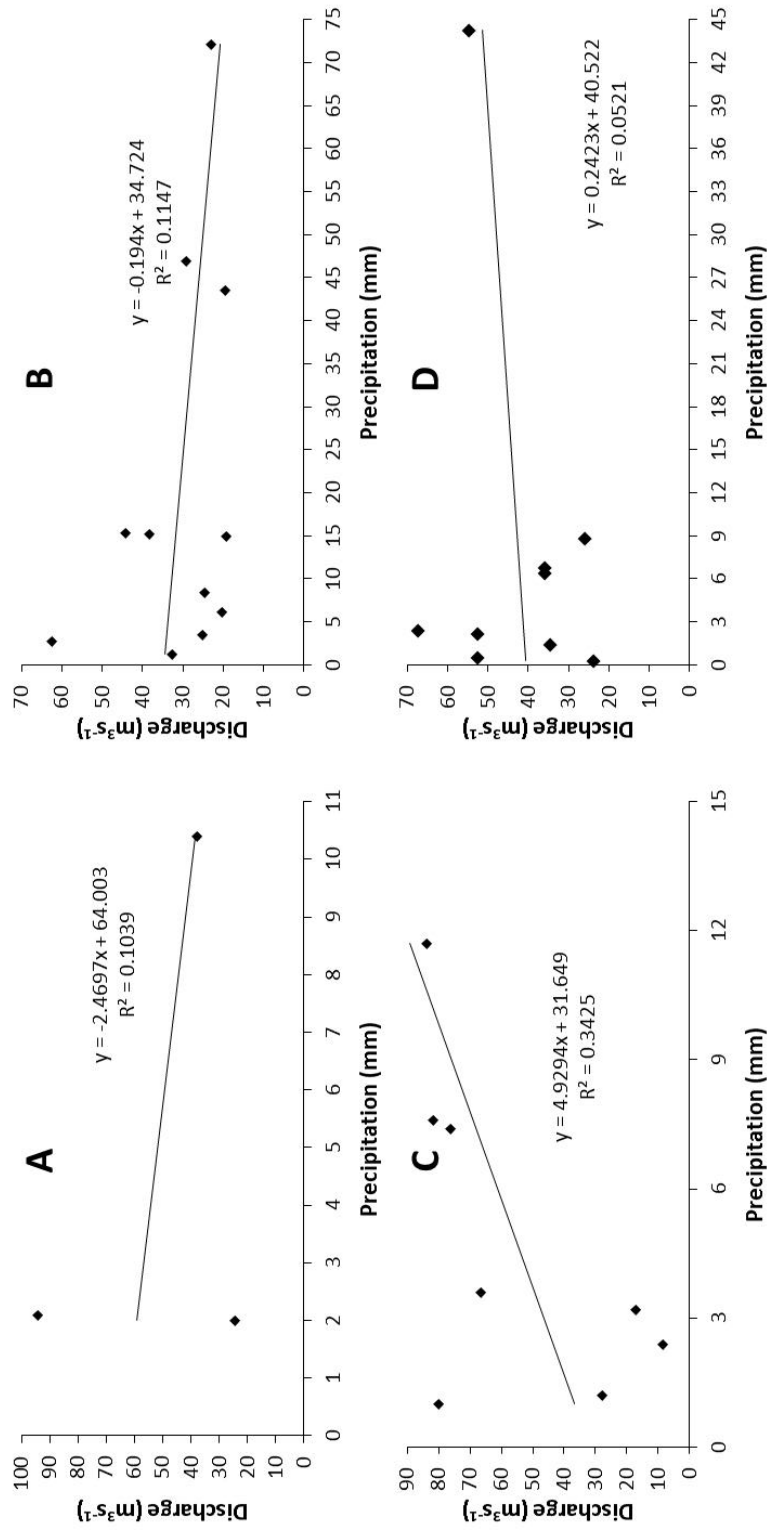
Figure 5.7: Discharge and precipitation for 2001 (A), 2002 (B), 2003 (C) and 2004(D) filtered for when the 0 °C isotherm was positioned below 5000 m, with their R^2 values and equations.

Furthermore, Figure 5.8 displays the relationship between discharge and precipitation for the years 2002 (Figure 5.8A) and 2004 (Figure 5.8B) under a 0 °C isotherm less than 4500 m filter. Out of all four years, 2002 and 2004 were the only two which experienced precipitation events when the 0 °C isotherm was below this point and are therefore the only two in which a relationship can be investigated.
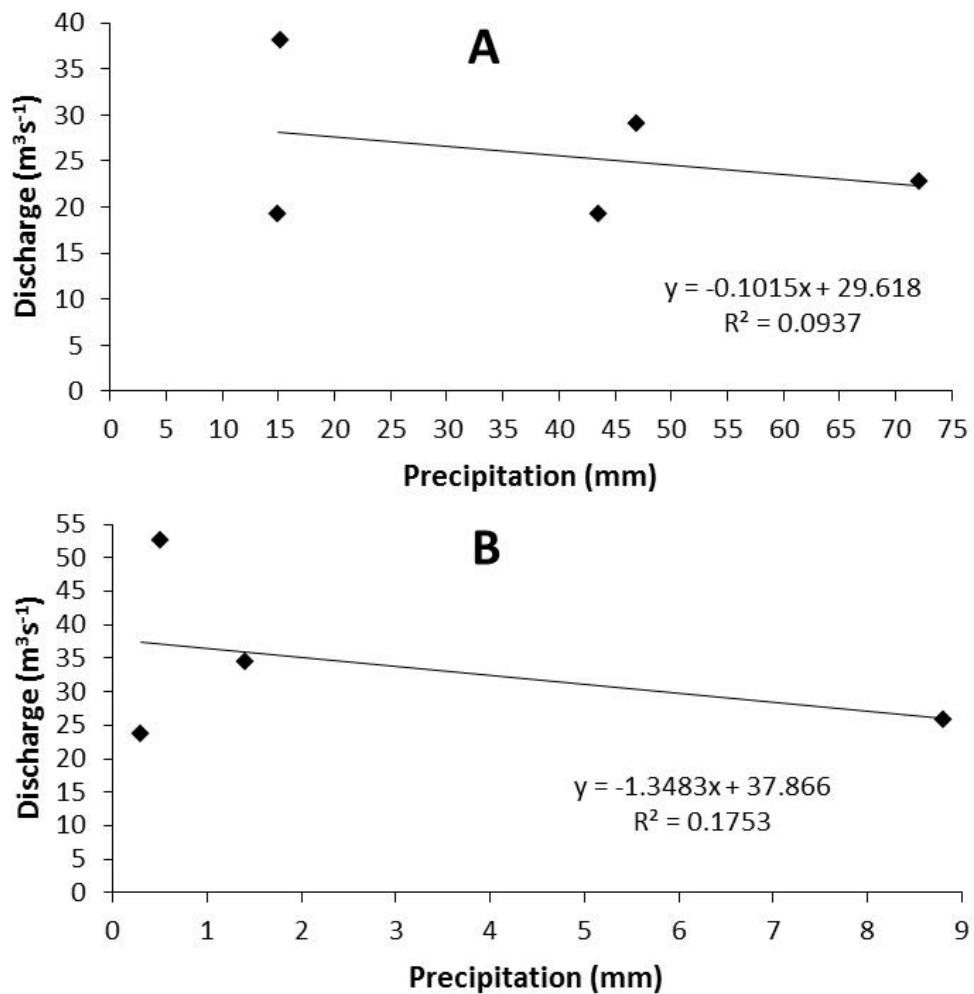
Figure 5.8: Discharge and precipitation for 2002 (A) and 2004 (B) filtered for when the 0 °C isotherm was positioned below 4500 m, with their R^2 values and equations.

Both graphs displayed in Figure 5.8 illustrate a negative relationship between discharge and precipitation via their trend lines under the 0 °C isotherm below 4500 m filter. This negative relationship is also reflected in the correlations for each year with 2002 (Figure 5.8A) displaying -0.31, slightly weaker than -0.34 for the less than 5000 m filter and 2004 (Figure 5.8B) displaying -0.42 (as opposed to a 0.23 for the 0 °C isotherm less than 5000 m filter). Precipitation occurring for 2004 appears to have a larger influence over discharge than that in 2002, with 2004 displaying an R^2 of 0.18 and 2002 only obtaining an R^2 of 0.09.

Table 5.3 summarises the regression coefficients with their corresponding p-values between daily average discharge and daily total precipitation, for each year investigated and each filter used.

Table 5.3: Summary of R^2 between daily average discharge and daily total precipitation for each year, under each filter with their corresponding p-value.

Unfiltered	R2	P-Value
2001	0.00	<0.05
2002	0.16	<0.05
2003	2E-06	<0.05
2004	0.02	<0.05

5500 m	R2	P-Value
2001	0.05	<0.05
2002	0.24	<0.05
2003	0.01	<0.05
2004	0.00	<0.05

5000 m	R2	P-Value
2001	0.10	0.39
2002	0.11	<0.05
2003	0.34	0.10
2004	0.05	<0.05

4500 m	R2	P-Value
2002	0.09	<0.05
2004	0.18	0.05

It is evident from Table 5.3 that all R^2 for the unfiltered data set and the data filtered for 5500 m are statistically significant p-values under 0.05. Moreover, under the 5000 m filter the R^2 for 2002 and 2004 appear to be significant, but not those for 2001 and 2004 with p-values of 0.39 and 0.10. Under the 4500 m filter the R^2 for 2002 is significant, but not for 2004 with a p-value of 0.05.

5.3 Interaction between discharge and air temperature in relation to the elevation of the 0 °C isotherm

The following series of graphs visualise the relationship between discharge and air temperature under different filters regarding to the elevation of the 0 °C isotherm for 2001 to 2004. As with precipitation and discharge, the filters utilised selected measurements of air temperature and discharge which occurred when the 0 °C isotherm was positioned below 5500 m, 5000 m and 4500 m.

Graphs displayed in Figure 5.9 illustrate the unfiltered relationship between discharge and air temperature for the periods of study. It is evident that all years investigated display a positive relationship between discharge and air temperature characterised by their linear trend line.

The year which air temperature and discharge appears to have the strongest relationship is 2003 (Figure 5.9C). The R^2 for 2003 is high with 0.67 with a correlation of 0.82, closely followed by 2002 (Figure 5.9B) with an R^2 of 0.58 and a correlation of 0.76. 2001 (Figure 5.9A) and 2004 (Figure 5.9D) display a similar relationship between discharge and air temperature, with 2001 indicating an R^2 of 0.39 and 2004 displaying an R^2 of 0.38 with correlations being 0.63 and 0.62 respectively.
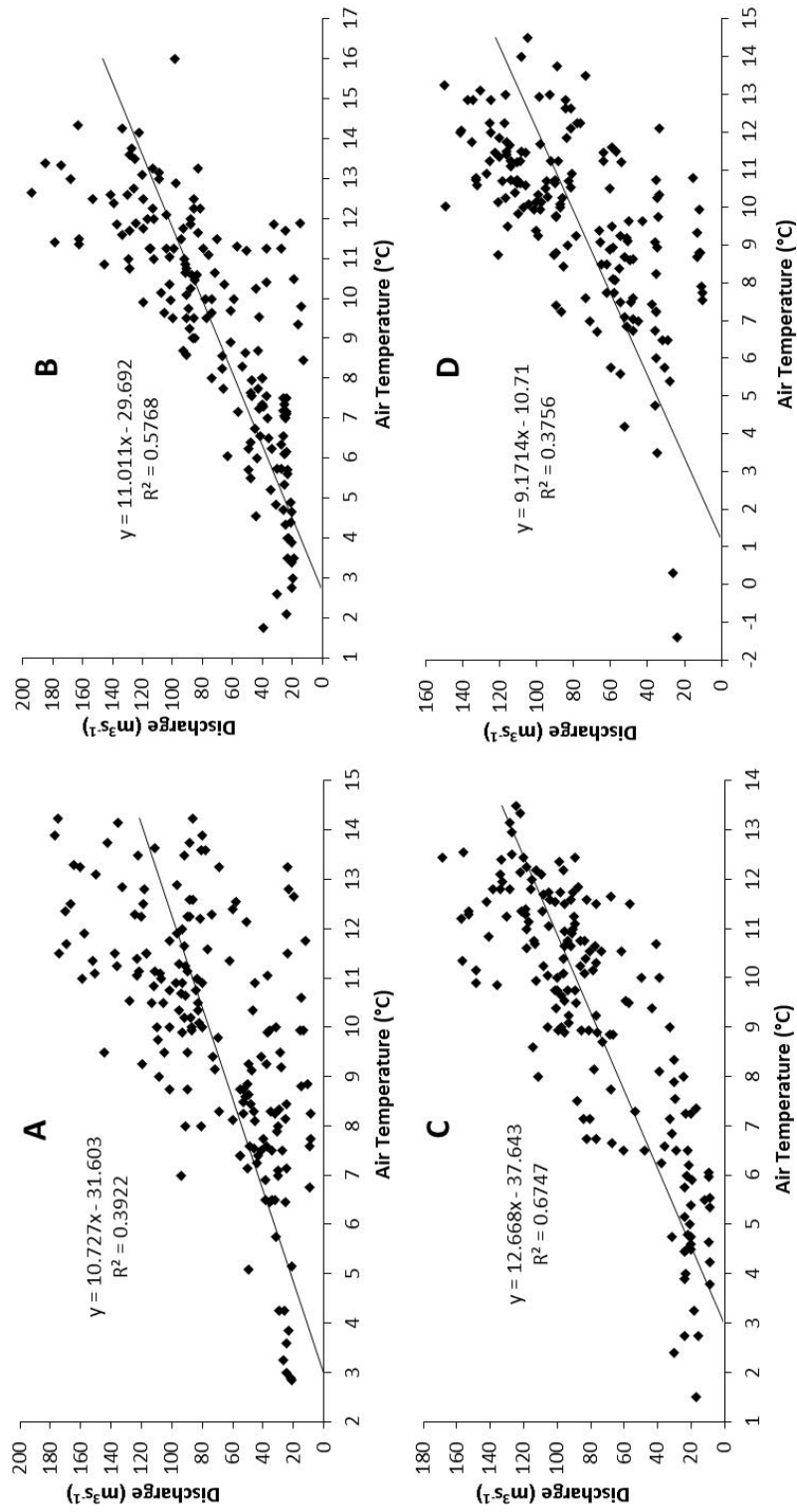
Figure 5.9: Discharge and air temperature for 2001 (A), 2002 (B), 2003 (C) and 2004(D), with their R^2 values and equations.

The relationship between discharge and air temperature when the 0 °C isotherm is situated below and elevation of 5500 m is displayed in Figure 5.10. For all years investigated in Figure 5.10 it appears that the relationship between variables decreases as indicated by each years R^2 and their corresponding correlations. For 2001 (Figure 5.10A) the R^2 decreases by 0.16 to 0.23 from 0.39, a decrease also evident within correlation dropping from 0.63 to 0.48. 2002 (Figure 5.10B) also shows a drop in R^2 decreasing from 0.58 to 0.47 indicating a decrease of 0.11. The decrease in relationship for 2002 is also evident within the correlation dropping from 0.76 to 0.69. As for 2003 (Figure 5.10C), it also indicates a decrease in relationship of 0.09 dropping from 0.67 to 0.58 with the correlation dropping from 0.82 to 0.76. Moreover, 2004 (Figure 5.10D) also displays a marked decrease, lowering by 0.18 from 0.38 to 0.20 accompanied by a decrease in correlation from 0.62 to 0.45.

The graphs displayed in Figure 5.11 show the interaction between discharge and air temperature filtered for when the 0 °C isotherm is positioned below an elevation of 5000 m.

Under the 0 °C isotherm less than 5000 m filter in Figure 5.11, years 2001 to 2003 all display an even further decrease in relationship between discharge and air temperature. For 2001 (Figure 5.11A), the R^2 indicates a further decrease of 0.09 from 0.23 to 0.14 with correlation also decreasing from 0.48 to 0.37. 2002 (Figure 5.11B) displays a very large decrease of 0.35 from 0.47 to 0.12, which is also evident within the correlation decreasing to 0.35 from 0.69. Furthermore, 2003 (Figure 5.11C) also displays a drop in R^2 from 0.58 to 0.28, a decrease of 0.30 also evident within the correlation dropping from 0.76 to 0.53.
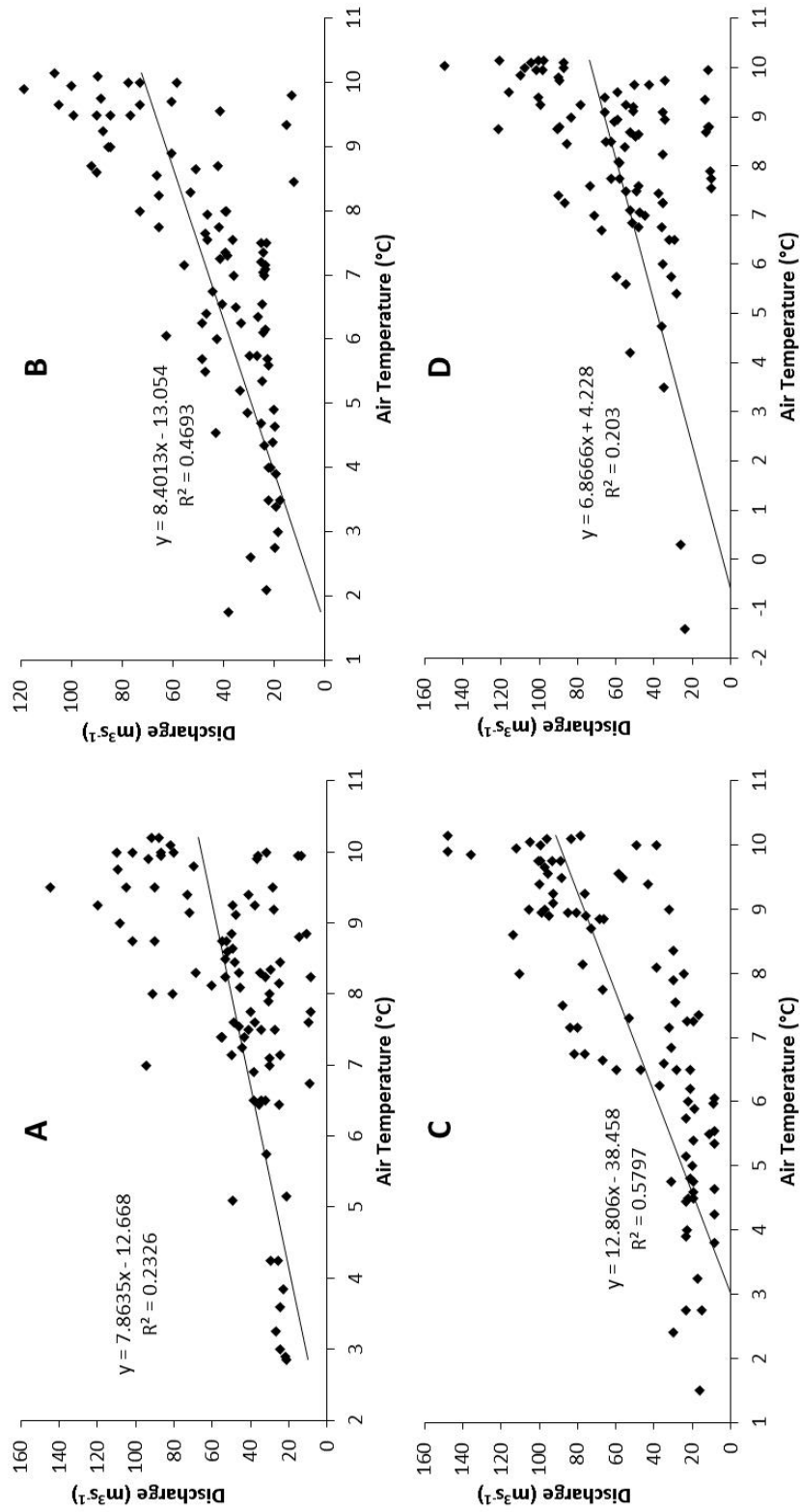
Figure 5.10: Discharge and air temperature for 2001 (A), 2002 (B), 2003 (C) and 2004(D) filtered for when the 0 °C isotherm is positioned below 5500 m, with their R^2 values and equations.

The year 2004 (Figure 5.11D) does not display the same response to the 0 °C isotherm less than 5000 m filter as other years displayed. The R^2 displayed shows an increase of 0.07 from 0.20 to 0.27. The increase in relationship between discharge and air temperature is also evident within the correlation for this year, which increases from 0.45 to 0.51.

The following graphs within Figure 5.12 display discharge and air temperature filtered for when the 0 °C isotherm is positioned below 4500 m. As opposed to graphs displayed from Figure 5.9 to 5.11, it is immediately evident from all graphs that there is no uniform relationship present between discharge and air temperature under the 0 °C isotherm less than 4500 m filter.

For 2001, illustrated in Figure 5.12A, a positive relationship between air temperature and discharge is evident with an R^2 of 0.10, which is a further decrease in relationship than that in Figure 5.11A, lowering by 0.04 from 0.14. This drop is also evident within the correlation, dropping from 0.37 to 0.32. The only other year which displays a positive relationship between discharge and air temperature is 2004 (Figure 5.12D). 2004 shows a positive relationship, with an R^2 of 0.75, an increase of 0.48 from 0.27 (Figure 5.11D). This is also evident in the correlation between discharge and air temperature for 2004 under the 0 °C isotherm less than 4500 m with a strong positive correlation of 0.87, increasing from 0.51 under the 0 °C isotherm less than 5000 m filter.

For 2002 (Figure 5.12B), the relationship appears to change from positive to negative, ascertaining an R^2 of 0.44, an increase of 0.32 from 0.12. The switch from a positive to a negative relationship is evident within the correlation, switching from 0.35 under the 0 °C isotherm less than 5000 m filter to -0.67. 2003 (Figure 5.12C) shows a weak relationship between air temperature and discharge, with the R^2 of 0.01 being 0.27 lower than that displayed for the same year in Figure 5.11C. There is a negative relationship evident for 2003 via the trend line, which is also evident within the correlation decreasing from a positive value of 0.53 to a negative value of -0.10.
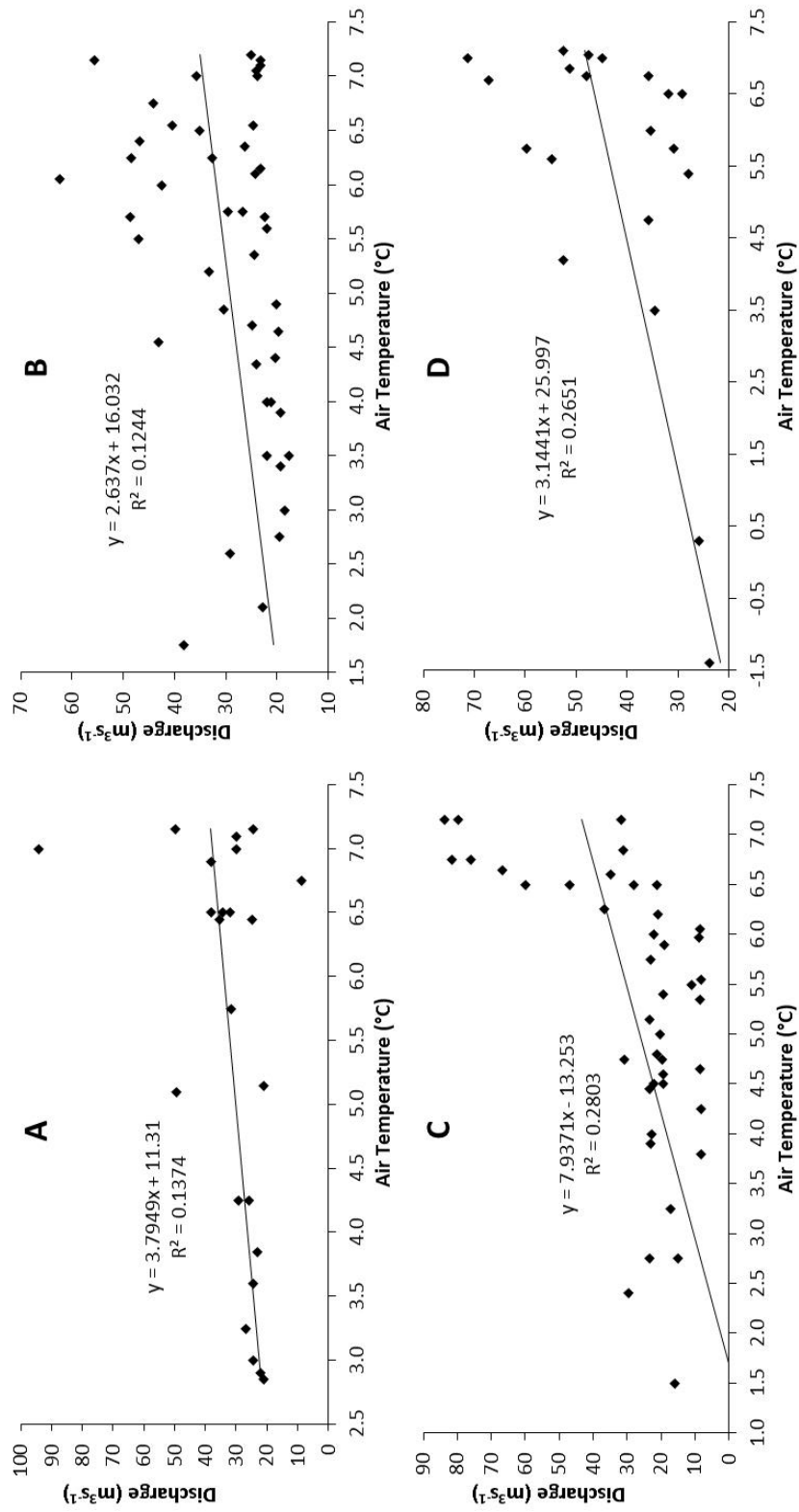
Figure 5.11: Discharge and air temperature for 2001 (A), 2002 (B), 2003 (C) and 2004(D) filtered for when the 0 °C isotherm is positioned below 5000 m, with their R² values and equations.
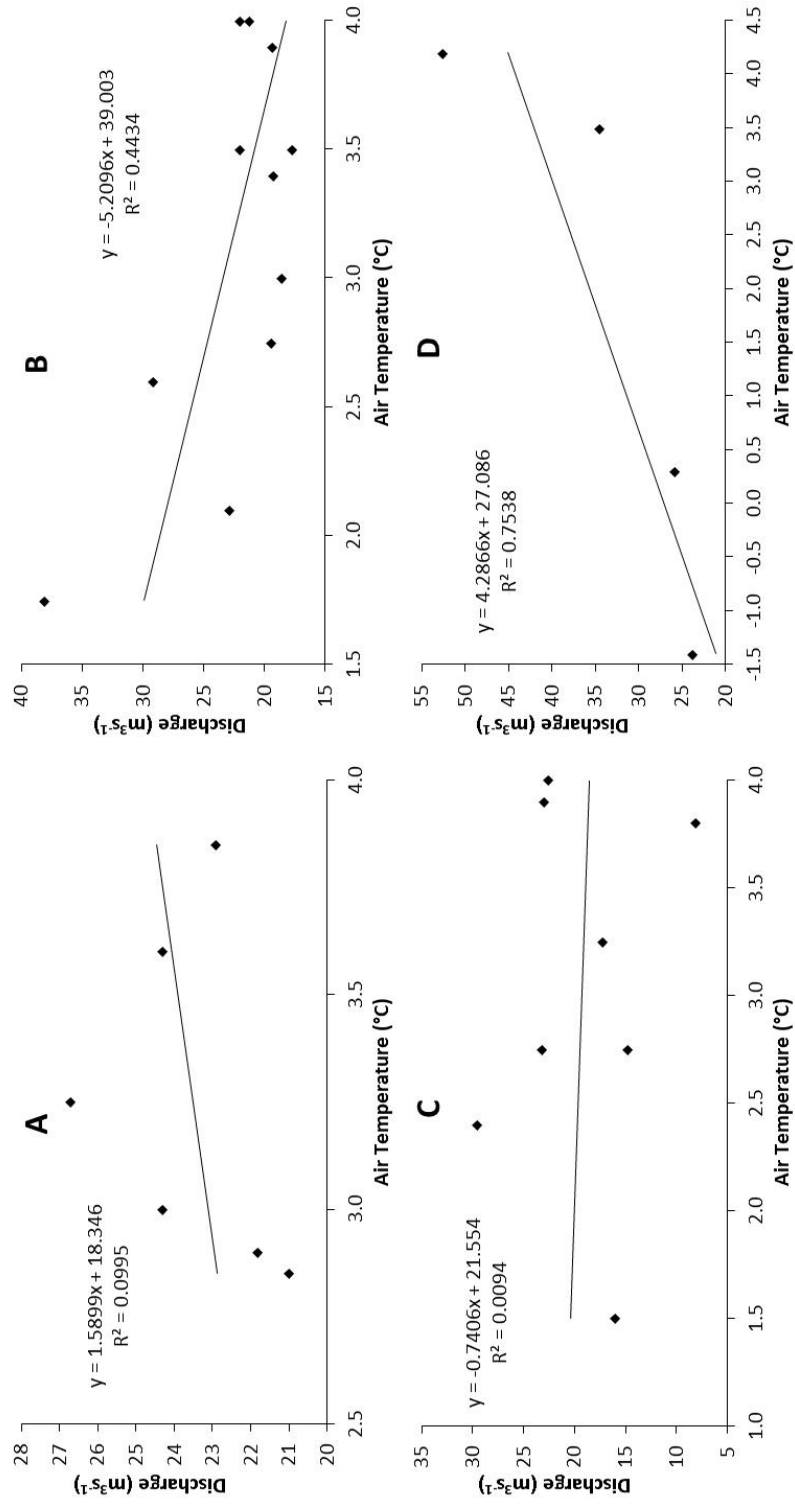
Figure 5.12: Discharge and air temperature for 2001 (A), 2002 (B), 2003 (C) and 2004(D) filtered for when the 0 °C isotherm was positioned below 4500 m, with their R² values and equations.

Table 5.4 displays a summary of R^2 and p-values between daily average discharge and daily average air temperature for the study period, under each 0 °C isotherm filter.

Table 5.4: Summary of R^2 between daily average discharge and daily average air temperature for each year, under each filter with their corresponding p-value.

Unfiltered	R2	P-Value
2001	0.39	<0.05
2002	0.58	<0.05
2003	0.67	<0.05
2004	0.38	<0.05

5500 m	R2	P-Value
2001	0.23	0.31
2002	0.47	0.07
2003	0.58	<0.05
2004	0.20	0.74

5000 m	R2	P-Value
2001	0.14	0.35
2002	0.12	<0.05
2003	0.28	0.23
2004	0.27	<0.05

4500 m	R2	P-Value
2001	0.10	0.08
2002	0.44	<0.05
2003	0.01	0.07
2004	0.75	<0.05

R^2 for the unfiltered data set all are significant with p-values below 0.05. Under the 5500 m filter the only significant R^2 is for 2003, with all other years displaying p-values higher than 0.05. For both data filtered for 5000 m and 4500 m R^2 for 2002 and 2004 are significant, but all other years under both filters display p-values larger than 0.05.

5.4 Specific summer snowfall events and the response of discharge

The following graphs display a specific summer precipitation event for years 2001, 2002 and 2004. These were identified using filters for when the 0 °C isotherm was below at least 5000 m, meaning any snowfall would cover a large majority of Gangotri glacier. Each graph includes air temperature, precipitation and discharge collected by Singh *et al.*, (2006b) and Singh *et al.*, (2005b) in order to determine the influence a precipitation event has on discharge in relation to air temperature.

The first precipitation event displayed in Figure 5.13 occurs between Julian days 126 (May 6) and 157 (June 6) for 2001, with the specific event in question spanning Julian days 135 (May 15) and 136 (May 16) reaching 1.40 mm and 10.40 mm respectively. It is evident that just before the precipitation event occurs the air temperature suffers a drop of 6.75 °C from 13.25 °C on Julian day 132 (May 12) to 6.50 °C on Julian day 136 (May 16). In terms of discharge from Gangotri glacier it appears to steadily rise until the precipitation event occurs across Julian days 135 (May 15) and 136 (May 16), where it peaks at 37.90 $m^3 s^{-1}$ on Julian day 136 (May 16) and begins to drop to 24.10 $m^3 s^{-1}$ on Julian day 140 (May 20) before recovering and increasing to 79.90 $m^3 s^{-1}$ on Julian day 155 (June 4).

Correlation for discharge and air temperature between Julian days 126 (May 6) & 157 (June 6) displayed in Figure 5.13, there is much fluctuation. Before the precipitation even occurs, correlation for air temperature and discharge between Julian days 126 (May 6) & 134 (May 14) attains a strong positive correlation of 0.69. After the summer precipitation event, correlation oscillates from a positive correlation to a negative correlation between Julian days 136 (May 16) & 140 (May 20) with -0.62 (the duration of the snowpack). Between Julian days 141 (May 21) & 157 (June 6) when discharge begins to increase again, the correlation returns positive but not as strong as before the large precipitation event with 0.34.
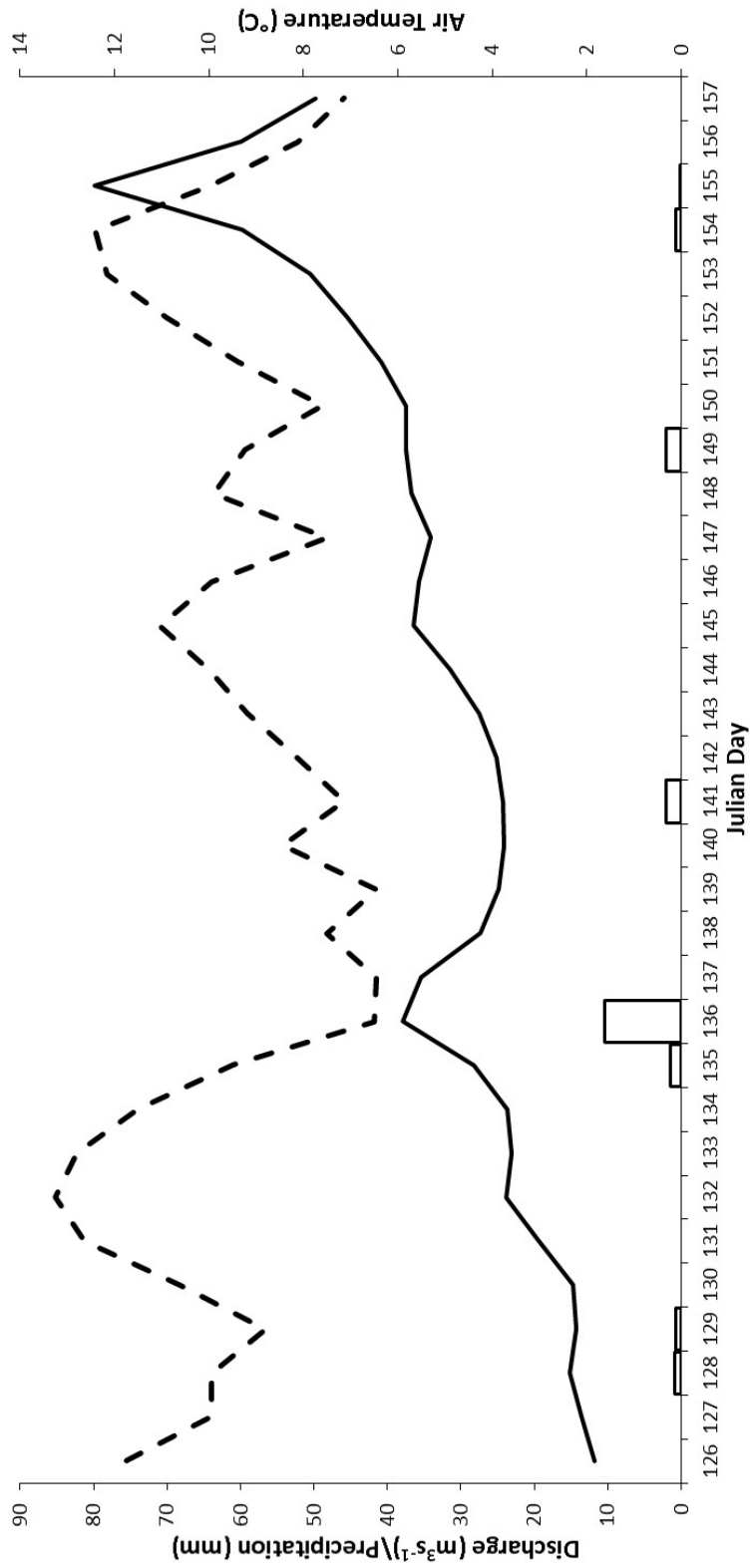
Figure 5.13: Example of a summer snowfall event occurring in 2001, including precipitation (columns), air temperature (dotted line) and discharge (solid line).

Figure 5.14 displays air temperature, discharge and precipitation between Julian days 241 (August 29) & 257 (September 14) for 2002. The precipitation event of interest occurs on Julian day 250 (September 7) when air temperature is at its lowest point for the period selected. Summer precipitation on Julian day 250 (September 7) is recorded as 15.20 mm and occurs when air temperature is 1.75 °C. Before this point discharge appears to follow roughly the same trend as daily air temperature, both steadily falling before a sharp drop in air temperature from 6.75 °C on Julian day 249 (September 6) to 1.75 °C on Julian day 250 (September 7). In terms of discharge emanating from Gangotri glacier during the period displayed for 2002, it is evident that discharge steadily drops with air temperature from Julian day 244 (September 1) with a value of $89.80\,\mathrm{m}^3\,\mathrm{s}^{-1}$ to $38.10\,\mathrm{m}^3\,\mathrm{s}^{-1}$ on Julian day 250 (September 7). After this point air temperature begins to reascend, yet discharge continues to decrease to a low of $19.20\,\mathrm{m}^3\,\mathrm{s}^{-1}$ on Julian day 254 (September 11).

Correlation between discharge and air temperature for the period displayed within Figure 5.14, before the summer precipitation event occurs on Julian day 250 (September 7) the correlation is a strong value of 0.80 between Julian days 241 (August 29) & 249 (September 6). After the precipitation event occurs on Julian day 250 (September 7) correlation for air temperature and discharge oscillates to a strong negative value of -0.73 between Julian days 250 (September 7) & 254 (September 11) (the duration of the snowpack). Similar to that displayed in Figure 5.13, once the discharge begins to increase after the summer precipitation event, the relationship between air temperature and discharge returns to a positive correlation of 0.56 between Julian days 254 (September 11) & 257 (September 14).
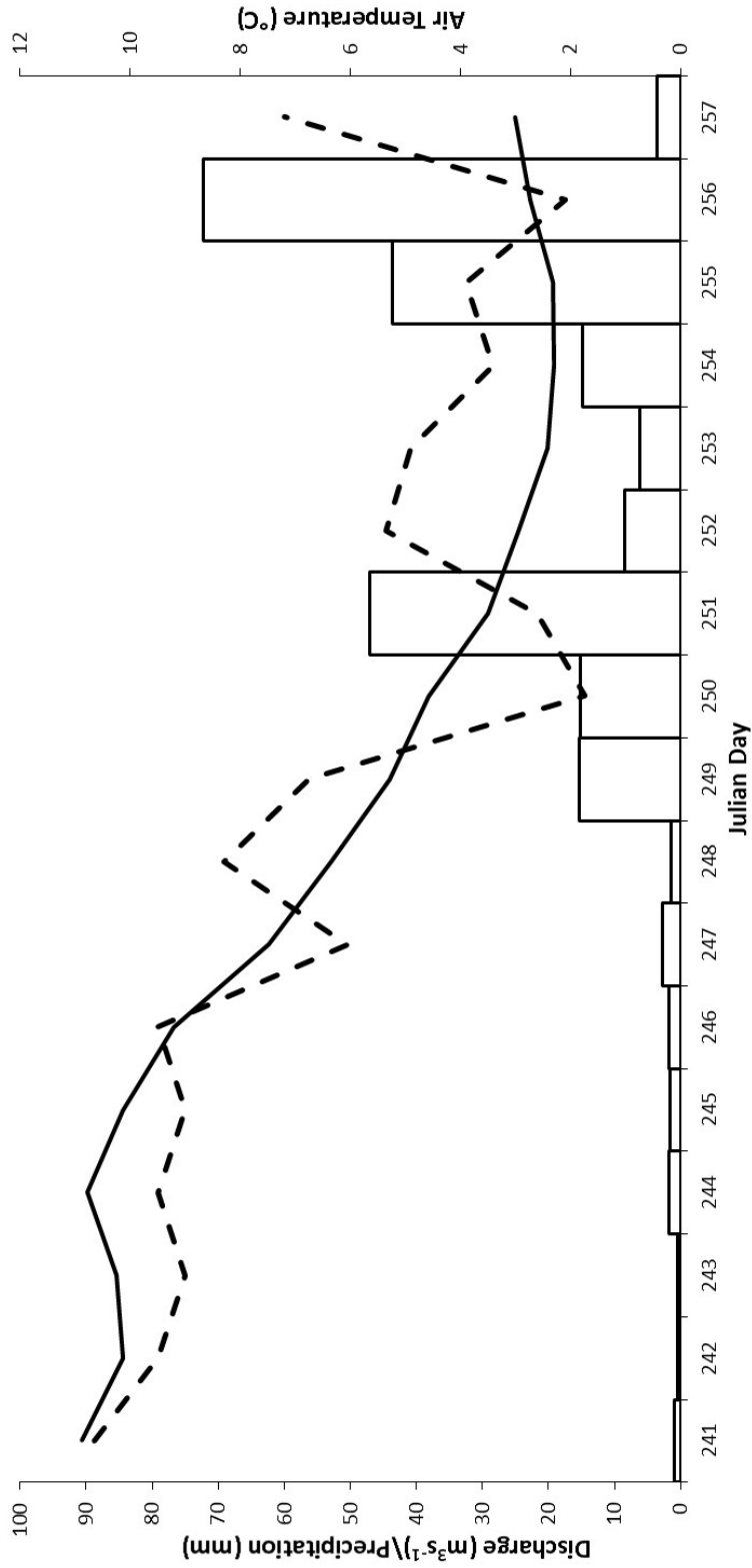
Figure 5.14: Example of a summer snowfall event occurring in 2002, including precipitation (columns), air temperature (dotted line) and discharge (solid line).

Air temperature, precipitation and discharge between Julian days 259 (September 15) & 279 (October 5) for 2004 are displayed in Figure 5.15. The summer precipitation event of interest takes place on Julian day 267 (September 23) with a large magnitude of 44.30 mm, when there is a sharp drop in air temperature from 9.50 °C on Julian day 266 (September 22) to 5.60 °C on Julian day 267 (September 23). Before Julian day 267 (September 23) discharge appears to closely follow air temperature experiencing similar fluctuations, but after the precipitation event air temperature begins a steady increase from 5.60 °C on Julian day 267 (September 23) to 10.75 °C on Julian day 272 (September 28). This is not followed by discharge which decreases from 54.71 $m^3 s^{-1}$ on Julian day 267 (September 23) to 34.07 $m^3 s^{-1}$ on Julian day 271 (September 27), before slightly increasing to 34.88 $m^3 s^{-1}$ on Julian day 272 (September 28).

The relationship between discharge and air temperature displayed through correlation for the precipitation event occurring within 2004 is similar to that for selected precipitation events occurring in 2001 (Figure 5.13) and 2002 (Figure 5.15). Before the precipitation event on Julian day 267 (September 23), correlation for air temperature and discharge was a positive value of 0.57 between Julian days 259 (September 15) & 266 (September 22). After the precipitation event between Julian days 267 (September 23) & 273 (September 29) (the duration of the snowpack), the relationship between discharge and air temperature flips to a strong negative value of -0.88. Furthermore, when discharge begins to slightly increase between Julian days 274 (September 30) and 279 (October 5) the correlation appears to be weak with 0.34, but has returned to a positive relationship.
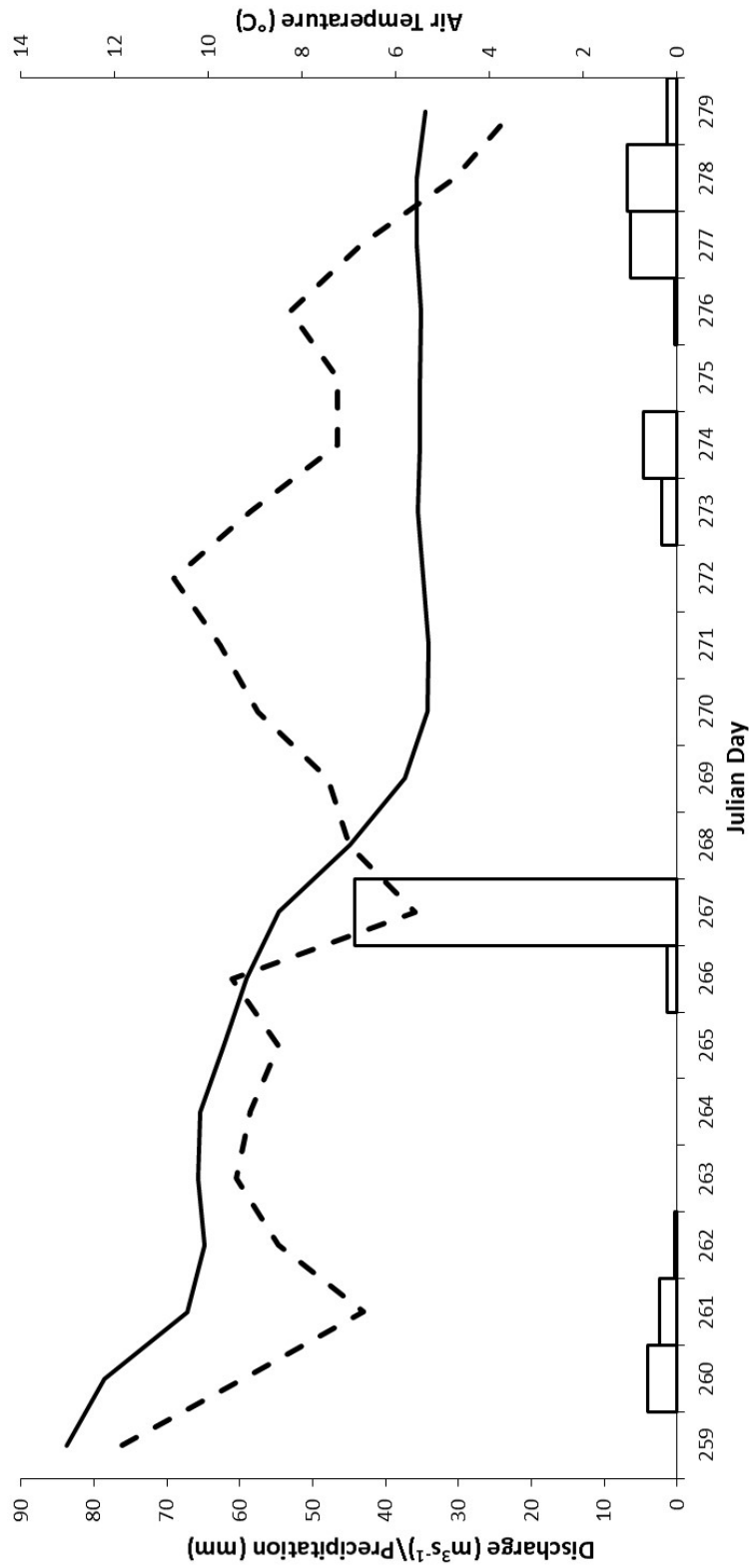
Figure 5.15: Example of a summer snowfall event occurring in 2004, including precipitation (columns), air temperature (dotted line) and discharge (solid line).

Chapter 6

Discussion

This study has illustrated the interaction between summer precipitation events and discharge for the Bhagirathi River sourcing from Gangotri glacier. Results span the summers of 2001 to 2004 and envisage the complex relationships between precipitation and discharge and also the effects of air temperature on discharge, utilising correlation and regression analysis to determine their relative magnitude of influence.

6.1 Year to year trends in discharge, air temperature and precipitation

The graphs displayed from Figure 5.1 to 5.4 display daily average discharge, daily average air temperature and daily total precipitation spanning the study period. In terms of discharge, each year displays a similar trend, with 2001 and 2004 only slightly differing from 2002 and 2003.

Summer discharge for each year displays a distinct rising section up until peak discharge is achieved, which in all cases occurs between Julian days 203 (July 22) & 218 (August 6) with the highest recorded daily average discharge for 2001 and 2002 both occurring on Julian day 203 (July 22). After this point

2002 & 2003 display a generally decreasing trend until the end of their series as opposed to 2001 & 2004, which both display a secondary peak in discharge with a value close to that but not quite as high as the primary peak, before beginning to show a general decline. 2001 & 2002 indicate a similar average discharge as displayed in Table 5.2 with $73.98 \, \mathrm{m^3 \, s^{-1}}$ for 2001 and $72.20 \, \mathrm{m^3 \, s^{-1}}$ for 2002. 2003 & 2004 display a comparatively larger average discharge of $78.18 \, \mathrm{m^3 \, s^{-1}}$ and $78.42 \, \mathrm{m^3 \, s^{-1}}$ respectively. This trend in discharge over the summer period is similar to findings of other studies which monitor discharge over summer within glacierised basins, including the findings of Collins and Hasnain, (1995) in Figure 3.12 for Batura glacier, previously presented and also those conducted by Bavay *et al.*, (2009) and Thayyen *et al.*, (2005).

Thayyen *et al.*, (2005) investigated monsoonal control on discharge sourcing from Dokriani glacier located within the Garhwal Himalaya, results of which are displayed in Figure 6.1.
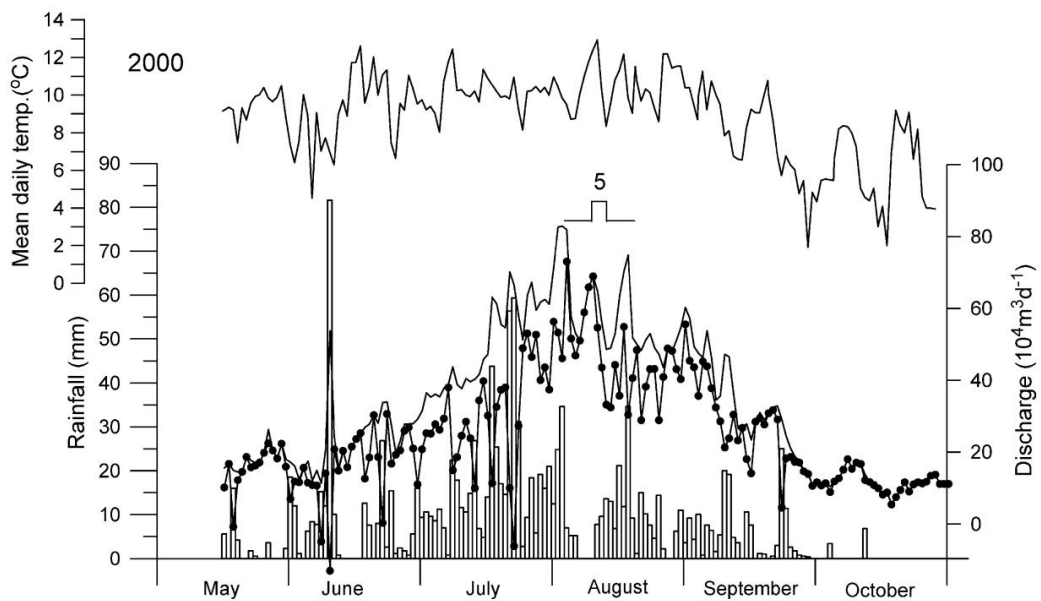
Figure 6.1: Daily total discharge (solid line) from Dokriani glacier and daily total rainfall (bars) including mean daily temperature and discharge without inclusion of the rainfall component (dotted line) for the summer of 2000 (Thayyen *et al.*, 2005)

Results illustrated in Figure 6.1 for Dokriani glacier tell an almost identical story to each of those in Figures 5.1 to 5.4 for the nearby Gangotri glacier. Discharge from Dokriani glacier for 2000 also indicates a similar trend, with a steady rise between May and July, reaching a peak between the end of July and the start of August then proceeding to steadily decrease, before almost plateauing around October. Discharge for Dokriani glacier is especially similar to that displayed for Gangotri glacier during 2002 in Figure 5.2 characterised by their dual peaks, both encountering two large drops in discharge in-between.

When compared to an Alpine catchment, where runoff is not dominated by a glacier, discharge from Gangotri glacier only indicates slight differences. Findings of Bavay *et al.*, (2009) are displayed in Figure 6.2, who investigated future snow cover and discharge from the Inn catchment and Dischma catchment located in Switzerland, both of which contain glaciers but do not contribute strongly to discharge.
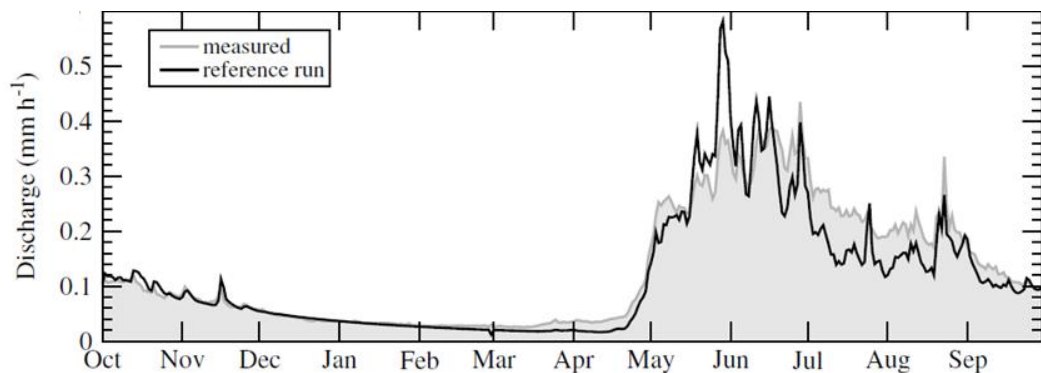
Figure 6.2: Modelled and measured daily discharge averaged over 2001 to 2006 for the Dischma catchment, Switzerland. (Bavay *et al.*, 2009)

Results regarding discharge within Figure 6.2 do not portray a dissimilar trend to those within Figures 5.1 to 5.4 for Gangotri glacier, with a particular similarity to Figure 5.2 in terms of composition. Despite displaying a similar shape to those within this study, it appears that discharge from the Dischma catchment experiences a much steeper rise than any of the years for Gangotri glacier which also occurs much earlier. The peak in discharge displayed within Figure 6.2 also appears to occur much earlier than any year for Gangotri glacier

occurring at the end of May, as opposed to the end of July or start of August. This is due to the fact that within the Dischma catchment, the glacier present appears to have little contribution to discharge indicating that the early rise and peak is due to melting winter snow cover as opposed to the glacier dominated catchment containing Gangotri glacier, where peak discharge is achieved due to melting ice (Bavay *et al.*, 2009).

In terms of air temperature each summer investigated also shows a similar trend to each other and also that displayed in Figure 6.1, illustrating a generic arc over summer with much fluctuation and a number of sharp drops. Air temperature also follows a similar pattern to discharge recorded in all cases, but the arc for air temperature is less pronounced and does not reach a clear peak. The highest recorded daily average air temperatures occur between Julian days 175 (June 24) & 188 (July 7) nearby to summer solstice when peak solar radiation is encountered, with 2001, 2003 and 2004 achieving their peaks on Julian days 188 (July 7), 185 (July 4) and 184 (July 2) respectively. Each year investigated also displays a similar average air temperature over the summer as displayed in Table 5.2 ranging from the lowest of 9.14 °C for 2003 to the highest of 9.84 °C for 2001. Air temperature is considered to be one of the most important and influential meteorological factors of discharge from a highly glacierised basin (Collins, 1987; Dyurgerov, 2003; Singh *et al.*, 2006a; Singh and Kumar, 1997).

Although daily average air temperature and daily average discharge display similar characteristics both year to year and with Figure 6.1, daily total precipitation does not appear to follow suit. Each year displays a varying precipitation pattern with the year attributing the lowest total precipitation being 2001 (131.35 mm), which is a large 84.15 mm lower than the second lowest recorded for 2003. The year which appears to have experienced a considerably large amount of precipitation was 2002 with 368.80 mm, 151.30 mm larger than any other year which appears to be primarily due to a large storm event occurring between Julian days 251 (September 8) & 257 (September 14), peaking at a sizeable 72.20 mm on Julian day 256 (September 13). Precipitation over the summers of 1999 and 2000 within the valley containing Gangotri glacier

were monitored by Kumar *et al.*, (2002) displayed within Figure 6.3.
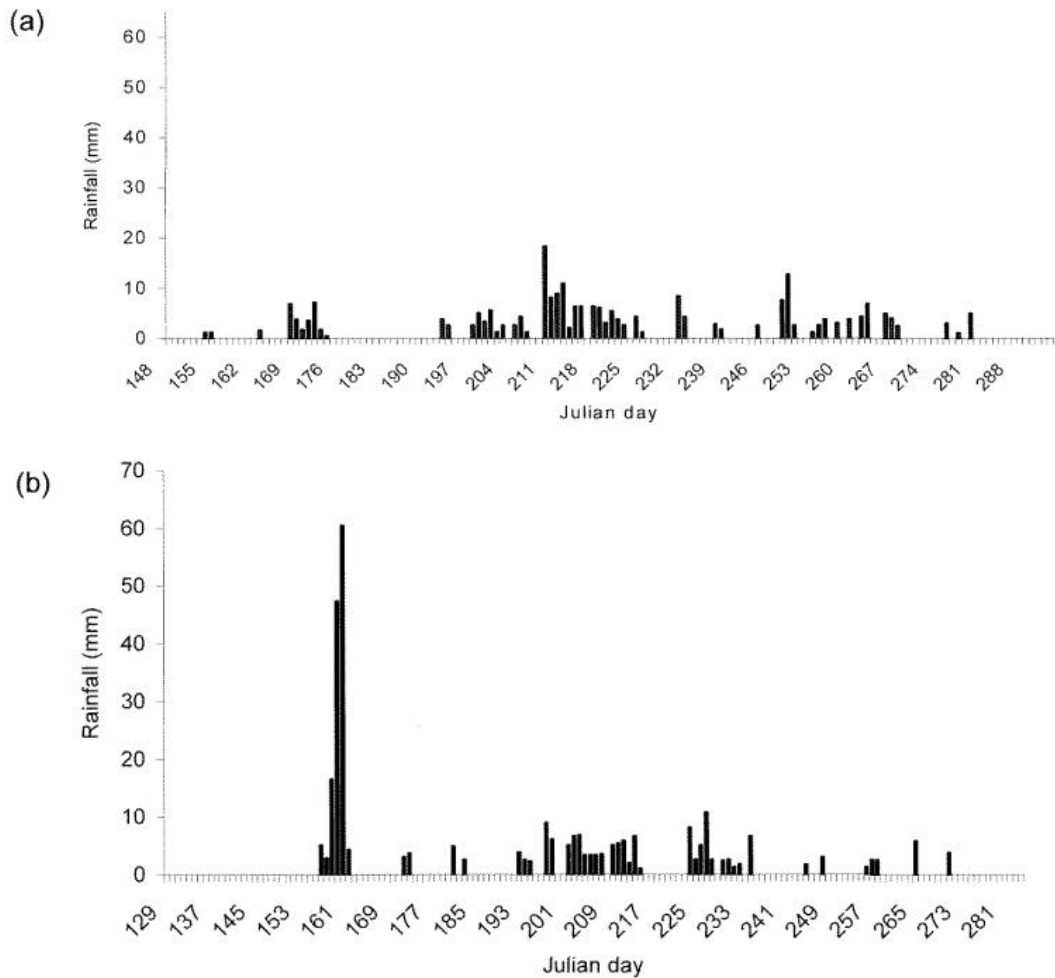
Figure 6.3: Precipitation within the Gangotri valley for 1999 (a) and 2000 (b) (Kumar *et al.*, 2002)

When precipitation displayed within Figures 5.1 to 5.4 are compared to those taken directly prior (years 1999 and 2000 illustrated in Figure 6.3), it is evident that 1999 appears to have resemblance to that of 2003 within Figure 5.3 in terms of frequency of precipitation events and their magnitude. Precipitation for 2000 (Figure 6.3) indicates the occurrence of a large storm event with around 60.00 mm of rainfall, a similar magnitude to that in 2002 displayed in Figure 5.2, although the storm event for 2000 materialised much earlier in the summer. Low amounts of precipitation such as that experienced during 2001

81

may be due to the fact that a large majority of the moisture contained by monsoonal clouds is precipitated before reaching high altitude areas such as that containing Gangotri glacier, similar to that displayed within Figure 1.3 (Singh *et al.*, 2005b). It is also suggested by Collins *et al.*, (2013) that basins in this area are on the margin of influence of the Indian summer monsoon, and therefore summer monsoon rainfall may not be as intense as other areas.

6.2 General influence of air temperature and precipitation on discharge

There are a number of variables that can effect discharge flowing from a highly glacierised basin including debris cover and a host of meteorological conditions, but this study concentrates on influence of air temperature and precipitation (Hock, 2005; Scherler *et al.*, 2011). The trend for discharge displayed for each summer appears to follow changes in air temperature as opposed to precipitation. Correlations between daily average discharge and air temperature for each year studied are collated in Table 6.1, with correlations between daily total precipitation and daily average discharge displayed in Table 6.2.

Table 6.1: Correlation between daily average discharge and daily average air temperature for each summer investigated.

	Correlation between air temperature and discharge
2001	0.63
2002	0.76
2003	0.82
2004	0.62

Table 6.2: Correlation between daily average discharge and daily total precipitation for each summer investigated.

	Correlation between precipitation and discharge
2001	-0.02
2002	-0.40
2003	0.00
2004	-0.12

Upon analysing Tables 6.1 and 6.2, it is evident that daily average air temperature in all instances has a much stronger relationship with daily average discharge than that of daily total precipitation. This relationship is especially evident for 2003, whereby the correlation between daily average air temperature and discharge is at its strongest with 0.82 and for the same period correlation between daily total precipitation and daily average discharge displays a weak relationship with 0.00. A strong positive relationship between daily average air temperature and discharge and weak negative relationship between daily total precipitation and daily average discharge is also evident for 2001 and 2004.

Additionally, 2002 appears to display both a strong positive relationship between daily average air temperature and daily average discharge with a correlation of 0.76, but also appears to display negative relationship between daily total precipitation and daily average discharge with a correlation of -0.40. This may be due to the fact that a majority of precipitation events occur after discharge has met its peak and has begun to decrease. Two large precipitation events also occur when air temperature is low, appearing to cause a large trough in discharge between Julian days 244 (September 1) & 254 (September 11).

A number of studies also conclude reporting similar relationships between these meteorological variables and discharge from a highly glacierised basin including those conducted by Collins, (1987; 1989), Escher-Vetter and Siebers, (2007), and Thayyen *et al.*, (2005). Collins, (1987) investigated the response of runoff

from glacierised basins within the Swiss Alps to climatic fluctuations such as summer air temperature, precipitation and also winter precipitation, the findings of which are displayed within Table 6.3.

Table 6.3: Correlations between climatic variables measured at Zermatt (Z), Sion (S) and Saas Almagell (SA) and total annual runoff (Collins, 1987).

River	Period	T_{5-9}	P_{11-10}	P_{11-5}	P_{6-9}
Vispa	1922-1956	S 0.62		S 0.20	
Lonza	1956-1977	S 0.39	S 0.25	S 0.31	
Saaser Vispa	1923-1963	Z 0.55	Z 0.23		
	1956-1977	S 0.79	Z -0.22	S 0.24	
Rhône	1968-1983	SA 0.81			SA 0.18
	1931-1964	S 0.91	Z -0.28	Z -0.20	Z -0.31
Massa	1965-1977	S 0.87		S 0.18	
	1968-1983	SA 0.92		SA -0.22	

Findings displayed within Table 6.3 indicate similar results to this investigation, in terms of relationship between summer air temperature and discharge and also summer precipitation and discharge for a number of glacial fed rivers located within the Swiss Alps. Correlation between summer air temperature and discharge generally ranges from 0.55 to 0.92, with the exception of an anomalous value of 0.39 for Lonza. These correlations are not entirely different from that found for Gangotri valley, and show a similarly positive relationship ranging from 0.62 to 0.82. In terms of summer precipitation, Collins, (1987) found both a weak positive correlation (0.18) and a negative correlation (-0.31) (Table 6.3) signifying no uniform relationship. This indicates that the relationship may be dependant on the form of precipitation (rain/snow). Although correlations between daily average discharge and daily total precipitation displayed in Table 6.2 do not display an instance of positive correlation, they do show much variability such as that encountered by Collins, (1987) ranging

from 0.00 to -0.40.

Conclusions of Collins, (1987) state that around 62.4% to 84.6% of variance in discharge can be explained by changes in summer air temperature, but only around 10% can be accounted for by precipitation. When compared to findings of this investigation, regression between daily average air temperature and daily average discharge indicates a similar finding for 2002 and 2003 (Figure 5.9), with 0.58 and 0.67 respectively. Although 2001 and 2004 do not show as strong relationship as that for 2002 and 2003 or indeed that found by Collins, (1987), they still display an R^2 of 0.39 for 2001 and 0.38 for 2004. In terms of the relationship between daily average discharge and daily total precipitation, similarly low values of R^2 are displayed in Figure 5.5, with the highest encountered recorded as 0.16 for 2002, but the rest indicating extremely low values for 2001, 2003 and 2004 with 0.00, 2E-06 (0.00) and 0.02 respectively.

Similar to Collins, (1987), Escher-Vetter and Siebers, (2007) also performed regression analysis on discharge in relation to a number of factors including summer snowfall days and summer air temperature for the Vernagtbach basin, Austria between May and September. Results of this study indicate an R^2 between discharge and summer snow fall days of 0.14, and an R^2 between discharge and summer air temperature of 0.60. The R^2 found for summer snowfall days and discharge by Escher-Vetter and Siebers, (2007) is similar to that displayed within Figure 5.5B for 2002 which reports an R^2 of 0.16 with a negative relationship, indicating that many of the precipitation events for this year portray a dampening effect on discharge. When regression between summer air temperature and discharge from Escher-Vetter and Siebers, (2007) are compared to this study, the R^2 of 0.60 is once again similar to that displayed for 2002 (Figure 5.5B), indicating an R^2 of 0.58 which also resembles that reported for 2003 (0.67).

Findings of this study are also further supported by Thayyen *et al.*, (2005) who concluded that the increase in summer discharge is predominantly due to increasing summer air temperatures, as opposed to monsoonal rainfall contribution. This was also found by Collins, (1989) for the Rhone catchment,

who found that summer air temperatures over summer months were highly correlated with total summer discharge.

6.3 Interaction of air temperature and precipitation with discharge, in relation to the elevation of the 0 °C isotherm

The relationship between daily average discharge and daily total precipitation are displayed in Figures 5.6 to 5.8, under filters for when precipitation events occur when the elevation of the 0 °C isotherm is below 5500 m, 5000 m and 4500 m. Figures 5.10 to 5.12 illustrate the relationship between daily average air temperature and daily average discharge also under filters for when the 0 °C isotherm is positioned below 5500 m, 5000 m and 4500 m.

In terms of the relationship between daily average discharge and daily total precipitation in relation to the elevation of the 0 °C isotherm, it was expected that under the filters for a progressively lowering 0 °C isotherm the relationship would become more negative as snow covered larger regions of the glacier. As each year is filtered in Figures 5.6 to 5.8, it quickly becomes apparent that this is not universal with the only years reaching a stronger negative relationship with a decreasing elevation of the 0 °C isotherm being 2001 and 2004, as displayed within a summary of correlations between daily average discharge and daily total precipitation in Table 6.4 and the R^2 in Table 5.3.

Table 6.4: Summary of correlations between daily average discharge and daily total precipitation under differing 0 °C isotherm filters.

	Unfiltered	5500 m	5000 m	4500 m
2001	-0.02	0.22	-0.32	N/A
2002	-0.40	-0.49	-0.34	-0.31
2003	0.00	-0.11	0.59	N/A
2004	-0.12	-0.02	0.23	-0.42

The unfiltered summer of 2001 displays a very weak R^2 of 0.00, which increases to 0.10 under the 0 °C isotherm less than 5000 m filter. This increase in relationship is further displayed within correlation between the variables, increasing from -0.02 to -0.32. Moreover, the unfiltered summer of 2004 begins with an R^2 of 0.02, which under the 0 °C isotherm less than 4500 m filter becomes a much stronger 0.18 which is also evident within correlation analysis, increasing from -0.12 to -0.42. For 2001 and 2003 under the 0 °C isotherm less than 4500 m filter there were no precipitation events for 2001 and only one for 2003 meaning investigating the effects of precipitation during these cold periods using correlation and regression was not possible for these years.

Despite a large majority of the relationships between daily average discharge and daily total precipitation displayed within Figures 5.5 to 5.8 being neutral or negative; 2001, 2003 and 2004 all display a positive relationship between variables under certain filters as displayed within Table 6.4. When under the 0 °C isotherm less than 5500 m, 2001 displays a weak positive relationship with an R^2 of 0.05 and a correlation of 0.22. Moreover, 2003 experiences a positive relationship when under the 0 °C isotherm lower than 5000 m filter with a positive R^2 of 0.34 and a correlation of 0.59. The summer of 2004 experiences a positive relationship also under the 0 °C isotherm less than 5000 m filter with a R^2 of 0.05 and a correlation value of 0.23.

From results discussed concerning the relationship between daily average discharge and daily total precipitation under differing 0 °C isotherm elevation filters, it is evident that precipitation has a varied influence on discharge providing both positive and negative relationships (Table 6.4). The positive relationships evident for 2003 and 2004 under the 0 °C isotherm lower than 5000 m filter may be due to precipitation events occurring when the 0 °C isotherm is at a high altitude, such is the case with 2003, where a majority of precipitation including a large event of 11.70 mm occur when the 0 °C isotherm is between 4908.33 m & 4991.67 m. Table 6.5 displays the glacierised area of elevation ranges within the basin containing Gangotri glacier.

Table 6.5: The glacierised area for different elevation ranges within the Gangotri glacier basin (Singh *et al.*, 2008).

Elevation range (m)	Glacierized area (km^2)
<3800	0
3800–4200	2.38
4201–4600	14.39
4601–5000	52.93
5001–5400	65.17
5401–5800	72.36
5801–6200	53.00
6201–6600	21.37
6600–7000	4.39
3800–7000	285.99

When compared to Table 6.5 a large amount of the glacier is still receiving rainfall and not snowfall when the 0 °C isotherm is situated at this elevation. This means much of the ablation zone is left exposed to solar radiation once the event has passed, with rainfall also adding quickly to runoff measurements where it falls on land between the glacier and gauging station situated 3 km downstream of the terminus. There is also an issue with distribution of snowfall as it can be redistributed by wind or avalanches potentially leaving large areas of the glacier bare, despite a precipitation event occurring when the 0 °C isotherm is positioned at a low altitude. (Archer, 2003; Collins and Taylor, 1990; Harris and Corte, 1992).

The negative relationship is caused when snowfall covers a large percentage of the glacier, especially the ablation zone, temporarily raising its albedo from 0.6 to 0.9. This increase of albedo is particularly important during the peak of summer as even a small amount of snowfall will raise the surface albedo, decreasing absorption of solar radiation and inhibiting discharge derived from bare ice melt (Collins, 1987).

Furthermore, in relation to the interaction between daily average air temperature and daily average discharge illustrated in Figures 5.9 to 5.12, it was expected that with a progressively lowering 0 °C isotherm filter the relationship would become weaker and potentially even negative by the 0 °C isotherm

less than 4500 m filter.

Upon analysis, it appears that the hypothesis of a decreasing relationship between daily average discharge and daily average air temperature with a decreasing elevation of the 0 °C isotherm is correct for 2001 to 2003 but not for 2004 as within Tables 6.6 & 5.4. When the data is filtered for the 0 °C isotherm less than 4500 m, a decrease in relationship is evident in all years investigated apart from 2004; with 2001 experiencing an decrease in R^2 from 0.39 to 0.10, 2002 decreasing from 0.58 to 0.44 (flipping to a negative relationship) and 2003 decreasing from 0.67 to 0.01 also changing to a slight negative relationship. This decrease and flip in relationship is also evident within correlations for 2001 to 2003; with 2001 decreasing from 0.63 to 0.32, 2002 switching from 0.76 to -0.67 and 2003 also switching from 0.82 to -0.10 also within Table 6.6.

Table 6.6: Summary of correlations between daily average discharge and daily average air temperature under differing 0 °C isotherm filters.

	Unfiltered	5500 m	5000 m	4500 m
2001	0.63	0.48	0.37	0.32
2002	0.76	0.69	0.35	-0.67
2003	0.82	0.76	0.53	-0.10
2004	0.62	0.45	0.51	0.87

The decreasing and shifting relationship between daily average discharge and daily average air temperature under a progressively lowering 0 °C isotherm filter is indicative of decreasing influence of air temperature on discharge, when air temperature within the glacierised basin is low. This coincides with the increasing relationship between daily average discharge and daily total precipitation under a progressively lowering filter of the 0 °C isotherm.

The relationship between daily average discharge and daily average air temperature for 2004 appears to at first decrease from an R^2 of 0.38 to 0.20, also evident within correlation lowering from 0.62 to 0.45 under the 0 °C isotherm less than 5500 m filter in line with other years studied. Unlike other years under the 0 °C isotherm less than 5000 m filter, the relationship between discharge and air temperature shows an increase with the R^2 slightly increasing

to 0.27 and correlation increasing to 0.51. Under the 0 °C isotherm less than 4500 m a strong relationship is portrayed with an R^2 of 0.75 and a correlation of 0.87. This may be due to the fact that there are very few values present under this filter and each value for daily average air temperature appears to closely follow daily average discharge, with both experiencing a sharp drop at the very end of the time series apparently due to a large precipitation event.

6.4 Relationship between discharge, air temperature and precipitation during specific summer snowfall events

Negative relationships between discharge and precipitation with a lowering elevation of the 0 °C isotherm found for 2001, 2002 and 2004, led to the selection precipitation events from these years (thought to be summer snowfall events). The precipitation events selected are illustrated within Figures 5.13 to 5.15 and used in order to determine the exact effect these events had on discharge.

In all three years, it was determined that the effect precipitation events had on discharge was not evident within correlation between daily total precipitation and daily average discharge, but was evident within correlation between daily average discharge and daily average air temperature. To view the effect a precipitation event had on discharge, correlation between daily average air temperature and daily average discharge was split into three sections; before the snowfall event, days for which the snowpack lasted and the days after the disappearance of the snowpack as displayed within Table 6.7.

Table 6.7: Correlation between daily total precipitation and daily average discharge before, during and after a specific precipitation event during the summers of 2001, 2002 and 2004.

	Before	During	After
2001	0.69	-0.62	0.34
2002	0.80	-0.73	0.56
2004	0.57	-0.88	0.34

In all three cases, correlation between daily average air temperature and daily average discharge indicated a strong positive relationship before the precipitation event, a strong negative relationship in the days immediately following the precipitation (duration of the snowpack) and returned to a positive relationship following the disappearance of the snowpack but not as strong as before the precipitation event.

Figures 6.4 to 6.6 illustrate the same precipitation events displayed in Figures 5.13 to 5.15, but with the snowfall event and subsequent influence of the snowpack highlighted within a red area.
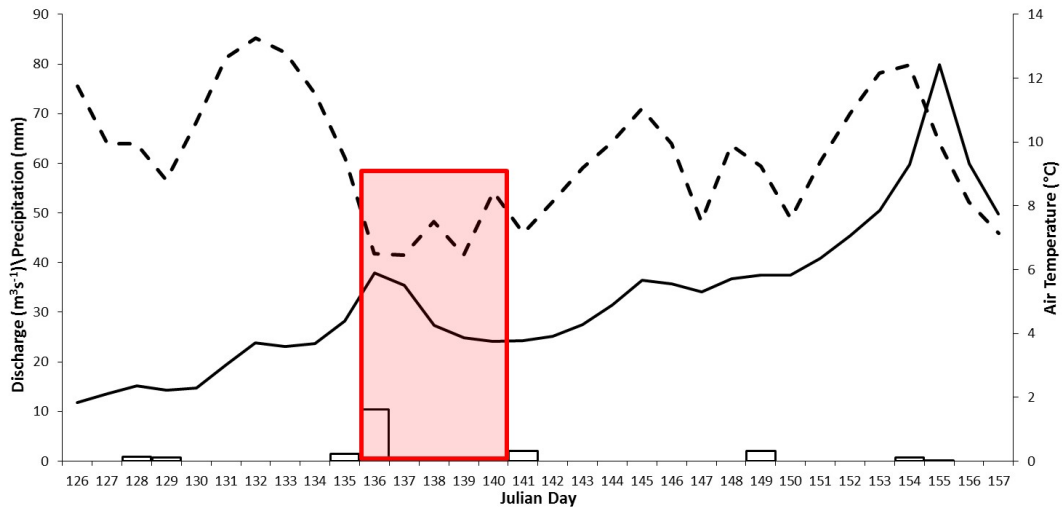
Figure 6.4: Example of a summer snowfall event occurring in 2001 highlighted within the red area, including precipitation (columns), air temperature (dotted line) and discharge (solid line).

91
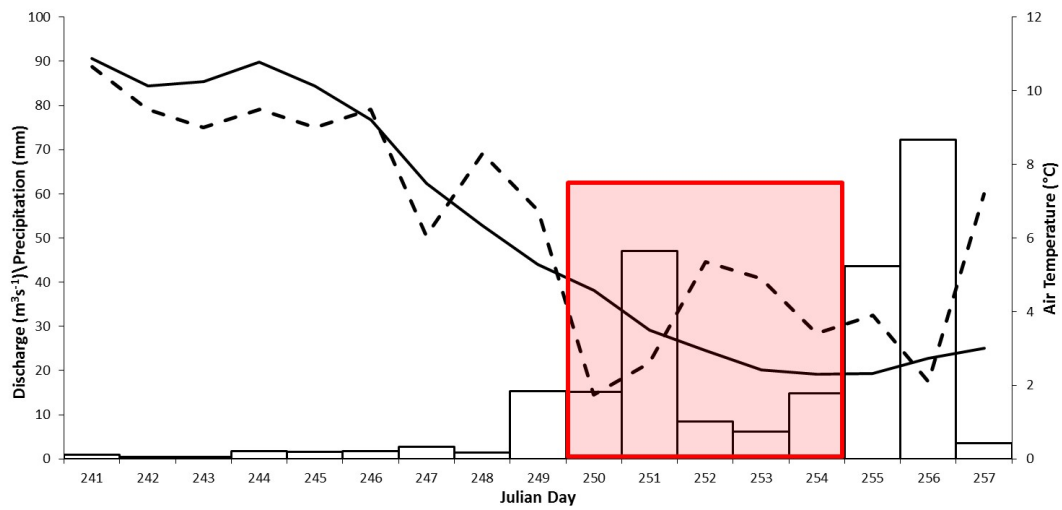
Figure 6.5: Example of a summer snowfall event occurring in 2002 highlighted within the red area, including precipitation (columns), air temperature (dotted line) and discharge (solid line).
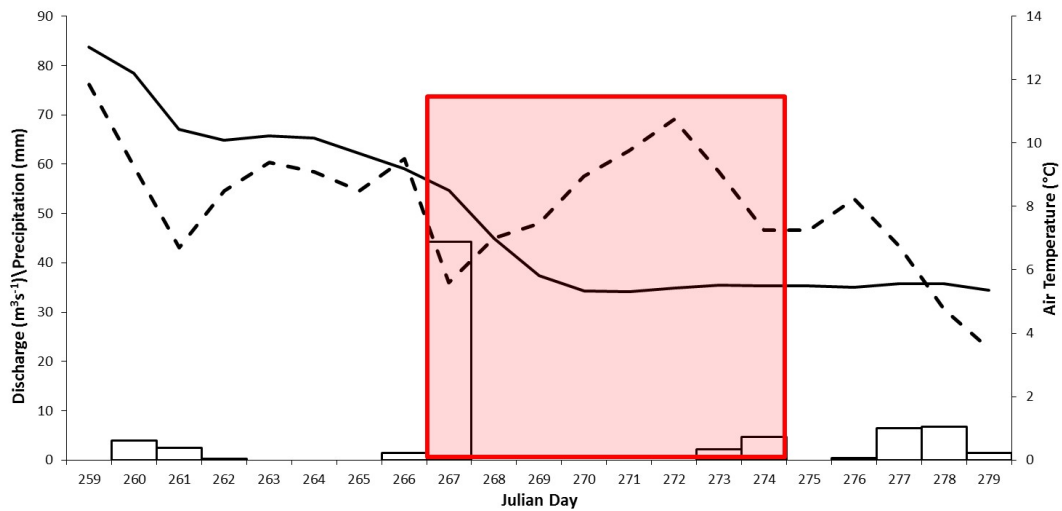
Figure 6.6: Example of a summer snowfall event occurring in 2004 highlighted within the red area, including precipitation (columns), air temperature (dotted line) and discharge (solid line).

The precipitation event selected which appears to have the most visible inhibiting effect on discharge is displayed within Figures 5.15 & 6.6, which occurs during 2004.

Figure 6.6 depicts a large precipitation event on Julian day 267 (September 23) of 44.30 mm when the 0 °C isotherm was on average around a low 4733.33 m. The lowest temperature recorded for that day was 0.20 °C meaning the snowfall event may have occurred when the 0 °C isotherm was as low as 3833.33 m. If the precipitation event occurred when the 0 °C isotherm was around 3833.33 m, Table 6.5 indicates that snow would have covered almost the entire area of the glacier. Despite an already decreasing discharge the decrease becomes sharper after this precipitation, indicating a decrease in ablation. Moreover, in the days following the snow fall, air temperature rapidly increases to an average of 10.75 °C on Julian day 272 (September 28) with the highest temperature recorded for this day abnormally warm with 16.50 °C. In defiance of this discharge continues to decline and plateau, only experiencing a small increase of 1.46 $m^3 s^{-1}$ nearing the peak of air temperature, despite a large increase in daily average air temperature of 5.15 °C experiencing a strong negative correlation of -0.88 during this period.

Therefore, this indicates a large amount of snow present on Gangotri glacier, offsetting the large increase in air temperature until the snow appears to show signs of depletion, with a small increase in discharge as air temperature peaks. Furthermore, when daily average air temperature previously reached a similar value to that on Julian day 272 (September 28) with similar maximum and minimum values recorded for Julian day 259 (September 15), the daily average discharge recorded was a considerable 48.89 $m^3 s^{-1}$ higher than that recorded for a similar air temperature when snow cover was present. These findings are supported by that of Brock *et al.*, (2000) who found that melt rate derived from Haut Glacier d'Arolla was reduced by more than 50% on the day of the summer snowfall event when compared to previous figures of discharge and concluded that this was caused by an increase of albedo to more than 70%, supported by the findings of Oerlemans and Klok, (2004) displayed within Figure 3.5.

A study with similar aims to this investigation was conducted by Escher-Vetter and Siebers, (2007) to understand the effect of summer snowfall on discharge from a glacierised basin located in Austria. Vernagtbach basin was investigated between the years of 1976 and 2005 using precipitation data obtained for each ablation season, with the type of precipitation derived from daily photographs. A number of issues were identified for using daily photographs to determine the type of precipitation including that small amounts of snowfall may have melted by the time a photograph was taken and the time series of the photographs is not always complete due to inaccessibility of the camera and potential technical problems. A summer snowfall event observed using daily photographs is displayed in Figure 6.7, taken before and after the summer snowfall event in the Vernagtbach basin during 2003, showing a distinct visual difference. The hydrograph from the Vernagtbach stream between August 27 & September 5 is also displayed in Figure 6.8, corresponding with the summer snowfall event in Figure 6.7.

Figure 6.7: Images of the Vernagtbach basin on the August 28, 2003 and September 4 (2003), before and after a summer snowfall event (Escher-Vetter and Siebers, 2007).
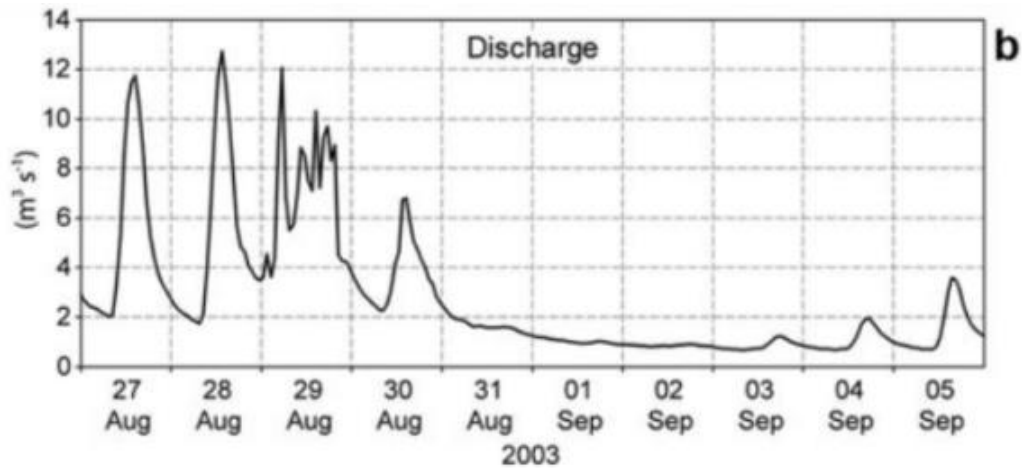
Figure 6.8: Discharge emanating from the Vernagtbach basin between August 27 and September 5, 2003 (Escher-Vetter and Siebers, 2007).

Results displayed in Figure 6.8 clearly demonstrate that a summer snowfall event occurred between August 30 & 31, confirmed by the images in Figure 6.7 taken on August 28 and September 4. It is evident that the summer snowfall event had a large impact on discharge from the glacierised basin, as before the summer snowfall event occurs daily discharge displayed in Figure 6.8 fluctuates greatly between day and night reaching peaks of over $12\,\mathrm{m}^3\,\mathrm{s}^{-1}$ and lows of around $2\,\mathrm{m}^3\,\mathrm{s}^{-1}$. After August 30 discharge stays low and continues to drop, with only very slight increases where peak discharge would usually occur after peak solar radiation until September 3 where discharge shows a small peak of $1\,\mathrm{m}^3\,\mathrm{s}^{-1}$ which continues to grow in subsequent days. This indicates that the higher albedo of fresh snow greatly inhibited discharge stemming from the glacierised basin. In this investigation the effect that snowfall had on the glacier was pronounced and also immediate, reducing the discharge from more than $12\,\mathrm{m}^3\,\mathrm{s}^{-1}$ to around $1\,\mathrm{m}^3\,\mathrm{s}^{-1}$.

The conclusions of Escher-Vetter and Siebers, (2007) strongly support the findings of this study with regards to Gangotri glacier. This is because the effect that the summer snowfall event had on the Vernagtbach basin illustrated within Figure 6.8 are remarkably similar to the effects that the summer snowfall events selected had on Gangotri glacier, in terms of reducing discharge from the

glacierised basin through increasing the surface albedo and reflecting incoming radiation but on a much smaller scale.

A number of other studies support the findings of this investigation regarding to summer snowfall events offsetting melt of the ablation zone of a glacier for a short period of time. Firstly Hock *et al.*, (2005) who investigated response of glacial discharge to climatic warming simply states that a large precipitation event can effectively stop discharge from a glacierised basin for an extended period of time similar to the findings of this study. A number of other studies including those conducted by Collins, (1987), Collins and Hasnain, (1995), Fujita and Ageta, (2000) and Pellicciotti *et al.*, (2010) also all state that summer snowfall events restrain ablation of glaciers through an increased albedo, reducing the amount of short wave radiation absorbed.

A study conducted by Rees and Collins, (2006) into regional differences in response of flow to climatic warming within glacier fed Himalayan rivers concluded that under a $0.06\,°C$ year^{-1} warming scenario, summer snowfall in the east would postpone the disappearance of ice. In terms of Gangotri glacier located in the west Himalaya, summer snowfall may have the same effect in postponing its disappearance but only slightly due to receiving less monsoonal rainfall.

The duration snow cover inhibits melt from Gangotri glacier is 5 days for both 2001 and 2002 and 7 days for 2004. These findings are supported by those of Oerlemans and Klok, (2004) who state that suppression of melt within the ablation zone of the Morteratschgletscher, located in Switzerland, caused by summer snowfall almost disappeared after 5 days. The extended period shown for 2004 is due to the fact that it appears to be a large snowfall event, meaning the duration of snow cover would be extended.

Chapter 7

Conclusion

Research regarding the influence of summer snowfall on discharge emanating from Alpine glaciers is of great importance, but appears to be sparse. This is especially evident within the Himalayan region due to issues with accessibility to high elevation regions and logistical issues with equipment making long term detailed data sets rare (Singh *et al.*, 2005b). This chapter summarises key findings where this study fills a gap in research and also provides limitations and recommends future considerations for research within this field.

7.1   Summary of key findings

This study set out to fill a gap in research by investigating the influence of summer snowfall events on runoff from Gangotri glacier, something which had not been previously investigated. The investigation explored the exact effect specific snowfall events had on discharge and the duration of its effect, utilising data previously collected for the summers of 2001 to 2004 for daily total precipitation, daily average air temperature and daily average discharge. The average elevation of the 0 °C isotherm was also calculated for each day in order to determine the elevation at which snow would fall during a precipitation event and to help identify whether a majority of the ablation zone of Gangotri

glacier would be concealed by snow. This was carried out using filters which only showed data for when the elevation of the 0 °C isotherm was positioned below 5500 m, 5000 m and 4500 m.

The general effect of meteorological influences including air temperature and precipitation on discharge flowing from Gangotri glacier was first determined. It was found using correlation and regression analysis that air temperature as opposed to precipitation was the driving factor for discharge within this glacierised basin. The regression and correlation indicated that air temperature can account for a large percentage of discharge during the study period, whereas the influence of precipitation was found to be small. These findings are supported by studies conducted by Collins, (1987), Collins, (1989), Escher-Vetter and Siebers, (2007) and Thayyen *et al.*, (2005).

The effect of precipitation and air temperature on discharge under filters whereby the 0 °C isotherm was positioned below 5500 m, 5000 m and 4500 m was also determined. It was thought that under a progressively lowering filter that the relationship between daily total precipitation and daily average discharge would became more strongly negative, but this was only evident within 2001 & 2004 which both indicate the presence of snowfall events occurring when the elevation of the 0 °C isotherm was low. A negative relationship when the elevation of the 0 °C isotherm is below 4500 m is also evident for 2002, despite indicating a weaker relationship than the unfiltered data. These findings suggest the presence of a snowfall event where an increase in precipitation causes a decrease in discharge, an element of research not previously investigated for Gangotri glacier.

Under a lowering filter of the 0 °C isotherm it was expected that the relationship between air temperature and discharge would become weaker. The results and consequent discussion show that this was the case for all years other than 2004 which appears to attain an increase in relationship. The relationship for 2002 & 2003 do in fact switch to negative relationships. This indicates that under the 0 °C isotherm less than 4500 m for 2002 & 2003 that discharge may decrease despite an increasing air temperature.

The most important findings of the study are related to that displaying specific snowfall events, along with discharge and air temperature. It was found in all three precipitation events chosen that correlation between air temperature and discharge before the event was strongly positive, the duration of the snowpack was strongly negative and after the snowpack had depleted returned to a positive relationship but not as strong as before the precipitation occurred. This indicates that the precipitation events chosen appear to have fallen as snow covering a majority of the ablation zone, increasing its albedo from around 0.6 to 0.9. This in turn has inhibited discharge despite an increasing air temperature following each event, before degrading and disappearing. The duration of which discharge was inhibited by snow cover appears to range from 5 to 7 days. This appears to be a new branch of study, filling a gap in research about the effects of summer precipitation events on discharge from Gangotri glacier. These findings are supported by and build upon the knowledge of a number of studies including those by Brock *et al.*, (2000), Collins, (1987), Collins and Hasnain, (1995), Escher-Vetter and Siebers, (2007), Fujita and Ageta, (2000), and Pellicciotti *et al.*, (2010).

7.1.1 Meeting the aim and objectives

The aim of this study was to investigate how summer snowfall events influence discharge emanating from Gangotri glacier as outlined in Chapter 1. This was to provide an insight as to how snowfall over the ablation area of Gangotri glacier during summer months influenced discharge produced. In order to achieve this aim three specific objectives were set:

1. Determine the discharge and meteorological regime for Gangotri glacier.

The first objective was completed utilising data gathered by Singh *et al.*, (2006b; 2005b), as outlined in Chapter 4. This provided data for air temperature, precipitation and discharge within Gangotri valley, which was then analysed providing the discharge and meteorological regime presented in Chapter 5 and discussed in Chapter 6.

2. Establish daily average elevation of the 0 °C isotherm for each summer day.

The second objective, to establish the daily average elevation of the 0 °C isotherm for each summer day, was fulfilled utilising the equation outlined in Chapter 4. This equation was applied to daily average air temperature which allowed for calculation of the 0 °C isotherm elevation within the atmosphere. This gave a good indication of which areas of Gangotri glacier would be receiving rain and which would receive snow on days in which precipitation events occurred. The use of this equation also allowed for data to be filtered in order to only show values when the 0 °C isotherm was positioned below certain elevations.

3. Identify precipitation events where snowfall covers a large amount of the ablation zone.

The final objective, to identify precipitation events where snowfall covers a large amount of the ablation zone, was completed using data filters, which appears to be the first in its kind to identify snowfall events in this way. Three filters were applied to the data in order to only show air temperature, precipitation and discharge for days where the daily average elevation of the 0 °C isotherm was positioned below 5500 m, 5000 m and 4500 m as illustrated within Chapters 5 & 6. These filters and calculated daily average elevation of the 0 °C isotherm subsequently allowed for identification of snowfall events which would have covered a large majority of Gangotri glacier, also evident in Chapters 5 & 6. Identification of such snowfall events led to completion of the overall aim of this thesis, through correlation analysis between daily average air temperature and discharge before the snowfall event, the duration of which the snow cover endured and immediately following the disappearance of the snowpack evident in Chapter 6. Such correlation analysis allowed for the determination of the influence three summer snowfall events had on discharge from Gangotri glacier and how long the influence of the snowfall event persisted.

7.2 Limitations

Most limitations encountered in this study revolve around data availability and issues with collecting data in this area, as opposed to methods used. The first limitation encountered by this research was that data were only available for the summers of four years (2001 to 2004), providing a short time series for analysis. This limitation restricted the number of potential snowfall events which influenced discharge identified and also did not allow for analysis of how the frequency and magnitude of summer precipitation events has changed with a warming climate.

Secondly, a further limitation of this investigation was that air temperature data available was only minimum and maximum, with precipitation daily total and discharge daily average, as opposed to hourly measurements of each. This limitation meant that selected summer snowfall events could only be analysed on a daily scale as opposed to an hourly, in order to gain a detailed view of the snowfalls exact effect. Furthermore, issues with data availability in the Himalayan region through an inadequate hydrological and meteorological network as stated by Bolch *et al.*, (2012) and Chalise *et al.*, (2003) meant there were few data sources used.

Moreover, an additional limitation linking to data availability is that the temperature lapse rate for the region was assumed to be $0.6\,°C$ derived from other studies conducted, as opposed to calculating the lapse rate specific to this valley.

7.3 Considerations for future research

There are a number of considerations research undertaken in this field may include in their investigations, from limitations of this study. The first consideration is the establishment and use of a long running data set of discharge, air temperature and precipitation in the vicinity of a Himalayan glacierised basin. This would be of use in order to investigate the effect of summer snow-

fall events on discharge over a long term scale. A long term data set would also be useful whilst investigating response of summer precipitation events to a warming climate, thought to be experienced in the future. Furthermore, a benefit would arise from collecting hydrometeorological data in the Himalayan region on an hourly schedule. This is particularly advantageous when aiming to view the exact effect of a summer snowfall event in detail and determine an accurate duration for these effects.

A weather station at the snout of the glacier and another 100 m higher would be of great benefit in order to calculate an accurate temperature lapse rate for the specific region, which would further allow accurate estimation of 0 °C isotherm elevation. It would also be ideal to have a camera taking regular images to ensure the ablation area of the glacier is snow covered, to collaborate with after a suspected snowfall event.

In conclusion, these considerations are given as an ideal for research in this subject area and it is understood that implementation of these may be extremely difficult within Alpine regions, especially the Himalayas due to its extreme elevation and difficult terrain. Despite difficulties in establishing such data sets, they would be extremely beneficial to the geographical area and its inhabitants, with regards to millions of people who rely on its water resources for both personal and commercial use. It would also be beneficial to accurately simulate future flows under differing climatic scenarios, to make informed decisions for the future.

References

Alford, D. and Armstrong, R. (2010). The role of glaciers in stream flow from the Nepal Himalaya. *The Cryosphere Discussions* **4** (2), 469–494.

Archer, D. (2003). Contrasting hydrological regimes in the upper Indus Basin. *Journal of Hydrology* **274** (1), 198–210.

Arora, M., Singh, P., Goel, N. K., and Singh, R. D. (2008). Climate variability influences on hydrological responses of a large Himalayan basin. *Water Resources Management* **22** (10), 1461–1475.

Bahuguna, I. M., Kulkarni, A. V., Nayak, S., Rathore, B. P., Negi, H. S., and Mathur, P. (2007). Himalayan glacier retreat using IRS 1C PAN stereo data. *International Journal of Remote Sensing* **28** (2), 437–442.

Bajracharya, S. and Shrestha, B. (2011). *The status of glaciers in the Hindu Kush-Himalayan region.* International Centre for Integrated Mountain Development (ICIMOD).

Bali, R., Awasthi, D. D., and Tiwari, N. K. (2003). Neotectonic control on the geomorphic evolution of the Gangotri Glacier Valley, Garhwal Himalaya. *Gondwana Research* **6** (4), 829–838.

Barnard, P. L., Owen, L. A., and Finkel, R. C. (2004). Style and timing of glacial and paraglacial sedimentation in a monsoon-influenced high Himalayan environment, the upper Bhagirathi Valley, Garhwal Himalaya. *Sedimentary Geology* **165** (3), 199–221.

Bavay, M., Lehning, M., Jonas, T., and Löwe, H. (2009). Simulations of future snow cover and discharge in Alpine headwater catchments. *Hydrological Processes* **23** (1), 95–108.

Bhambri, R. and Bolch, T. (2009). Glacier mapping: a review with special reference to the Indian Himalayas. *Progress in Physical Geography* **33** (5), 672–704.

Bhambri, R., Bolch, T., Chaujar, R. K., and Kulshreshtha, S. C. (2011). Glacier changes in the Garhwal Himalaya, India, from 1968 to 2006 based on remote sensing. *Journal of Glaciology* **57** (203), 543–556.

Bolch, T., Kulkarni, A., Kääb, A., Huggel, C., Paul, F., Cogley, J. G., Frey, H., Kargel, J. S., Fujita, K., and Scheel, M. (2012). The state and fate of Himalayan glaciers. *Science* **336** (6079), 310–314.

Brock, B. W., Willis, I. C., Sharp, M. J., and Arnold, N. S. (2000). Modelling seasonal and spatial variations in the surface energy balance of Haut Glacier d'Arolla, Switzerland. *Annals of Glaciology* **31** (1), 53–62.

Chalise, S. R., Kansakar, S. R., Rees, G., Croker, K., and Zaidman, M. (2003). Management of water resources and low flow estimation for the Himalayan basins of Nepal. *Journal of Hydrology* **282** (1), 25–35.

Chhetri, A., Kayastha, R. B., and Shrestha, A. (2016). Assessment of Sediment Load of Langtang River in Rasuwa District, Nepal. *Journal of Water Resource and Protection* **8** (1), 84.

Collins, D. N. (1987). Climatic fluctuations and runoff from glacierised Alpine basins. *The influence of climate change and climatic variability on the hydrologic regime and water resources. IAHS Publication* **168**, 77–89.

Collins, D. N. (1989). Hydrometeorological conditions, mass balance and runoff from alpine glaciers. In: *Glacier fluctuations and climatic change.* Springer, 235–260.

Collins, D. N. (1998a). Outburst and rainfall-induced peak runoff events in highly glacierized Alpine basins. *Hydrological processes* **12** (15), 2369–2381.

Collins, D. N. (1998b). Rainfall-induced high-magnitude runoff events in highly-glacierized Alpine basins. *IAHS Publications-Series of Proceedings and Reports Intern Assoc Hydrological Sciences* **248**, 69–78.

Collins, D. N., Davenport, J. L., and Stoffel, M. (2013). Climatic variation and runoff from partially-glacierised Himalayan tributary basins of the Ganges. *Science of the Total Environment* **468**, S48–S59.

Collins, D. N. and Hasnain, S. I. (1995). Runoff and sediment transport from glacierized basins at the Himalayan scale. *IAHS Publications-Series of Proceedings and Reports-Intern Assoc Hydrological Sciences* **226**, 17–26.

Collins, D. N. and Taylor, D. (1990). Variability of runoff from partialy glacierised alpine basins. *Hydrology in Mountainous Regions*, 365–372.

De Scally, F. A. (1997). Deriving lapse rates of slope air temperature for meltwater runoff modelling in subtropical mountains: An example from the Punjab Himalaya, Pakistan. *Mountain Research and Development*, 353–362.

Diaz, H. F., Eischeid, J. K., Duncan, C., and Bradley, R. S. (2003). Variability of freezing levels, melting season indicators, and snow cover for selected high-elevation and continental regions in the last 50 years. In: *Climate Variability and Change in High Elevation Regions: Past, Present & Future.* Springer, 33–52.

Dobhal, D. P. and Mehta, M. (2010). Surface morphology, elevation changes and terminus retreat of Dokriani Glacier, Garhwal Himalaya: implication for climate change. *Himalayan Geology* **31** (1), 71–78.

Dyurgerov, M. (2003). Mountain and subpolar glaciers show an increase in sensitivity to climate warming and intensification of the water cycle. *Journal of Hydrology* **282** (1), 164–176.

Dyurgerov, M. B. (2001). Mountain glaciers at the end of the twentieth century: global analysis in relation to climate and water cycle. *Polar Geography* **25** (4), 241–336.

Dyurgerov, M. B. and Meier, M. F. (2005). *Glaciers and the changing Earth system: a 2004 snapshot*. Vol. 58. Institute of Arctic and Alpine Research, University of Colorado Boulder.

Escher-Vetter, H. and Siebers, M. (2007). Sensitivity of glacier runoff to summer snowfall events. *Annals of Glaciology* **46** (1), 309–315.

Fu, C. and Fletcher, J. O. (1985). The relationship between Tibet-tropical ocean thermal contrast and interannual variability of Indian monsoon rainfall. *Journal of climate and applied meteorology* **24** (8), 841–847.

Fujita, K. (2008). Influence of precipitation seasonality on glacier mass balance and its sensitivity to climate change. *Annals of Glaciology* **48** (1), 88–92.

Fujita, K. and Ageta, Y. (2000). Effect of summer accumulation on glacier mass balance on the Tibetan Plateau revealed by mass-balance model. *Journal of Glaciology* **46** (153), 244–252.

Ghatak, D., Sinsky, E., and Miller, J. (2014). Role of snow-albedo feedback in higher elevation warming over the Himalayas, Tibetan Plateau and Central Asia. *Environmental Research Letters* **9** (11), 114008.

Gurung, D. R., Maharjan, S. B., Shrestha, A. B., Shrestha, M. S., Bajracharya, S. R., and Murthy, M. S. R. (2017). Climate and topographic controls on snow cover dynamics in the Hindu Kush Himalaya. *International Journal of Climatology.*

Hagemann, S., Shiqiang, Z., Xu, M., Xu, J., and Zhao, Q. (2013). Estimating the characteristics of runoff inflow into Lake Gojal in ungauged, highly glacierized upper Hunza River Basin, Pakistan. *Journal of Earth Science* **24** (2), 234–243.

Haritashya, U. K., Singh, P., Kumar, N., and Singh, Y. (2006). Hydrological importance of an unusual hazard in a mountainous basin: flood and landslide. *Hydrological Processes* **20** (14), 3147–3154.

Harris, S. A. and Corte, A. E. (1992). Interactions and relations between mountain permafrost, glaciers, snow and water. *Permafrost and Periglacial Processes* **3** (2), 103–110.

Higuchi, K. and Ohata, Y. (1996). Specific features of snow and ice regime under the conditions of Central Asia. *Variations of Snow and Ice in the Past and Present on a Global and Regional Scale. Paris: UNESCO*, 45–51.

Hock, R. (2005). Glacier melt: a review of processes and their modelling. *Progress in physical geography* **29** (3), 362–391.

Hock, R., Jansson, P., and Braun, L. N. (2005). Modelling the response of mountain glacier discharge to climate warming. In: *Global Change and Mountain Regions.* Springer, 243–252.

Hood, J. L. and Hayashi, M. (2015). Characterization of snowmelt flux and groundwater storage in an alpine headwater basin. *Journal of Hydrology* **521**, 482–497.

Immerzeel, W. W., Droogers, P., De Jong, S. M., and Bierkens, M. F. P. (2009). Large-scale monitoring of snow cover and runoff simulation in Himalayan river basins using remote sensing. *Remote sensing of Environment* **113** (1), 40–49.

Jain, S. K. (2008). Impact of retreat of Gangotri glacier on the flow of Ganga River. *Current Science* **95** (8).

Khan, A. A., Pant, N. C., Sarkar, A., Tandon, S. K., Thamban, M., and Mahalinganathan, K. (2017). The Himalayan cryosphere: A critical assessment and evaluation of glacial melt fraction in the Bhagirathi basin. *Geoscience Frontiers* **8** (1), 107–115.

Kulkarni, A. V. and Bahuguna, I. M. (2002). Correspondence. Glacial retreat in the Baspa basin, Himalaya, monitored with satellite stereo data. *Journal of glaciology* **48**, 171–172.

Kulkarni, A. V., Bahuguna, I. M.., Rathore, B. P., Singh, S. K., Randhawa, S. S., Sood, R. K., Dhar, S., *et al.* (2007). Glacial retreat in Himalaya using Indian Remote Sensing satellite data. *Current science* **92** (1), 69–74.

Kumar, A., Gokhale, A. A., Shukla, T., and Dobhal, D. P. (2016). Hydroclimatic influence on particle size distribution of suspended sediments evacuated from debris-covered Chorabari Glacier, upper Mandakini catchment, central Himalaya. *Geomorphology* **265**, 45–67.

Kumar, K., Dumka, R. K., Miral, M. S., Satyal, G. S., and Pant, M. (2007). Estimation of retreat rate of Gangotri glacier using rapid static and kinematic GPS survey. *CURRENT SCIENCE* **94** (2), 258.

Kumar, K., Miral, M. S., Joshi, V., and Panda, Y. S. (2002). Discharge and suspended sediment in the meltwater of Gangotri Glacier, Garhwal Himalaya, India. *Hydrological Sciences Journal* **47** (4), 611–619.

Le Fort, P. (1975). Himalayas: the collided range. Present knowledge of the continental arc. *American Journal of Science* **275** (1), 44.

Luetschg, M., Lehning, M., and Haeberli, W. (2008). A sensitivity study of factors influencing warm/thin permafrost in the Swiss Alps. *Journal of Glaciology* **54** (187), 696–704.

Mathew, J., Jha, V. K., and Rawat, G. S. (2007). Weights of evidence modelling for landslide hazard zonation mapping in part of Bhagirathi valley, Uttarakhand. *CURRENT SCIENCE* **92** (5), 628.

Molnar, P. (1986). The Geologic History and the Structure of the Himalayas. *American Scientist* **74**, 144–154.

Negi, H. S., Thakur, N. K., and Ganju, A. (2012). Monitoring of Gangotri glacier using remote sensing and ground observations. *Journal of Earth System Science* **121** (4), 855–866.

Ninh, N. H. (2007). Asia, Climate Change 2007: Impacts, Adaptation and Vulnerability. *Fourth assessment report of the intergovernmental panel on climate change. Cambridge University Press, Cambridge*, 469.

Oerlemans, J. and Klok, E. J. (2004). Effect of summer snowfall on glacier mass balance. *Annals of Glaciology* **38** (1), 97–100.

Pandey, S. K., Singh, A. K., and Hasnain, S. I. (1999). Weathering and geochemical processes controlling solute acquisition in Ganga headwater–Bhagirathi river, Garhwal Himalaya, India. *Aquatic Geochemistry* **5** (4), 357–379.

Pellicciotti, F., Bauder, A., and Parola, M. (2010). Effect of glaciers on streamflow trends in the Swiss Alps. *Water Resources Research* **46** (10).

Raina, V. K. and Srivastava, D. (2014). Glacier atlas of India. *GSI Publications* **7** (1).

Rees, H. G. and Collins, D. N. (2006). Regional differences in response of flow in glacier-fed Himalayan rivers to climatic warming. *Hydrological processes* **20** (10), 2157–2169.

Sangewar, C. V., Shukla, S. P., and Singh, R. K. (2009). Inventory of the Himalayan glaciers.

Scherler, D., Bookhagen, B., and Strecker, M. R. (2011). Spatially variable response of Himalayan glaciers to climate change affected by debris cover. *Nature geoscience* **4** (3), 156–159.

Sharma, M. C. and Owen, L. A. (1996). Quaternary glacial history of NW Garhwal, central Himalayas. *Quaternary Science Reviews* **15** (4), 335–365.

Singh, P., Arora, M., and Goel, N. K. (2006a). Effect of climate change on runoff of a glacierized Himalayan basin. *Hydrological Processes* **20** (9), 1979–1992.

Singh, P., Haritashya, U. K., and Kumar, N. (2008). Modelling and estimation of different components of streamflow for Gangotri Glacier basin, Himalayas/Modélisation et estimation des différentes composantes de l'écou-

lement fluviatile du bassin du Glacier Gangotri, Himalaya. *Hydrological sciences journal* **53** (2), 309–322.

Singh, P., Haritashya, U. K., Kumar, N., and Singh, Y. (2006b). Hydrological characteristics of the Gangotri glacier, central Himalayas, India. *Journal of Hydrology* **327** (1), 55–67.

Singh, P., Haritashya, U. K., Ramasastri, K. S., and Kumar, N. (2005a). Diurnal variations in discharge and suspended sediment concentration, including runoff-delaying characteristics, of the Gangotri Glacier in the Garhwal Himalayas. *Hydrological processes* **19** (7), 1445–1457.

Singh, P., Haritashya, U. K., Ramasastri, K. S., and Kumar, N. (2005b). Prevailing weather conditions during summer seasons around Gangotri Glacier. *Current Sciences* **88** (5).

Singh, P. and Jain, S. K. (2002). Snow and glacier melt in the Satluj River at Bhakra Dam in the western Himalayan region. *Hydrological Sciences Journal* **47** (1), 93–106.

Singh, P. and Jain, S. K. (2003). Modelling of streamflow and its components for a large Himalayan basin with predominant snowmelt yields. *Hydrological sciences journal* **48** (2), 257–276.

Singh, P., Kumar, A., and Kishore, N. (2011). Meltwater storage and delaying characteristics of Gangotri Glacier (Indian Himalayas) during ablation season. *Hydrological Processes* **25** (2), 159–166.

Singh, P. and Kumar, N. (1997). Impact assessment of climate change on the hydrological response of a snow and glacier melt runoff dominated Himalayan river. *Journal of Hydrology* **193** (1), 316–350.

Singh, P., Ramasastri, K. S., Kumar, N., and Arora, M. (2000). Correlations between discharge and meteorological parameters and runoff forecasting from a highly glacierized Himalayan basin. *Hydrological Sciences Journal* **45** (5), 637–652.

Singh, V. B., Ramanathan, A. L., Pottakkal, J. G., and Kumar, M. (2014). Seasonal variation of the solute and suspended sediment load in Gangotri glacier meltwater, central Himalaya, India. *Journal of Asian Earth Sciences* **79**, 224–234.

Six, D. and Vincent, C. (2014). Sensitivity of mass balance and equilibrium-line altitude to climate change in the French Alps. *Journal of Glaciology* **60** (223), 867–878.

Srivastava, D., Kumar, A., Verma, A., and Swaroop, S. (2014). Analysis of climate and melt-runoff in Dunagiri Glacier of Garhwal Himalaya (India). *Water Resources Management* **28** (10), 3035–3055.

Thayyen, R. J. and Gergan, J. T. (2010). Role of glaciers in watershed hydrology: a preliminary study of a" Himalayan catchment". *The Cryosphere* **4** (1), 115–128.

Thayyen, R. J., Gergan, J. T., and Dobhal, D. P. (2005). Monsoonal control on glacier discharge and hydrograph characteristics, a case study of Dokriani Glacier, Garhwal Himalaya, India. *Journal of Hydrology* **306** (1), 37–49.

Vohra, C. P. (1988). Gangotri Glacier. *Indian Mountaineer*, 51–58.

Wang, S., Zhang, M., Pepin, N. C., Li, Z., Sun, M., Huang, X., and Wang, Q. (2014). Recent changes in freezing level heights in High Asia and their impact on glacier changes. *Journal of Geophysical Research: Atmospheres* **119** (4), 1753–1765.

Watson, R. T., Zinyowera, M. C., and Moss, R. H. (1996). *Climate Change 1995 impacts, adaptations and mitigation of climate change: Scientific-technical analysis*. Cambridge University Press.

Yao, T., Pu, J., Lu, A., Wang, Y., and Yu, W. (2007). Recent glacial retreat and its impact on hydrological processes on the Tibetan Plateau, China, and surrounding regions. *Arctic, Antarctic, and Alpine Research* **39** (4), 642–650.

Zhang, G., Sun, S., Ma, Y., and Zhao, L. (2010). The response of annual runoff to the height change of the summertime 0 C level over Xinjiang. *Journal of Geographical Sciences* **20** (6), 833–847.

Zhang, Y. and Guo, Y. (2011). Variability of atmospheric freezing-level height and its impact on the cryosphere in China. *Annals of Glaciology* **52** (58), 81–88.

Zhisheng, A., Clemens, S. C., Shen, J., Qiang, X., Jin, Z., Sun, Y., Prell, W. L., Luo, J., Wang, S., Xu, H., *et al.* (2011). Glacial-interglacial Indian summer monsoon dynamics. *science* **333** (6043), 719–723.